CALCULATIONS OF PHOTO-IONIZATION CROSS SECTIONS FOR DIATOMIC MOLECULES.

by

H. C. TUCKWELL, B.Sc.

A thesis submitted in accordance with the requirements of the Degree of Master of Science.

Department of Mathematical Physics,
University of Adelaide,
South Australia.

February, 1969.

I give consent to this copy of my thesis, when deposited in the University Library, being available for loan and photocopying.

Date ....6/9/69..... Signed .

CONTENTS

SUMMARY.

In this thesis we present calculations of photo-ionization cross sections for the diatomic molecules N_2, O_2 and NO. These are expected to have important astrophysical applications.

The necessary formulae and the justification of the one electron approach for evaluating electronic matrix elements for many-electron systems are given in Chapter 1, where an attempt is also made to survey briefly the relatively well known field of atomic calculations. The Chapter concludes with a resume of previous theoretical work on photo-ionization cross sections for molecules.

In Chapters 2 and 3 the electronic wave functions needed for the evaluation of the matrix elements are presented and discussed. It is apparent that approximate methods must be used for both the initial and final states. S.C.F.-L.C.A.O.-M.O. wave functions are found most convenient for the bound states and analytic expressions for these M.O.'s are derived for the case of Slater type A.O.'s, using prolate spheroidal co-ordinates. For the first attempt at calculations of the cross sections,

Flannery and Opik's final state model is chosen by analogy with Coulomb waves which are a first approximation for atomic calculations.

The first parts of Chapter 4 are concerned with the evaluation of the electronic matrix elements with the initial and final states of Chapters 2 and 3. In the final part, a calculation of the cross section using plane wave final states is presented for a $1\pi_g$ electron, this approach not being pursued in subsequent numerical work.

The results of the calculations for fixed nuclei reveal several interesting features. Each bound state orbital type has a characteristic cross section curve and this is explained. In the high energy behaviour of the cross sections for $1\pi_g$ and $3\sigma_g$ orbitals, we observe peaks which are interpreted as the basis of Cohen and Fano's "shoulder" effect. We also incorporate changes in the parameters for π M.O.'s and also in the amount of hybridization for σ M.O.'s and discuss their effects.

The inclusion of the vibrational eigenstates is considered necessary in the evaluation of the cross

sections near threshold and in Chapter 6 we develop formulae for the cross section using the Franck-Condon factor approximation. Comparison with experiment reveals that our approach is reliable for the $1\pi_g$, $1\pi_u$ and $3\sigma_g$ orbitals of N_2 and O_2 (if occupied). For the transitions to $O_2^+(a^4\Pi_u, A^2\Pi_u)$ an anomalous effect is found near threshold but for all $2\sigma_g$ and $2\sigma_u$ orbitals, the model meets with a radical failure which is discussed in detail. Before the total cross sections for N_2 and O_2 are discussed, we investigate the validity of the Franck-Condon factor approximation in the case of photo-ionization of the $1\pi_g$ electron (of zero kinetic energy) in O_2. We find the variation of the electronic transition moment with internuclear separation and reach the conclusion that the Franck-Condon factor approximation is valid to within a few percent.

In Chapter 7 we evaluate the electronic matrix elements for the 2π electron of nitric oxide. We find that much computational work can be avoided with an approximate approach which proves reliable near threshold.

Finally in Chapter 8, general conclusions are given with a discussion of possible methods for further work in this field.

STATEMENT

This thesis contains no material which has been accepted for the award of any other degree and to the best of my knowledge and belief, contains no material previously published or written by another person except where due reference is made in the text.

H. C. TUCKWELL

ACKNOWLEDGEMENTS.

The author would like to thank Professor C.A. Hurst for his supervision and encouragement throughout this work and also for his critical reading of the manuscript. Thanks are also due to Professor J.H. Carver and other members of the Adelaide University Physics Department for many useful discussions. In particular, Dr. A.J. Blake for providing cross sections for O_2 and N_2 prior to publication, Mr. J.L. Bahr for providing Franck-Condon factors for ionization to $O_2^+(^2\Sigma_g^-)$, and Mr. Vijay Kumar for providing experimental results for nitric oxide.

Further thanks are due to Dr. G.J. Iverson for valuable criticisms and help during the earlier stages of this work and also to Dr. Forrest R. Gilmore for providing spectroscopic constants and potential energy curve data for various states of N_2^+ and O_2^+. Finally it is a pleasure to acknowledge the untiring efforts of Miss N. Adams in her excellent typing of the manuscript.

CHAPTER 1.

INTRODUCTION.

1.1. INTERACTIONS OF PHOTONS WITH BOUND ELECTRONIC SYSTEMS.

A bound system of electrons in an atom may interact with photons in a variety of distinct ways. A photon of frequency $\nu_{nn'}$ can be spontaneously emitted when a transition occurs between two discrete levels of energies E_n and $E_{n'}$, where $\nu_{nn'} = (E_{n'} - E_n)/h$, or photon emission can be induced by an external radiation field. The presence of an external field may also give rise to absorption of a photon with a transition from a lower to a higher electronic state. If the incident radiation is of sufficiently short wavelength, the atom can absorb the photon and an electron may be ejected, in which case a transition to the continuum of positive energy states occurs. This phenomenon is called photo-ionization and the kinetic energy ε of the ejected electron is given by the Einstein relation.

$$\varepsilon = h\nu - E_i \qquad (1)$$

where ν is the frequency of the incident quanta and E_i is the ionization potential of the initial electronic state.

For a molecular system the above remarks also apply except that the bound states available then consist of a

series of vibrational and rotational eigenstates superimposed on the electronic states. Thus the spectra of molecules have many features not found in those of atoms. Further, the absorption of a photon can produce dissociation of a molecule into one or more of its atomic components so that the total absorption coefficient has this additional contribution. Thus photons of sufficient energy to produce ionization can also produce dissociation and experimentalists have the additional task of determining the relative contributions of photo-ionization and dissociation from the total measured absorbtion coefficients.

There is one other important process that incident photons can produce. The photon energy may be sufficient to promote an inner shell electron to a higher energy state i.e. a bound-bound transition may occur. The final state of this transition may be in the continuum relative to the ionization potential of a less negative stationary state. This enhances the probability of an electron spontaneously- or auto-ionizing. Thus the continuous absorption spectra of atoms may be characterized by a number of autoionization lines. For molecules the corresponding process is called pre-ionization.

1.2 TIME DEPENDENT PERTURBATION THEORY. FORMULAE FOR PHOTOIONIZATION CROSS SECTIONS.

The expression for the photoionization cross section for a bound system can be deduced by quantum electrodynamics[1,2] or by the method of time dependent perturbation theory[3,4]. In the latter approach the perturbation which ensures a finite probability for a transition from a bound state of negative energy eigenvalue to a state belonging to the continuum of positive energy states is the vector potential $\underline{A}(\underline{r},t)$ of the radiation field, providing $h\nu \geq E_i$. Letting the unperturbed Hamiltonian Ho have eigenstates according to the Schrodinger equation

$$H_o \psi_n = E_n \psi_n \qquad (1.2)$$

where $E_n (< 0)$ are the eigenvalues of the energy, and then considering the perturbed Hamiltonian $H = H_o + H'(t)$, we can write down the time dependent Schrodinger equation satisfied by the wave solutions ψ of the whole system,

$$i\hbar \frac{\partial \psi}{\partial t} = [H_o + H'(t)]\psi \qquad (1.3)$$

as an expansion in terms of the stationary states $\psi_n(t) = \psi_n e^{-iE_n t/\hbar}$ of the undisturbed system, with time dependent coefficients. Following the method and notation of Schiff[3] it can be readily shown that the differential cross section

for photo-ionization is,

$$\sigma_r(\theta_0,\phi_0) = \frac{e^2 k\, \omega_{kn} m}{6\pi c \hbar^2 \omega} \left| \int e^{-i\underline{k}\cdot\underline{r}}\, \underline{r}\, \psi_n \, d\tau \right|^2 \qquad (1.4)$$

where e = electronic charge, $k = p/\hbar$, $\omega_{kn} = (E_k - E_n)/\hbar$, ω = angular frequency of radiation, m = electronic mass. In deriving (1.4) the average has been taken over the polarization directions of the incident radiation. Two assumptions have been made, namely that the final states can be represented by momentum eigenstates $e^{i\underline{k}\cdot\underline{r}}$, and that the wavelength λ of the incident radiation is sufficiently greater than the dimensions of the atomic or molecular system involved in the process to render the approximation $e^{i\underline{K}\cdot\underline{r}} \sim 1$ a valid one, $\underline{K}$ being the propagation vector of the radiation. This latter approximation is known as the dipole approximation because it leads to the evaluation of the dipole length matrix elements $(e\underline{r})_{kn}$. Integration of (1.4) over all (θ_0, ϕ_0) yields a formula for the total cross section which is essentially that quoted by Bates[5],

$$\sigma(v) = \frac{32\pi^4 m^2 e^2}{3h^3 c} \sum_f (vv) \left| \int \bar{\psi}_n\, \underline{r}\, \psi_f \, d\tau \right|^2 \qquad (1.5)$$

where v is the velocity of the ejected photo-electron,

Ψ_f being the more general final state wave function. The formula derived in Quantum Electrodynamics[1] is usually written

$$\sigma(\nu) = \frac{8\pi^3 \nu e^2}{3c} \left| \int \bar{\Psi}_n \pm \Psi_f \, d\tau \right|^2 \qquad (1.6)$$

the different factors outside the matrix elements being due to the different normalization conditions. From equation (1.6) we obtain the formula which is most suitable for calculations;

$$\sigma(\varepsilon) = \frac{4\pi^2 \alpha a_0^2}{3} (E_i + \varepsilon) \sum_f \left| \int \bar{\Psi}_i \pm \Psi_f \, d\tau \right|^2 \qquad (1.7)$$

where α = fine structure constant, a_0 = Bohr radius and E_i, ε are both measured in units of I_H, the first ionization potential of atomic hydrogen $(= 13.595\ eV)$. Evaluating the constant factors in (1.7) gives the result

$$\sigma(\varepsilon) = 2.689 \times (E_i + \varepsilon) \times \times \sum_f \left| \int \bar{\Psi}_i \pm \Psi_f \, d\tau \right|^2 \times 10^{-18}\ cm^2. \qquad (1.8).$$

In formula (1.7) the normalization conditions for the bound states Ψ_i and the continuum states Ψ_f are respectively

$$\int \bar{\Psi}_i \Psi_i \, d\tau = 1 \qquad (1.9)$$

and

$$\int \bar{\psi}_f(\varepsilon'|\underline{r})\psi_f(\varepsilon|\underline{r})\,d\tau = \delta(\varepsilon-\varepsilon') \qquad (1.10)$$

The application of (1.9) to the various bound states appropriate to the problems to be treated in this work, will be discussed in Appendix 1; that of (1.10) will be discussed in Ch.3.

There are two other forms which the matrix elements in (1.6) may take. These are known as the dipole velocity and dipole acceleration forms and the usefulness of having these alternatives was pointed out by Chandrasekhar[6]. To derive the dipole velocity form we utilize the standard relations

$$(\underline{r})_{fi} = \int \bar{\psi}_f \underline{r}\,\psi_i\,d\tau = (im\omega_{fi})^{-1}(\underline{p})_{fi} \qquad (1.11)$$

and

$$\underline{p} \longrightarrow -i\hbar\,\underline{\nabla} \qquad (1.12)$$

whence the result follows,

$$(\underline{r})_{fi} = -\hbar\,(m\omega_{fi})^{-1}\int \bar{\psi}_f \underline{\nabla}\psi_i\,d\tau \qquad (1.13).$$

The dipole acceleration form follows by using the relations

$$E \longrightarrow i\hbar\frac{\partial}{\partial t} \qquad (1.14)$$

and

$$(\dot{\underline{p}})_{fi} = \int \bar{\psi}_f(-\underline{\nabla}V)\psi_i\,d\tau \qquad (1.15)$$

whereupon the final result is

$$(\underline{r})_{fi} = -(m\omega_{fi}^2)^{-1}\int \bar{\psi}_f\,\underline{\nabla}V\psi_i\,d\tau \qquad (1.16)$$

Considering the dipole acceleration form, it is clear that the quantity ∇V will become less appreciable at large distances from the bound system so this form relies most heavily on an accurate knowledge of ψ_i and ψ_f at small values of the radial co-ordinate r. Similarly, it can be argued that by virtue of the factor r, the dipole length form requires an accurate knowledge of the initial and final state wave functions at large values of r. The dipole velocity form, by virtue of the factor $\nabla\psi_i$ depends for its evaluation more on the values of ψ_i and ψ_f at intermediate values of r. Thus the choice of which of the three equivalent forms of the matrix elements to use for a photoionization calculation on a given system depends on the relative accuracies of one's knowledge of the state functions concerned at the various distances from the centre of mass. In our treatments of N_2 and O_2 we adopt the dipole length form of the matrix elements for reasons which will become apparent in Ch. 3, where the final state waves are presented and discussed.

1.3. MANY PARTICLE WAVE FUNCTIONS AND THE ONE ELECTRON APPROXIMATION.

In a full treatment of photo-ionization of an N - electron system, one should use an antisymmetric product wave function Ψ of the Slater determinant type, in accordance with the Pauli exclusion principle;

$$\Psi(\underline{r}_1, \underline{r}_2, \ldots \underline{r}_N) = (N!)^{-\frac{1}{2}} \begin{vmatrix} \psi_1(\underline{r}_1)\psi_1(\underline{r}_2) \ldots & \psi_1(\underline{r}_N) \\ \psi_2(\underline{r}_1)\psi_2(\underline{r}_2) \ldots & \psi_2(\underline{r}_N) \\ \vdots & \vdots \\ \psi_N(\underline{r}_1)\psi_N(\underline{r}_2) \ldots & \psi_N(\underline{r}_N) \end{vmatrix} \qquad (1.17)$$

where the ψ_i $(i = 1, 2, \ldots N)$ are one particle wave functions, appropriately normalized. If we denote the initial and final many particle state functions by Ψ_i and Ψ_f, then the appropriate dipole length matrix elements to evaluate are

$$M_{fi} = \int \cdots \int \bar{\Psi}_f(\underline{r}_1, \underline{r}_2, \ldots \underline{r}_N) \times \left[\sum_{\mu=1}^{N} \underline{r}_\mu \right] \Psi_i(\underline{r}_1, \underline{r}_2, \ldots \underline{r}_N)\, d\underline{r}_1 d\underline{r}_2 \ldots d\underline{r}_N \qquad (1.18).$$

We wish to show that this many-particle matrix element can be written as a one electron transition integral multiplied by a numerical distortion factor. To this end we write our initial state determinantal function as

$$\Psi_i(\underline{r}_1, \underline{r}_2, \ldots \underline{r}_N) = (N!)^{-\frac{1}{2}} \sum_P (-)^P \psi_1(\underline{r}_a)\psi_2(\underline{r}_b) \ldots \psi_i(\underline{r}_c) \ldots \psi_N(\underline{r}_d) \qquad (1.19)$$

and our final state function as

$$\Psi_f(\underline{r}_1, \underline{r}_2, \cdots \underline{r}_N) = (N!)^{-\frac{1}{2}} \sum_P (-)^P \phi_1(\underline{r}_a)\phi_2(\underline{r}_b)\cdots\phi_f(\underline{r}_c)\cdots\phi_N(\underline{r}_d) \qquad (1.20)$$

where $\sum_P$ a..b..c..d represents the sum over all permutations of 1,2,...N, $(-)^P$ is + 1 if a permutation is even and is - 1 if it is odd. Further, $\psi_1, \psi_2, \cdots \psi_N$ are the individual bound orbitals in the system before ionization; $\phi_1, \phi_2, \cdots \phi_N$ are the corresponding bound state orbitals in the final system, and generally ψ_j and $\phi_j\ (j \neq l)$ have the same set of quantum numbers (n, l, m_l, m_s). In (1.19) ψ_i is the bound state orbital which is not present in the final state and in (1.20), ϕ_f represents the one particle continuum wave function for the ejected electron. We notice that ψ_i and ϕ_f being eigenstates of the same hamiltonian of different energy eigenvalues, must be orthogonal, so that $\int \bar{\phi}_f \psi_i \, d\tau = 0$. Furthermore, we require that

$$\int \bar{\phi}_k \psi_l \, d\tau = d_l \delta_{kl}, (k \neq f, l \neq i) \qquad (1.21)$$

and this defines the factors d_l . We now use the notation of alternation, used by Roothaan[7], whereby the quantities in (1.17) are written $(N!)^{\frac{1}{2}} \psi_1^{[1} \psi_2^{2} \cdots \psi_N^{N]}$. Then from (1.18) we obtain

$$\underline{M}_{fi} = (N!) \int\cdots\int \overline{\phi_1^{[1} \phi_2^{2} \cdots \phi_f^{i} \cdots \phi_N^{N]}} \times \qquad (1.22)$$

$$\times \left[\sum_{\mu=1}^{N} \underline{r}_\mu\right] \psi_1^{[1} \psi_2^{2} \cdots \psi_i^{i} \cdots \psi_N^{N]} d\tau_1 \cdots d\tau_N$$

which, on invoking Roothaan's relation for an operator which acts symmetrically on all superscripts of an anti-symmetric product wave function, can be written

$$N!\int\cdots\int \overline{\phi_1(1)\phi_2(2)\ldots\phi_f(i)\ldots\phi_N(N)}\Big[\sum_{\mu=1}^{N} t_\mu\Big]\times$$
$$\times\ \psi_1^{[1}\psi_2^{2}\ldots\psi_i^{i}\ldots\psi_N^{N]}\,d\tau_1\ldots d\tau_N \qquad (1.23).$$

Using the relation of alternation to the determinantal wave function we obtain,

$$\underline{M}_{fi} = \int\cdots\int \overline{\phi_1(1)\phi_2(2)\ldots\phi_f(i)\cdots\phi_N(N)}\Big[\sum_{\mu=1}^{N} t_\mu\Big]\times$$
$$\times\ \sum_P (-)^P \psi_1(\alpha)\psi_2(\beta)\ldots\psi_i(\gamma)\ldots\psi_N(\delta)\,d\tau_1\ldots d\tau_N \qquad (1.24).$$

Let

$$\underline{M}_{fi} = \sum_{\mu=1}^{N} \underline{M}_{fi}^{\mu} \qquad (1.25)$$

where $\underline{M}_{fi}^{\mu}$ is the dipole length matrix element for the μ-th electron. Then

$$\underline{M}_{fi}^{\mu} = \sum_P (-)^P \int\cdots\int \overline{\phi_1(1)\phi_2(2)\ldots\phi_f(i)\ldots\phi_N(N)}\ \underline{t}_\mu\times$$
$$\times\ \psi_1(\alpha)\psi_2(\beta)\ldots\psi_i(\gamma)\ldots\psi_N(\delta)\,d\tau_1\ldots d\tau_N \qquad (1.26).$$

Suppose μ = i and further that $\{1\ 2..i..N\} \neq \{a\ b\ ..c..d\}$; then at least one electron is in orthogonal initial and final bound states.and all such terms vanish. Thus the only contribution is

$$\int\cdots\int \overline{\phi_1(1)\phi_2(2)\ldots\phi_f(i)\ldots\phi_N(N)}\ \underline{t}_i\,\psi_1(1)\psi_2(2)\ldots\psi_i(i)\ldots\psi_N(N)\,d\tau_1\ldots d\tau_N$$

$$= d_1 d_2 \ldots d_{i-1} d_{i+1} \ldots d_N \int \overline{\phi_f}(\underline{r}) \pm \psi_i(\underline{r}) d\underline{r} \qquad (1.27).$$

Consider now the case $\mu \neq i$. The result is then

$$\sum_P (-)^P \int \ldots \int \overline{\phi_1(1)\phi_2(2) \ldots \phi_f(i) \ldots \phi_N(N)} \underline{r}_j \times$$

$$\times \psi_1(a)\psi_2(b) \ldots \psi_i(c) \ldots \psi_N(N) d\tau_1 \ldots d\tau_N \qquad (1.28).$$

Then terms with $\{1\ 2..i..N\} \not\equiv \{a\ b..c..d\}$ vanish because at least one electron is in orthogonal initial and final bound states and that with $\{1\ 2..i..N\} \equiv \{a\ b..c..d\}$ also vanishes by the orthogonality of ψ_i and ϕ_f.

Thus we can write, from (1.27),

$$|\underline{M}_{fi}|^2 = D^2 \left| \int \overline{\phi_f} \pm \psi_i d\tau \right|^2 \qquad (1.29)$$

which is the required result. Providing the initial and final one-electron bound states are not very much different, each $d_\ell \simeq 1$ so that $D^2 \simeq 1$ and the cross section for the process can be found once the one-electron wave functions ϕ_f and ψ_i are known.

1.4. ATOMIC PHOTO-IONIZATION CROSS SECTIONS.

Since 1927 the quantum mechanical calculation of photo-ionization cross sections for many atoms and atomic ions have been performed by one or more methods. Surveys of the progress made at different times have been made by Bates[8], Ditchburn and Opik[9], and Marr[10]. The only system that can be treated exactly is atomic hydrogen where there exist analytic expressions for the bound state functions and the well known Coulomb scattered waves expanded (Messiah's notation[11]), thus

$$\psi_c = (kr)^{-1} \sum_{\ell=0}^{\infty} (2\ell+1)\, i^{\ell} e^{i\sigma_\ell} F_\ell(\gamma; kr) P_\ell(\cos\theta) \qquad (1.30)$$

for the continuum waves. Although the experimental result is only known at 850·6Å[12], the value lies precisely on the theoretical curve.[13] Furthermore, the calculations of the photo-ionization cross section of 1s electrons have not been restricted to non relativistic energies. See for instance the work of Erber[14] who employed exact Dirac wave functions for the bound and free states.

Turning our attention to systems which contain more than one bound electron, we recall that in section 1.3 it was indicated that in such cases sufficiently accurate calculations could be performed if reliable one electron wave functions could be found for the photo-electron's

initial and final states. The best first approximation, which has the advantage of an analytic formulation, is to use Slater type atomic orbitals[15,16] for the bound states and ordinary Coulomb scattered waves, as given by (1.30) for the final states. Such a calculation was performed by Bates[17] who wrote the bound state radial wave function as

$$R^{i}_{n,\ell}(r) = \sum_{t}\sum_{s} \alpha(s,t) r^{t} e^{-\alpha(s,t)r} \qquad (1.31)$$

and adjusted the values of the coefficients $\alpha(s,t)$ so that $R^{i}_{n,\ell}(r)$ was a good approximation to the corresponding function calculated by the Hartrees using the self consistent field method.[18] It can be seen that substituting (1.31) and (1.30) in (1.29) will give rise to contributing radial transition integrals whose form is

$$\int_{0}^{\infty} r^{l} e^{-qr} {}_1F_1(a,b;cr)\,dr \qquad (1.32).$$

An integral of this type yields an analytic result, due to Burhop[19]

$$\frac{p!}{q^{p+1}} {}_2F_1(a, p+1; b; c/q) \qquad (1.33)$$

where ${}_1F_1$ and ${}_2F_1$ are the confluent hypergeometric function and the hypergeometric function respectively. Generally, due to the dipole selection rule for the angular momentum quantum number

$$\Delta\ell = \pm 1 \qquad (1.34)$$

there are two final state waves which contribute. The exception of course is a bound s- state which gives rise only to p-continuum waves. The above method was applied by Bates[17] to the ions C^+, N^+, O^+, F^+, Ne^+, Na^+ and to neutral Be. This work supplemented his previous work[5] where the neutral atoms B,C,N,O,F,Ne had been treated but self consistent field radial bound state functions were employed and a continuum function calculated from the self consistent potential for the case of oxygen. It is interesting to compare the results obtained for the individual systems. For Be the cross section‡ diminishes rapidly from its value at the spectral head ($\epsilon = 0$) and the rate of decline decreases as Z (atomic number) increases until Z=7 (Nitrogen); for $Z > 7$ the cross section increases from threshold, the rate of increase itself increasing until Z=10 (Neon). The explanation of the differences in behaviour near threshold lies in the relative placement of the nodes of the continuum functions with respect to the regions where the bound state functions attain their maximum or minimum values. Such an explanation will not be enlarged upon here, the reader being referred to the relevant papers by Bates[5,8,17].

" ‡ " The term cross section will hereafter mean photo-ionization cross section unless stated otherwise.

Most attempts at reliable calculations on atomic systems have employed bound and free wave functions calculated by the self consistent field method, originally introduced by Hartree[20] and expounded in several texts[21,22] on atomic physics. In the calculations of atomic spectra, it is essential to find the bound wave functions; if this is done by the Hartree method then the resulting self consistent potentials can be used in the Schrodinger equation for the continuum eigenfunctions and hence the dipole length matrix elements can be calculated numerically. However, results obtained by such methods may not be accurate unless exchange effects are taken into account. This was made clear by the two sets of results of Bates and Massey[23], who found the cross sections for Ca and Ca^+ with and without the inclusion of exchange terms in the radial equations. The effect of exchange was to make the nodes of the free radial wave functions occur at smaller radial distances. Thus if the chances of cancellation in the transition integrals are high, then exchange can have a radical effect on the cross section versus energy curve. More recent work, when aimed at as accurate results as possible within the central field framework at non relativistic energies, has thus used the Hartree-Fock form of the wave equations which include the exchange integrals. See for instance the calculations of

Bates and Seaton[24] on C, N, O at the spectral head and those of Dalgarno et al[25] for O at energies from threshold to photon wavelengths of 25Å (and therefore including the photoejection of the inner shell electrons, except 1s).

Before discussing recent works which have aimed at treating a large number of atomic systems in an approximate fashion, we mention two other refinements in the wave functions used in special cases. These make allowance for the polarization of the core electrons and the non-separability of the core electron functions together with the inclusion of correlation terms in the bound states. Only one calculation including each of these is known to the author.

Bates[26] included in the wave equation for the continuum functions for potassium an attractive potential

$$V_\rho(r) = -\tfrac{1}{2}\left(\rho/(r^2+\rho^2)^2\right) \qquad (1.35)$$

where ρ is the polarizability (in cm^3), and ρ is the core radius. This potential represents the influence of the electric dipole induced in the core by the ejected electron on the force field in which the latter moves. As mentioned above, inclusion of exchange terms tends to pull in the continuum functions so in a sense including the potential (1.35) compensates for the neglect of exchange.

Values of P for atoms and their ions can be obtained theoretically and experimentally by many methods, as indicated in the comprehensive work of Dalgarno[27], and previously by Buckingham[28]. However, because the experimental curve for the potassium cross section showed a distinct minimum near threshold[29] indicating that cancellation effects would be so important that small errors in either the initial or final state functions could lead to drastic changes in the results, Bates chose to treat P as a parameter. The effects of varying P from 0 to $2 \times 10^{-24} cm^3$ were investigated and the value at which theory best agreed with experiment was found to be $1{\cdot}6 \times 10^{-24} cm^3$. That this was higher than the independent result of Buckingham was attributed to the neglect of exchange.

Turning to Tait's calculation[30] on the 2s electron of lithium we see the only attempt to take account of electron correlation. For the initial state the wave function of James and Coolidge[31], a 17 term function depending on r_1, r_2, and r_3 and also the inter-electron distances r_{12} etc, was used. For the final state the ion + free electron functions were written

$$\Psi(\underline{r}_1, \underline{r}_2, \underline{r}_3) = \qquad (1.36)$$
$$3^{-\frac{1}{2}}\left[\psi_i(\underline{r}_1,\underline{r}_2)\psi_k(\underline{r}_3) + \psi_i(\underline{r}_2,\underline{r}_3)\psi_k(\underline{r}_1) - \psi_i(\underline{r}_1,\underline{r}_3)\psi_k(\underline{r}_2)\right]$$

where ψ_i is the core function and ψ_k is that of the free electron, so that the separability of the core electron functions is not assumed. No electron correlation terms r_{ij} are included in (1.36).

Celtman[32] had found such terms made a negligible difference to the cross section of H^-, and correlation effects should be even less important in the more compact Li atom. Tait used both the dipole length and dipole velocity forms of the matrix elements (cf. section 1.3) and found that the length calculations gave better agreement with the experimental cross sections of Marr[33], indicating that the wave functions employed were less accurate at intermediate values of r.

Two facts that have probably become apparent by now are that in seeking an accurate determination of the cross section curve for a given system, there is a large amount of computational labour involved and that each system presents its own special difficulties. Furthermore, it is almost too great a task to work in a completely rigorous framework and include all possible refinements in the wave functions, a summary of which is given at the end of this section. Owing to

this state of affairs some theorists have aimed at less accuracy and sought application to a greater number of systems. Such are the methods of Cooper[34] and Burgess and Seaton[35], whose work will now be briefly described before we discuss the less investigated field of molecular calculations.

Cooper has calculated cross section curves for He, Ne, Ar, Kr, Na, Cu^+ and Ag^+. The "unrelaxed ionic core" assumption was made so that the distortion factor D in (1.29) was assumed equal to unity. Further, the radial transition integrals

$$R_{\ell\pm1} = \int_0^\infty P_{n\ell}(r)\, r\, P_{\varepsilon,\ell\pm1}(r)\, dr \qquad (1.37)$$

were evaluated by using bound orbitals $P_{n\ell}$ satisfying the radial Hartree-Fock equation.

$$\left[\frac{d^2}{dr^2} + G_{n\ell}(r) + \varepsilon_{n\ell} - \frac{\ell(\ell+1)}{r^2}\right] P_{n\ell} = X_{n\ell} \qquad (1.38)$$

where $G_{n\ell}$ is the potential and $X_{n\ell}$ represents the exchange terms, with continuum orbitals satisfying the same radial equation but with $\varepsilon_{n\ell}$ replaced by ε, the positive energy of the free electron. The results were in fair agreement with experiment but somewhat surprising was the agreement to within 10% of the length, velocity and acceleration

results, for He, Ne, Cu^+. However, the bound state functions have no nodes and hence, at relatively low electron energies, there is no strong cancellation in the transition integrals. This however, is in contrast with the apparently more accurate above mentioned calculations of Tait[30] on lithium, where the length and velocity results differed by a factor of almost 2. Burgess and Seaton used the quantum defect method (QDM) to calculate cross sections for He, Li, Na, Mg^+, Si^+, K, Ca^+, O, O^+, O^{++} and O^{+++} for transitions involving s, p and d electrons. QDM is based on the ideas of Bates and Damgaard[36] for calculations on bound-bound transition probabilities. The major contributions to transition integrals $\int R_i r^3 R_f dr$, which arise in the dipole length form for oscillator strengths may come from large values of r. At such values the accurate Hartree-Fock potential reaches its asymptotic form $\sim 2Z/r$ and the radial wave functions for positive energy have reached their asymptotic form which can be written

$$P_\varepsilon(r) \underset{r\to\infty}{\sim} \sin\left(kr - \tfrac{1}{2}\ell\pi + \gamma \ln 2kr + \arg\Gamma(1+i\gamma) + \delta(\varepsilon)\right) \quad (1.39).$$

where $\delta(\varepsilon)$ is the phase shift with respect to ordinary Coulomb waves. Following Seaton[37] the effective

quantum number $\nu_{n\ell}$ of an energy level $T_{n\ell}$ is defined by

$$T_{n\ell} = RZ^2/\nu_{n\ell}^2 \qquad (1.40)$$

where R is the Rydberg constant, Z = the residual charge on the ion after the removal of the electron. Comparing this with the energy level of the corresponding hydrogenic system leads to the natural definition of the quantum defect

$$\mu_{n\ell} = n - \nu_{n\ell} \qquad (1.41) .$$

As n increases for a given ℓ, the energy levels of a given series become closer spaced until at $n = \infty$ the spectral head is attained. It had been shown previously by Seaton[38] that at such an energy the phase shift $\delta(0)$ was given by $\pi\mu_{\infty\ell}$. In general $\delta(\varepsilon) = \pi\mu(\varepsilon)$ and the values of the quantum defects are obtained by extrapolating from known values of $\mu_{n\ell}$ for discrete levels. With this technique for finding the asymptotic form for the continuum functions, Burgess and Seaton derived general formulae for the cross sections but these are too lengthy to be displayed here. In general, the results compare favourably with those obtained with Hartree-Fock wave functions but in cases where comparison with experiment is possible, the results are as often as not in disagreement with measured values.

The discussion in this section of calculations of atomic cross sections has served a useful purpose, we hope, in that knowledge of the difficulties and relative importances of the different approximations used may help in estimating the important factors in calculations on molecular cross sections. We now give a list of the factors which may or may not be important in a particular calculation, most of which have already been discussed in some detail.

(1) Relativistic effects - negligible at low energies.

(11) Separability of the many electron wave functions into products of one electron functions. Probably not a significant source of error.

(111) Electron correlation - may be large near threshold, especially for loosely bound electrons.

(1V) Exchange - may be large near threshold, especially in heavier systems.

(V) Dipole approximation - should be valid for photon wavelengths $> \sim 25\text{Å}$.

(V1) Core distortion - possible error $\sim$ 10%.

(V11) Polarizability of the core - may be very important for sensitive cases e.g. K.

(V111) Configuration interaction - not yet investigated - only important for non closed shells.

(1X) Transitions to <u>excited states</u> of the ion - not investigated. Could be appreciable.

(X) <u>Auto-ionization</u> - can be very important at and near specific energies.

Finally, it is worth pointing out that the published method and results of Herman and Skillman[39] on calculations of potential functions and normalized radial waves for atoms by the Hartree-Fock-Slater method should make it possible to estimate, fairly reliably, by a method such as that of Cooper[34] the cross section for any known atomic system.

1.5. PREVIOUS WORK ON MOLECULES.

Cross sections for molecular systems have not enjoyed the same attention as atoms and their ions. This is surprising if one realizes the importance of absorption by molecules, chiefly N_2 and O_2, in upper atmosphere studies, and of gases such as NO, which is used in ion chambers for rocket experiments on absorption of solar radiation by O_2 so that the gas density as a function of altitude can be found. There have been many laboratory studies of absorption by the above gases (see Ch. 6) as well as certain polyatomic molecules such as NH_3, H_2O, and CH_4. The discrepancy between the advances of the theoretical and experimental studies is due to the difficulty at present in finding suitable one electron wave functions for bound and free molecular orbitals in all cases except the H_2^+ ion. The first system studied in detail was thus H_2^+ as reported by Bates et al[40]. The bound state functions for this system had been given by Bates et al[41] in an earlier paper where the Schrodinger equation for the electronic motion was solved in prolate spheroidal co-ordinates. Writing the total wave function as

$$\Psi(\lambda,\mu,\phi) = \Lambda(\lambda) M(\mu) \Phi(\phi) \qquad (1.42)$$

with $\lambda = (r_1 + r_2)/R$, $\mu = (r_1 - r_2)/R$, ϕ = azimuthal angle where r_1 and r_2 are the distances of the electron from the protons and R is the inter-proton distance, the solutions for M and Φ can be obtained (see Ch. 3) analytically. The bound state "radial"‡ functions can be written in the form (1.43)

$$\Lambda(\lambda) = (\lambda^2-1)^{m/2}(\lambda+1)^{\sigma} e^{-p\lambda} y(\lambda) \qquad (1.44)$$

after Jaffe[42]. For the continuum waves M and Φ can again be written down but the radial functions must be obtained numerically. (See Ch. 3). Bates et al[40] studied in detail the cross section for the process in which R is fixed at $2a_0$ while the energy of the electron, ε, varies, and they also considered the effects of different values of R for the case $\varepsilon = 0$. In these cases the dipole length matrix elements were regarded as functions of ε only and not of the interproton distance. Transitions from the $1s\sigma_g$, $2s\sigma_g$ and $3s\sigma_g$ states were studied and in all cases the $p\pi_u$ final state waves gave the greatest contributions, with appreciable cross sections for transitions to $p\sigma_u$ states only if R is appreciably greater or less than $2a_0$.

---

‡ In future, we will refer to functions of λ in prolate spheroidal co-ordinates as "radial" functions, without the use of inverted commas.

The calculations were extended to include the vibrational and rotational eigenfunctions and hence necessitated the evaluation of the electronic matrix elements as functions of R. The final state vibrational wave functions were approximated by δ - functions (this method being due to Winans and Stueckelberg[43]; see Herzberg[44] for further discussion) and transitions were considered from the zeroth vibrational level and the rotational levels J = 0, 4, 8. The cross section for a given J is small near threshold and rises to a maximum near photon wave numbers of $2{\cdot}5 \times 10^5 cm^{-1}$, after which it decreases steadily as the energy increases. It will be seen in Ch. 5, that this behaviour is characteristic for bound state molecular orbitals of the $s\sigma_g$ type. Furthermore, the different values of J in the initial state give rise to only minor differences in the magnitudes of the cross section at a given photon energy.

Dalgarno[45] had treated the case of CH_4 by approximate methods. The calculation was essentially reduced to an atomic one because it was assumed that the motion of the electrons and protons of the H atoms in the tetrahedral CH_4 structure could be averaged to give a central potential,

with the occupation of electronic subshells $(1s)^2$, $(2s)^2$, $(2p)^6$. The effect of the 4 protons (from the H atoms) on the self consistent field wave functions had been found previously by Buckingham et al[46]. The value obtained for the cross section at the spectral head, is about twice the experimental value reported by Metzger and Cook[47] and Ditchburn[48], assuming an ionization efficiency of 100%.

Two distinct calculations for H_2 have appeared, one by Shimizu[49] and more recently by Flannery and Opik[50]. Shimizu determined the ratio of concentrations of H^+ and H_2^+, produced by photon bombardment, as a function of the mixing parameter λ in the synthesis of the $^1\Sigma_g^+$ state written as $\sigma_g^2 + \lambda\sigma_u^2$, where σ_g and σ_u are obtained as linear combinations of 1s atomic orbitals. For the final states, momentum eigenfunctions $e^{i\underline{k}.\underline{r}}$ were used and compared with waves scattered from two half elementary positive charges separated by a distance $\underline{R}$. It was found that the Born approximation should be valid at photon wavelengths $< 20\text{Å}$. No magnitudes for the cross section were obtained however, but interesting results were given for the dependence of the relative yields of H^+ and H_2^+ on the parameter λ.

In contrast with the earlier calculation, that of Flannery and Opik, was concerned with the near threshold values of the cross section. The same bound state functions, i.e. those of Weinbaum,[51] were employed. Results from threshold to photon wavelengths of about 640Å

were found for the case of fixed nuclei, using final state waves appropriate to an electron moving in the field of two half elementary positive charges placed at such a separation that the quadrupole moment of the system ($\frac{1}{2}qR^2$, with $q = \frac{1}{2}e$) was the same as that of the H_2^+ ion, which had been previously given by Bates and Poots[52]. Quantum defects (see Section 1.4) were estimated for several excited states of H_2 but these were not employed in the determination of the final state radial wave functions. The results were in very good agreement with the experimental results of Wainfain[53] and Cook and Metzger[54] over the range of energies considered. The initial state rotational quantum numbers J = 0 and J = 6 were used but again the effects of including rotational eigenfunctions are small. Furthermore, at a photon wavelength of 700Å, the relative transition probabilities for different vibrational quantum numbers of the final state were found with an assumed zeroth level initial state (V = 0). For the V = 0 vibrational state of H_2 a series of harmonic oscillator wave functions was used whereas for the vibrational states of H_2^+ the Schrodinger equation for the eigenfunctions was solved numerically with the previously determined potential energy function of Bates et al[41]. The results show a widespread distribution over the final vibrational states as is expected when the initial and

final electronic states have greatly differing equilibrium internuclear separations (see Ch. 6 for a detailed explanation).

To complete our resume of calculations on molecules, we have yet to discuss the threshold dependence of the cross sections and the relatively high energy phenomenon of "shoulders". The first topic was studied by Geltman[55], chiefly for the photodetachment of negative diatomic molecular ions. This process is similar to photo-ionization except that the products are a free electron and a neutral molecule. The validity of Geltman's assumption that the energy dependence of the photodetachment cross section is contained entirely in the quantity $\nu k \left|\int \bar{U}_k \, r U_0 \, d\tau\right|^2$ can be questioned on the following grounds. A photo-detachment process involves a transition from some initial molecular ion state for whose complete description in the Born-Oppenheimer approximation[56] one needs a knowledge of the 3 eigenfunctions; electronic, vibrational and rotational. To accurately evaluate the transition probability to even a single final vibrational state, one must include the dependence of the transition integrand on the internuclear separation and the photo-electron's co-ordinates.

The integrations can be carried out by regarding the electronic matrix element as a function of R and then performing the integration over the latter variable. An easier treatment is to separate the R and $\underline{r}$ integrations altogether. In this case only vibrational overlap integrals need be determined and these multiply the above quantity involving the electronic matrix elements for each possible combination of initial and final vibrational states. These points will be enlarged upon in Ch. 6 where similar problems arise in the case of photo-ionization of N_2 and O_2. Geltman's remarks are thus only approximately true but his results for photodetachment are nevertheless interesting in that they indicate how the cross section might depend on the initial state's component of angular momentum along the internuclear axis and, in the case of homonuclear diatomic molecules on the symmetry type .

Furthermore, Geltman has claimed that for photo-ionization of neutral diatomic molecules, the threshold dependence of the cross section should be of the form $\nu(1-e^{-2\pi/k})^{-1}(1+a_1k^2+a_2k^4+\dots)$ where ν = frequency of radiation and k = p/h, independent of the initial molecular orbital or the type of molecule. This prediction can be immediately seen to be false if one considers the

expression for the cross section; the latter quantity's dependence on the energy is clearly different for different types of initial orbital because these will have different radial functions. As the energy increases, the cross section may fall or rise or remain almost steady with respect to its value at the spectral head according to the cases of diminishing, increasing or steady transition integrals. This point too will become clearer in Ch. 5 where the results for different bound state molecular orbitals in N_2 and O_2 will be discussed.

The last topic in this section, that of the shoulders or bumps in the experimental absorption cross sections of N_2 and O_2 as found by Samson and Cairns[57] at photon wavelengths of around 200Å, was first investigated theoretically by Cohen and Fano[58]. They regarded the atoms of diatomic molecules as independent absorbers of light and argued that scattered electron waves from each centre should produce interference effects. Thus the undulations in the cross sections were explained qualitatively on the basis of the resulting modulation factor for the net intensity from the two sources. It was also suggested on a quantum mechanical basis that since the selection rule for atoms is no longer valid for an axially symmetric field,

but rather Δl can take any odd value, the transition probabilities for successively higher l final state waves should increase with increasing energy. Further, an estimate of the photo-electron energy k^2 at which cross sections for a given l should become important is obtained from

$$k^2 + 2Z/r - l(l+1)/r^2 = 0 \qquad (1.45)$$

where Z is the effective charge on the ion. To investigate tentatively their hypotheses Cohen and Fano made an approximate calculation for a $1s\sigma_g$ state of H_2^+ using a free spherical wave ($\underline{r}$ | k l m) for the calculation of the dipole length matrix elements. With somewhat crude arguments they deduced an expression for the total cross section

$$\sigma(k) = \sum_l \sigma_l = \sigma_H \left[1 + \sin kR/(kR)\right]/(1+S) \qquad (1.46)$$

where σ_H is the cross section for a hydrogen like atom, and S = ·46.

Thus the total cross section has the modulation factor 1 + s in k R/(kR) but because $\sigma_H(k)$ is a rapidly decreasing function, the total cross section should only show undulations of a small magnitude.

In response to Cohen and Fano's work, Bates and Opik[59] have extended their cross sections for H_2^+ to electron energies of 16 rydbergs. The results for the total cross section decline steadily with no trace of a shoulder effect at high energies. The partial cross sections for $f\sigma$ and $f\pi$ continuum waves do however grow from threshold to 1·44 rydbergs whereupon they also steadily diminish. The effects of the maxima in these partial cross sections are nevertheless masked in the overall cross section, because of the dominance of the steadily decreasing contributions from the $p\sigma$ and $p\pi$ continuum waves. We will see in Ch. 5 that the shoulder effect is noticeable in the computed cross sections for $3\sigma_g$ and $1\pi_g$ (or $1\bar{\pi}_g$) orbitals.

Finally, we note that Bates and Opik[59] have also investigated the cross section for a model complex molecule, for which they used the same final state waves as for H_2^+ and initial bound state $3s\sigma_g$ functions appropriate for a single electron moving in the field of two nuclei separated by $R = 2a_0$ and each carrying a charge +2e. The results obtained show no discernible shoulder effect due to higher angular momentum states but a slight bump near threshold as certain electronic matrix elements pass through zero when cancellation in the transition integrals is complete.

CHAPTER 2.

ELECTRONIC STATES OF N_2, N_2^+, O_2, O_2^+

2.1. ELECTRONIC TERMS.

In the Born-Oppenheimer approximation the total wave function for a molecule is separated into the 3 components which describe the electronic motion, and the vibrational and rotational motions, thus

$$\Psi(\underline{r},\underline{R}) = \psi_{elect.}(\underline{r},\underline{R})\,\psi_{vib.}(R)\,\psi_{rot.}(\Theta,\Phi) \qquad (2.1)$$

$\psi_{vib.}$ and $\psi_{rot.}$ can be regarded as functions of the nuclear co-ordinates $\underline{R}(R,\Theta,\Phi)$ only, because of the smallness of the ratio of the electronic to the nuclear mass. $\psi_{elect}(\underline{r},\underline{R})$ can be regarded as depending only parametrically on $\underline{R}$. These topics are discussed in greater detail in Ch. 6 where the rotational and vibrational eigenstates are taken into account in the calculation of the cross sections. This section is meant only to define the spectroscopic notation for the electronic states, further details of which can be found in reference 44.

In atoms the (assumed) spherically symmetric potential renders the angular momentum quantum number ℓ a "good" quantum number but for diatomic molecules there

is only axial symmetry about the internuclear axis, so that only the component of angular momentum along this axis has an associated quantum number. Denoting this quantum number by λ , the electronic states are called $\Sigma, \Pi, \Delta,$ etc as $|\lambda| = 0, 1, 2, \ldots$. Further, there is 2 fold degeneracy when $|\lambda| \neq 0$. To further identify the electronic state the multiplicity 2S+1 is used, S being the total spin quantum number, and this is attached as a left superscript e.g. ${}^3\Sigma , {}^2\Pi, \ldots$. The symmetry of the state under inversion in the mid point between the nuclei is usually attached as a right subscript which will be either g or u corresponding to total wave functions which are even or odd under inversion. It is worth noting that inversion in the prolate co-ordinates defined in equation (1.43) is equivalent to the transformations

$$\lambda \rightarrow \lambda , \mu \rightarrow -\mu , \phi \rightarrow \phi + \pi . \qquad (2.2).$$

Σ states are also distinguished by their properties under reflection in a plane containing the nuclei. Thus Σ^+ states are even under such a reflection whereas Σ^- states are odd. Finally lower and upper case letters are used for convenience to identify states of different energies. X denotes the ground state, A, B, C are used for higher states of same multiplicity.

For N_2 and O_2 the ground electronic states are $X^1\Sigma_g^+$

and $X^3\Sigma_g^-$ respectively. If we use "+" and "-" to represent the 2 spin states for a molecular orbital, then the electronic configurations of these states are given in Table 2.1.

TABLE 2.1

ELECTRONIC CONFIGURATIONS OF THE GROUND STATES.

STATE ↓	ORBITAL								
	$1\sigma_g$	$1\sigma_u$	$2\sigma_g$	$2\sigma_u$	$3\sigma_g$	$1\pi_u$	$1\bar{\pi}_u$	$1\pi_g$	$1\bar{\pi}_g$
$N_2(X^1\Sigma_g^+)$	+ −	+ −	+ −	+ −	+ −	+ −	+ −		
$O_2(X^3\Sigma_g^-)$	+ −	+ −	+ −	+ −	+ −	+ −	+ −	+	+

In the above table $1\sigma_g$, $2\sigma_u$.. etc. represent one electron spatial wave functions, usually called molecular orbitals (M.O.), and these together with the spin functions are molecular spin orbitals (M.S.O.). We will now see how the initial state wave functions for a given photo-ionization process in N_2 and O_2 can be found from the above electronic configurations.

2.2. S.C.F. - L.C.A.O. - MOLECULAR ORBITALS.

The starting point for self consistent field (S.C.F.) wave functions for the electronic states of molecules is the determinantal expression (1.17). Each ψ_i then represents a one-electron M.S.O. The individual M.S.O's are assumed to form an orthonormal set and the total wave function satisfies the normalization condition (1.9). Roothaan[7] has developed the theory of two approaches to the problem of determining the best M.O.'s. The better but more difficult method results in the Hartree-Fock M.O.'s while that which is more amenable to computational work finds the best L.C.A.O. - M.O.'s (Linear Combination of atomic orbitals). In the L.C.A.O. method an orthonormal set of atomic orbitals χ_ρ is used to construct the ψ_i

$$\psi_i = \sum_\rho \chi_\rho C_{\rho i} \tag{2.3}$$

where the $C_{\rho i}$ are the L.C.A.O. coefficients. Starting with (2.3) and (1.17), one asks for the sets of $C_{\rho i}$ which minimize the electronic energy

$$E = \int \bar{\Psi} \mathcal{H} \Psi \, d\tau \tag{2.4}$$

where $\mathcal{H}$ is the total hamiltonian operator

$$\mathcal{H} = \sum_\mu H^\mu + \tfrac{1}{2} e^2 \sum_{\mu \neq \nu} \frac{1}{r_{\mu\nu}} \tag{2.5}$$

where the H^μ is the hamiltonian operator for the μ-th electron consisting of its kinetic energy and potential

energy due to the nuclei only. After setting up the variational equations for $\delta E = 0$, the task remains, having chosen the atomic orbitals, to solve the secular equation

$$Det(F - \underline{\varepsilon} S) = 0 \qquad (2.6)$$

where S is the matrix whose elements are defined by

$$(S)_{pq} = \int \bar{\chi}_p \chi_q d\tau \qquad (2.7)$$

and for F

$$(F)_{pq} = \int \bar{\chi}_p F_{op.} \chi_q d\tau \qquad (2.8)$$

where $F_{op.}$ is the Hartree-Fock hamiltonian operator. The eigenvalues ε_i and the corresponding set of C_{pi} give the energies of the different orbitals and the optimum L.C.A.O. coefficients.

Roothaan's treatment of the L.C.A.O. method for closed shell systems was extended to electronic configurations with open shells by Pople and Nesbet[60]. Many calculations of S.C.F. - L.C.A.O. - M.O.'s for different molecules have since appeared in the literature. Those of special interest here are those of Scherr[61] on N_2 and in particular those of Sahni and Lorenzo[62] who treated several electronic states of N_2, N_2^+, O_2 and O_2^+.

The formulation of a given M.O. is in terms of a basic set of <u>primitive symmetry M.O.'s</u>. Those needed in the

present cases have been given by Scherr:

$$\sigma_g 1s = 2^{-\frac{1}{2}}(1s_a + 1s_b) \qquad \sigma_u 1s = 2^{-\frac{1}{2}}(1s_a - 1s_b) \tag{2.9}$$

$$\sigma_g 2s = 2^{-\frac{1}{2}}(2s_a + 2s_b) \qquad \sigma_u 2s = 2^{-\frac{1}{2}}(2s_a - 2s_b) \tag{2.10}$$

$$\sigma_g 2p_z = 2^{-\frac{1}{2}}(2p_{za} + 2p_{zb}) \qquad \sigma_u 2p_z = 2^{-\frac{1}{2}}(2p_{za} - 2p_{zb}) \tag{2.11}$$

$$\pi_g 2p_x = 2^{-\frac{1}{2}}(2p_{xa} - 2p_{xb}) \qquad \pi_u 2p_x = 2^{-\frac{1}{2}}(2p_{xa} + 2p_{xb}) \tag{2.12}$$

$$\pi_g 2p_y = 2^{-\frac{1}{2}}(2p_{ya} - 2p_{yb}) \qquad \pi_u 2p_y = 2^{-\frac{1}{2}}(2p_{ya} + 2p_{yb}) \tag{2.13}$$

where $1s_a$ represents a 1s atomic orbital on centre a etc. and the axes Z_a and Z_b lie along the internuclear axis and have their positive directions towards one another.

The normalized orbitals used are of the real Slater type:

$$1s = (\zeta_1^3/\pi)^{\frac{1}{2}} e^{-\zeta_1 r} \tag{2.14}$$

$$2s^* = (\zeta_2^5/3\pi)^{\frac{1}{2}} r e^{-\zeta_2 r} \tag{2.15}$$

$$2p \begin{Bmatrix} x \\ y \\ z \end{Bmatrix} = (\zeta_2^5/\pi)^{\frac{1}{2}} r e^{-\zeta_2 r} \begin{Bmatrix} \sin\theta\cos\phi \\ \sin\theta\sin\phi \\ \cos\theta \end{Bmatrix} \tag{2.16}$$

except that the $2s^*$ orbital is usually replaced by a 2s function which is orthogonal and has a node:

$$2S = (1 - S_1^2)^{-\frac{1}{2}} [2s^* - S_1 1s] \qquad (2.17)$$

where $S_1 = (1s|2s^*)$ is the monon~~u~~clear overlap integral which can easily be shown to be

$$(1s|2s^*) = 2^4 \zeta_1^{\frac{3}{2}} \zeta_2^{\frac{3}{2}} (\zeta_1\zeta_2/3)^{\frac{1}{2}}/(\zeta_1 + \zeta_2)^4 \qquad (2.18).$$

The values of the orbital exponents ζ_1 and ζ_2 obtained from Slater's rules[15] are $\zeta_1 = 7{\cdot}7$, $\zeta_2 = 2{\cdot}275$ for O and $\zeta_1 = 6{\cdot}7$, $\zeta_2 = 1{\cdot}95$ for N.

From the primitive M.O.'s defined in (2.9)-(2.13) the wave function for a given M.O. is constructed by (2.3) with the restriction that each primitive so used has the same symmetry. Complete mixing within an L.C.A.O. - M.O. class is allowed so that, for example, the $3\sigma_g$ M.O. consists of a combination of $1S\sigma_g$, $2S\sigma_g$ and $2p_z\sigma_g$ primitive orbitals.

For closed shell structures such as N_2, the spatial parts of the M.S.O.'s for a given M.O. are the same and there is a 2-fold degeneracy in the energy eigenvalues for such states. For an open shell structure such as O_2 there is no such degeneracy and in general the M.S.O.'s for a given M.O. type have different spatial wave functions (except for the case of an M.O. containing only one kind of primitive

M.O. in which case the spatial function is completely determined by the normalization condition to unit total probability density, whether or not the system is the closed or open shell type). Sahni and Lorenzo performed two sets of calculations for O_2 ($X^3\Sigma_g^-$). In their restricted treatment the spatial parts of the M.S.O. pairs for a given M.O. were identical, whereas in their spin polarized treatment 2 sets of secular equations were solved, one for each spin set. We have chosen to use the results of their restricted treatment and this choice has one notable consequence. The electronic matrix elements in (1.29) for two M.S.O.'s of the same shell are then the same at a given kinetic energy of the ejected electron. For transitions involving such M.S.O.'s the only difference in the partial cross section curves will then be due to the difference in ionization energies between the 2 processes. Since such differences are only of the order of a few eV, and the ionization potentials are of order 12-40eV, the partial cross section curves will differ only slightly (see Ch.5).

In our calculations we have adopted the L.C.A.O. - M.O.'s of Sahni and Lorenzo as the one electron initial state wave functions. The coefficients of (2.3.) which result from the solution of (2.6) are thus basic input data for our

computations and are displayed in Table 2.2.

TABLE 2.2.

A. L.C.A.O.-M.O.'s FOR O_2 ($X^3\Sigma_g^-$) FROM THE RESTRICTED TREATMENT.(62)

M.O	L.C.A.O.			‡ ε_i^+	ε_i^-
$1\sigma_g$	$+0.9996(\sigma_g 1s)$	$+0.0127(\sigma_g 2s)$	$+0.0002(\sigma_g 2p_z)$	-20.6305	-20.5997
$2\sigma_g$	$-0.0410(\sigma_g 1s)$	$+0.8054(\sigma_g 2s)$	$+0.2153(\sigma_g 2p_z)$	-1.5986	-1.4750
$3\sigma_g$	$+0.0206(\sigma_g 1s)$	$+0.4232(\sigma_g 2s)$	$-0.8749(\sigma_g 2p_z)$	-0.5965	-0.5259
$1\sigma_u$	$+1.0006(\sigma_u 1s)$	$+0.0204(\sigma_u 2s)$	$+0.0065(\sigma_u 2p_z)$	-20.6311	-20.5994
$2\sigma_u$	$+0.0033(\sigma_u 1s)$	$+1.0798(\sigma_u 2s)$	$-0.2010(\sigma_u 2p_z)$	-1.0820	-0.8862
$1\pi_u$	$+0.9340(\pi_u x)$			-0.6965	-0.4227
$1\pi_g$	$+1.0824(\pi_g x)$			-0.3969	
$1\bar{\pi}_u$	$+0.9340(\pi_u y)$			-0.6965	-.4227
$1\bar{\pi}_g$	$+1.0824(\pi_g y)$			-0.3969	

‡ In units of I_H.

B. L.C.A.O.-M.O.'s FOR N_2 ($X^1\Sigma_g^+$).[62]

M.O.	L.C.A.O.			ε_i
$1\sigma_g$	$+0.9990(\sigma_g 1s)$	$+0.0116(\sigma_g 2s)$	$+0.0026(\sigma_g 2p_z)$	-15.7219
$2\sigma_g$	$-0.0815(\sigma_g 1s)$	$+0.6723(\sigma_g 2s)$	$+0.3391(\sigma_g 2p_z)$	-1.4527
$3\sigma_g$	$-0.0430(\sigma_g 1s)$	$-0.5589(\sigma_g 2s)$	$+0.8531(\sigma_g 2p_z)$	-0.5446
$1\sigma_u$	$+1.0025(\sigma_u 1s)$	$+0.0272(\sigma_u 2s)$	$+0.0121(\sigma_u 2p_z)$	-15.7197
$2\sigma_u$	$-0.0106(\sigma_u 1s)$	$-1.0207(\sigma_u 2s)$	$+0.3759(\sigma_u 2p_z)$	-0.7306
$1\pi_u$	$+0.8831(\pi_u x)$			-0.5797
$1\bar{\pi}_u$	$+0.8831(\pi_u y)$			-0.5797

2.3 PHOTO-IONIZATION PROCESSES FROM O_2 $(X^3\Sigma_g^-)$ AND N_2 $(X^1\Sigma_g^+)$ FOR FIXED NUCLEI.

Ionization potentials for molecular or atomic systems can be found by electron impact or photon bombardment experiments. At incident particle energies of 12·08 eV and 15·6 eV for O_2 $(X^3\Sigma_g^-)$ and N_2 $(X^1\Sigma_g^+)$ respectively the most loosely bound electrons, which occupy the $1\pi_g$ (or $1\bar{\pi}_g$) and $1\pi_u$ (or $1\bar{\pi}_u$) orbitals, may be ejected according to the general scheme

$$M_2 + h\nu \longrightarrow M_2^+ + \bar{e} \qquad (2.19).$$

The thesholds for dissociation are at 3·65 eV and 9·75 eV respectively so that the continuous absorption coefficient is finite at lower photon energies. Measurement of ion chamber currents, however enables the absorption due to ionization to be found, despite these competing processes. We expect that photo-ionization would take precedence over dissociation and dissociative ionization above the 1st ionization potentials on account of the smallness of the ratio of the electronic to the nuclear mass. This makes it difficult to understand why the ionization efficiencies, Y_i, defined by

$$Y_i = \frac{\text{photo-ionization cross section}}{\text{total absorption cross section}} \times 100 \qquad (2.20)$$

are relatively small well above the 1st ionization potentials of O_2 and N_2 (see for instance the experimental results of Cook and Metzger[63]). Further discussion on this and similar questions will, however, be postponed until Ch.6. As the photon energy is increased above the 1st ionization potentials, other states of the ions M_2^+ become accessible when the ionization potentials for the inner orbitals are attained. Many dissociative and pre-ionizing transitions also become possible but it is not our purpose here to investigate their absorption cross sections. In table 2.3 are displayed the possible final <u>electronic</u> states resulting from the ejection of a single electron from the various orbitals in N_2 $(X^1\Sigma_g^+)$ and O_2 $(X^3\Sigma_g^-)$ together with their corresponding appearance thresholds. We ignore photo-ionization from the inner most orbitals, $1\sigma_g$ and $1\sigma_u$, from which photo-ejection only occurs for $\lambda^{\ddagger} < 30\text{Å}$. It is worth noting that many of the excited states of O_2^+ and N_2^+ shown in Table 2.3 have not been experimentally identified. Most of these therefore carry a "?" alongside their term designations. The ionization potentials for such states are thus subject to considerable uncertainty as they are obtained by using the relation

$$\mathcal{E}_i = E(\Phi^0) - E(\Phi_i^*) \qquad (2.21)$$

---

‡ The same symbol λ is used for photon wavelength and the prolate spheroidal co-ordinate $(r_1 + r_2)/R$, but the context should make it clear which use is intended.

where $E(\bar{\Phi}^{o})$ and $E(\bar{\Phi}_{i}^{*})$ are the energies obtained from the S.C.F.-L.C.A.O.-M.O. method for the ground state of M_2 and a particular state of M_2^+.

For all transitions from N_2 to N_2^+ there are degenerate initial states. For the process

$$N_2(X^1\Sigma_g^+) + h\nu \longrightarrow N_2^+(A^2\Pi_u) + \bar{e} \qquad (2.22)$$

there is a 4-fold degeneracy as each M.S.O. connected with the spatial orbitals $1\pi_u$ and $1\bar{\pi}_u$ has the same energy. For all other processes in N_2 the order of degeneracy is 2. We follow Bates[5] and assume that the total cross section for such processes as (2.22) are obtained by multiplying the cross section for one electron by the order of degeneracy, d,

$$\sigma_{tot} = \sum_{i=1}^{d} \sigma_i \qquad (2.23).$$

Similarly for the process

$$O_2(X^3\Sigma_g^-) + h\nu \longrightarrow O_2^+(X^2\Pi_g) + \bar{e} \qquad (2.24)$$

the one electron cross section is multiplied by 2 as the orbitals $1\pi_g$ and $1\bar{\pi}_g$ have the same energies. For transitions to O_2^+ $(A^2\Pi_u)$ and $O_2^+(a^4\Pi_u)$ a factor of 2 must also be employed but for all other processes in O_2 no multiplicative factors are needed.

TABLE 2.3

ELECTRONIC STATES OF N_2^+ AND O_2^+.

ION M_2^+	STATE	THRESHOLD eV	THRESHOLD λ(Å)	MOLECULAR ORBITAL VACATED (ψ_i) IN M_2
N_2^+	$X^2\Sigma_g^+$	15·6	795	$3\sigma_g$
	$A^2\Pi_u$	16·7	742	$1\pi_u$ OR $1\bar{\pi}_u$
	$B^2\Sigma_u^+$	18·8	661	$2\sigma_u$
	$?^2\Sigma_g^+$	39·5‡	314	$2\sigma_g$
O_2^+	$X^2\Pi_g$	12·1	1025	$1\pi_g$ OR $1\bar{\pi}_g$
	$a^4\Pi_u$	16·1	770	$1\pi_u$ OR $1\bar{\pi}_u$
	$A^2\Pi_u$	16·9	734	$1\pi_u$ OR $1\bar{\pi}_u$
	$b^4\Sigma_g^-$	18·2	681	$3\sigma_g$
	$?^2\Sigma_g^-$	20·3	611	$3\sigma_g$
	$c^4\Sigma_u^-$	24·5	506	$2\sigma_u$
	$?^2\Sigma_u^-$	29·4‡	422	$2\sigma_u$
	$?^4\Sigma_g^-$	40·1‡	309	$2\sigma_g$
	$?^2\Sigma_g^-$	43·5‡	285	$2\sigma_g$

‡ Data obtained from self consistent field calculations of Sahni and Lorenzo (1965).[62] The remaining data were taken from the potential energy curves of Gilmore (1965).[64]

2.4 EXPRESSIONS FOR BOUND STATE M.O. WAVE FUNCTIONS IN PROLATE SPHEROIDAL CO-ORDINATES.

In table 2.2 we have given the L.C.A.O.-M.O.'s for $O_2\ (X^3\Sigma_g^-)$ and $N_2\ (X^1\Sigma_g^+)$. For a given photo-ionization process we take the appropriate one electron initial state wave function ψ_i to be the molecular spin orbital which is occupied in the molecule and vacated in the ion. Thus for the process (2.22), for example, ψ_i is the wave function for the orbital $1\pi_u$ or $1\bar{\pi}_u$. In order to compute the cross sections, we find it convenient to work in prolate spheroidal co-ordinates. We now deduce expressions for each basic orbital type π_g, $\bar{\pi}_g$, π_u, $\bar{\pi}_u$, σ_g and σ_u in these co-ordinates. The 3 sets of axes involved, one on each nucleus and one at the C.O.M. are shown in figure 2.1 (c.f. Scherr[61]).

FIG. 2.1

CO-ORDINATE SYSTEMS IN THE ATOMS AND MOLECULE.

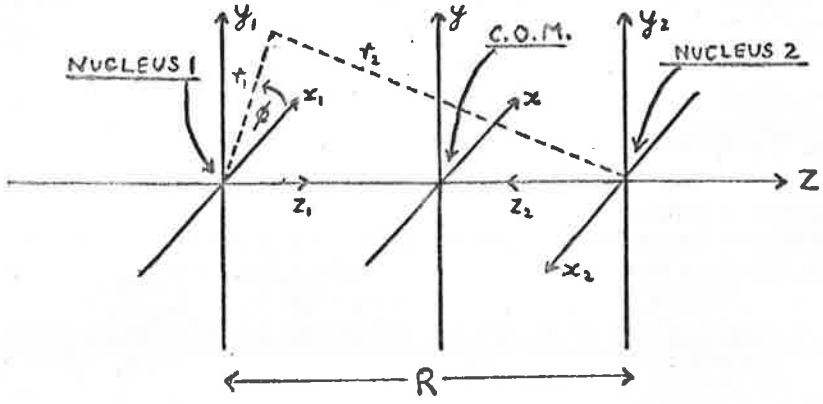

With this choice of axes we have

$$\psi_i^{(\bar{\pi}_y)} = C\left[(2p_{y_1}) - (2p_{y_2})\right]$$

$$= C\left[e^{-\zeta_2 r_1} r_1 \sin\theta_1 \sin\phi_1 - e^{-\zeta_2 r_2} r_2 \sin\theta_2 \sin\phi_2\right]$$

$$= C_y\left[e^{(-\zeta_2 R/2)(\lambda+\mu)} - e^{(-\zeta_2 R/2)(\lambda-\mu)}\right]$$

and since $\quad y = (R/2)(\lambda^2-1)^{\frac{1}{2}}(1-\mu^2)^{\frac{1}{2}}\sin\phi$

we have

$$\psi_i^{(\bar{\pi}_y)} = (CR/2)(\lambda^2-1)^{\frac{1}{2}}(1-\mu^2)^{\frac{1}{2}}\sin\phi \times \qquad (2.25)$$

$$\times\left[e^{-(\zeta_2 R/2)\lambda}\right]\left[e^{-(\zeta_2 R/2)\mu} - e^{+(\zeta_2 R/2)\mu}\right]$$

$$= -CR(\lambda^2-1)^{\frac{1}{2}}(1-\mu^2)^{\frac{1}{2}} e^{-\alpha\lambda} \times$$

$$\times \sinh(\alpha\mu)\sin\phi \qquad (2.26)$$

where $\alpha^{\ddagger} = \zeta_2 R/2$ and C is a normalization constant. Utilizing the expression

$$x = (R/2)(\lambda^2-1)^{\frac{1}{2}}(1-\mu^2)^{\frac{1}{2}}\cos\phi \qquad (2.27)$$

we see that the expression for a π_y orbital is identical to (2.26) except that $\sin\phi$ is replaced by $\cos\phi$.

---

‡ We have previously used the symbol α to represent the fine structure constant but that use will not occur again in this part, so no ambiguity should arise.

Further, that the above expression (2.26) has g symmetry can be verified by making the transformations (2.2) and observing that there is no change of sign of ψ_i .

For a $\bar{\pi}_u$ orbital we have,

$$\psi_i^{(1\bar{\pi}_u)} = C[(2p_{y_1}) + (2p_{y_2})]$$

$$= CR(\lambda^2-1)^{\frac{1}{2}}(1-\mu^2)^{\frac{1}{2}} e^{-\alpha\lambda} \cosh(\alpha\mu) \sin\phi \qquad (2.28)$$

and for a π_u state $\sin\phi$ is replaced by $\cos\phi$.

For the σ states the expressions are more complicated because 3 primitive orbitals are involved. Thus for σ_g states we let the L.C.A.O. coefficients of table 2.2 be a_1, a_2, a_3, for $1s\sigma_g$, $2s\sigma_g$ and $2p_z\sigma_g$ primitives respectively and also write

$$1s = b_1 e^{-\beta_1 r}, \quad 2s^* = b_2 e^{-\beta_2 r}, \quad 2p_z = b_3 e^{-\beta_2 r}\cos\theta \qquad (2.29).$$

We let

$$c_1 = a_1 b_1/\sqrt{2} \quad , \quad c_2 = (1-s_i^2)^{-\frac{1}{2}} b_2 a_2/\sqrt{2} \qquad (2.30)$$

$$c_3 = (1-s_i^2)^{\frac{1}{2}} b_1 s_i a_2/\sqrt{2} \quad , \quad c_4 = a_3 b_3/\sqrt{2} \qquad (2.31)$$

so that

$$\psi_i^{(\sigma_g)} = (c_1-c_3)(e^{-\beta_1 r_1} + e^{-\beta_1 r_2}) + c_2(r_1 e^{-\beta_1 r_1} + r_2 e^{-\beta_1 r_2})$$

$$+ c_4(r_1 e^{-\beta_2 r_1}\cos\theta_1 + r_2 e^{-\beta_2 r_2}\cos\theta_2) \qquad (2.32)$$

Since $$r_1 \cos\theta_1 = Z_1 = Z + R/2 = (\lambda\mu + 1)R/2 \qquad (2.33)$$

$$r_2 \cos\theta_2 = Z_2 = R/2 - Z = (1 - \lambda\mu)R/2 \qquad (2.34)$$

we obtain

$$\begin{aligned}\psi_i^{(\sigma_g)} &= (C_1 - C_3)\left[e^{-(\zeta_1 R/2)(\lambda+\mu)} + e^{-(\zeta_1 R/2)(\lambda-\mu)}\right] \\ &+ C_2\left[(R/2)(\lambda+\mu)e^{-(\zeta_2 R/2)(\lambda+\mu)} + (R/2)(\lambda-\mu)e^{-(\zeta_2 R/2)(\lambda-\mu)}\right] \\ &+ C_4\left[(\lambda\mu+1)(R/2)e^{-(\zeta_2 R/2)(\lambda+\mu)} + (1-\lambda\mu)(R/2)e^{-(\zeta_2 R/2)(\lambda-\mu)}\right] \qquad (2.35)\end{aligned}$$

which after letting $\beta = \zeta_1 R/2$ and some simple manipulation yields the result

$$\begin{aligned}\psi_i^{(\sigma_g)} &= 2(C_1 - C_3)e^{-\beta\lambda}\cosh(\beta\mu) \\ &+ Re^{-\alpha\lambda}\left[\{C_2\lambda + C_4\}\cosh(\alpha\mu) - \{C_2 + C_4\lambda\}\mu\sinh(\alpha\mu)\right] \qquad (2.36)\end{aligned}$$

Similarly we find for σ_u orbitals

$$\begin{aligned}\psi_i^{(\sigma_u)} &= (C_1 - C_3)(e^{-\zeta_1 r_1} - e^{-\zeta_1 r_2}) \\ &+ C_2(r_1 e^{-\zeta_2 r_1} - r_2 e^{-\zeta_2 r_2}) + C_4(e^{-\zeta_2 r_1} r_1\cos\theta_1 - e^{-\zeta_2 r_2} r_2\cos\theta_2) \qquad (2.37)\end{aligned}$$

$$= -2(c_1 - c_3)e^{-\beta\lambda}\sinh(\beta\mu)$$

$$+ Re^{-\alpha\lambda}\left[\{c_4\lambda + c_2\}\mu\cosh(\alpha\mu) - \{c_4 + c_2\lambda\}\sinh(\alpha\mu)\right] \quad (2.38).$$

The properties of expressions (2.28), (2.36) and (2.38) under the operation of inversion can also be shown to be correct by applying (2.2).

In sections 5.3 and 5.4 we will use the above expressions for the molecular orbitals with different values of ζ_2 for π orbitals and different values of the L.C.A.O. coefficients for σ orbitals. These modifications mean that the wave functions given by Sahni and Lorenzo which are displayed in Table 2.2 are no longer normalized. Thus we had to determine normalization coefficients from (2.26)(2.28,) (2.36)and(2.38)in accordance with (1.9). The formulae involved tend to be somewhat long and of little interest to the main purpose of the work. They are given, for the sake of completeness in Appendix 1.

The above expressions for the bound state molecular orbitals will be used in Ch.4 to evaluate the electronic matrix elements for the processes shown in Table 2.3. We now turn our attention to the continuum waves that will be employed in the evaluation of the matrix elements.

CHAPTER 3.

ELECTRONIC STATES OF THE CONTINUUM.

3.1 DISCUSSION OF THE FINAL STATE MODEL.

We have seen in Ch. 1 that for calculations on atomic cross sections one has the choice of the following continuum wave functions:

(1) Plane waves

(11) Coulomb scattered waves for Z = +1 or some effective nuclear charge.

(111) Waves calculated from a Hartree type self consistent potential.

(1V) Waves calculated from a Hartree-Fock potential, including exchange terms.

From (1) to (1V) the results obtained should be progressively more accurate. Plane waves should only yield the correct magnitudes at high energies where $\mathcal{E} \gg V(r)$, $V(r)$ being the potential energy function and $\mathcal{E}$ being the photo-electron's kinetic energy. As $\mathcal{E} \to \infty$, the Coulomb waves will of course approximate to plane waves. Coulomb type functions can give a reasonable degree of accuracy even at low energies if the dipole length form of the matrix elements is used and a suitable method is used to determine the phase shifts $\delta(\mathcal{E})$. The results of calculations

with type (1V) functions may or may not give significantly more accurate results than those with type (111) but in any case the latter should generally give at least the right order of magnitude for the cross sections even if the details of the variation with energy are not correct.

The most striking feature of the above continuum waves for atoms is that they are based on models which assume a central potential $V = V(r)$ (except in the trivial case (1) where $V = 0$). Spherical harmonics can then be used for the angular dependence of the one electron wave functions which are used to construct either the product wave functions (Hartree method) or the determinantal wave functions (Fock method).

Turning to the present problems connected with finding continuum waves for electrons moving in the field of a homonuclear diatomic ion, such as N_2^+ or O_2^+, we see that type (1) wave functions go straight over from the atomic case providing the kinetic energy of the photoelectron is high enough. One has a convenient expansion for free particle states in prolate spheroidal co-ordinates,[65] satisfying $\nabla^2\psi + k^2\psi = 0$,

$$e^{i\underline{k}\cdot\underline{r}} = 2\sum_{m,l}\left(\varepsilon_m i^l / N_{ml}(h)\right) \times \qquad (3.1)$$

$$\times S_{m\ell}(k,\cos\theta_0)\cos[m(\phi-\phi_0)]\,S_{m\ell}(k,\mu)\,je_{m\ell}(k,\lambda)$$

where $\underline{k} = (k,\theta_0,\phi_0), \underline{r} = (r,\theta,\phi)$, $N_{m\ell}(k)$ is the normalization factor for the "angular"‡ functions $S_{m\ell}$

$$N_{m\ell} = \int_{-1}^{1} |S_{m\ell}|^2 d\mu \qquad (3.2)$$

$$k = \tfrac{1}{2} R k \qquad (3.3)$$

and ϵ_m is the Neumann factor (=1 if m = 0, =2 otherwise). The radial solutions $je_{m\ell}(\lambda)$ can be expanded in terms of spherical Bessel functions $j_n(\lambda)$ of the 1st kind;

$$je_{m\ell}(k,\lambda) = \frac{(\ell-m)!}{(\ell+m)!}\left(\frac{\lambda^2-1}{\lambda^2}\right)^{\frac{1}{2}m} \times$$
$$\times \sum_{n=1}^{\infty}{}' i^{n+m-\ell} d_n(k|m,\ell)\frac{(n+2m)!}{n!} j_{n+m}(k\lambda) \qquad (3.4).$$

It can be seen that for any initial state ψ_i, described in section 2.4 for each molecular orbital type, one merely has to substitute (3.1) and the expression for ψ_i in equation (1.7) for the differential cross section whereupon all integrations that occur in the evaluation of the dipole length matrix elements can be performed analytically.

---

‡ Functions of μ and ϕ in prolate spheroidal coordinates will subsequently be referred to as angular functions without the use of inverted commas.

Integration over all angles (θ_o, ϕ_o) will of course give the cross section for the process in which ψ_i is vacated. We do not wish to pursue this method in detail however, because we are primarily interested in the cross sections at low energies. Furthermore the calculations we shall describe should give identical results to the above Born approximation calculation when used at high energies. Nevertheless we did perform the above integrations for a $1\pi_g$ initial state in O_2 (see Ch.4) but did not find numerical results.

Since we are interested in low energy cross sections we seek an approximation for the final state waves for diatomic molecules which is of the same degree of accuracy as type (11) waves for atoms. Such waves have already been used in the calculations of Flannery and Opik[50] on H_2 and were discussed by Shimizu[49]. These are the waves for an electron moving in the field of 2 half elementary positive charges placed at the nuclei. Such spheroidal waves bear much the same mathematical and physical relationships to diatomic molecules as Coulomb scattered waves do to atomic systems. We have noted in section 1.5 that Flannery and Opik adjusted the

separation of the positive charges in the final state so that the quadrupole moment was the same as that of H_2^+. While there is no doubt that such a modification has an appealing physical foundation, we found, after estimating quadrupole moments in O_2^+ and N_2^+, based on data from the microwave collision experiments of Smith and Howard[66], that such a modification would make the integrations in the matrix elements exceedingly difficult. This would be the case if there were any difference between the internuclear separation of the ground states of the neutral molecules and the separation of the 2 half elementary charges, because, if we worked in prolate spheroidal co-ordinates there would be 2 sets $(\lambda_1, \mu_1, \phi_1)$ and $(\lambda_2, \mu_2, \phi_2)$ involved and no simple relations could be found to write either the bound state functions in terms of the set $(\lambda_2, \mu_2, \phi_2)$, for the final state internuclear separation or the continuum waves in terms of $(\lambda_1, \mu_1, \phi_1)$. Consequently, we have chosen the separation of the half elementary charges to be the equilibrium internuclear separation of the ground state neutral molecules, so that integrations over the angular variables can be performed analytically and those over the radial variable can be done straightforwardly by numerical methods.

It is natural to ask why we should stop our considerations of final state waves at the analogue to type (11), especially since type (11) waves for atoms are only an approximation and can be improved by using Hartree or Hartree-Fock methods. A brief discussion should justify our choice.

The difference between the symmetries of atoms and diatomic molecules is the major factor, as we have already pointed out in section 2.1. It is true of course that the use of spherically symmetric potentials is not completely accurate for atoms but the departures from the approximation are either expected to be small[21] or at least to take them into account is too much labour for too little improvement, so in either case they are usually ignored.

However, if we use the Hartree method, we can find from the one electron wave functions at any stage of the self consistency calculations a potential $V(r)$ from the charge density distribution function. Similarly the Hartree-Fock method results in a potential function for the motion of each electron. Since Hartree-Fock M.O.'s are not usually found but rather the best L.C.A.O.-M.O.'s in the case of molecules, there is no analogous self

consistent potential; the usual criterion[62] is that the energy eigenvalues reach a pre-determined degree of consistency in successive iterative solutions of the Fock equations (2.6). It is certain that a "self consistent potential" could be found from the resulting L.C.A.O.-M.O.'s by obtaining the total charge density distribution function from the individual one electron wave functions. The potential so obtained would, however, be a function of the 2 variables λ and μ. Only under extremely fortuitous conditions, such as the fitting of this $V(\lambda,\mu)$ to a function of the form[67]

$$V(\lambda,\mu) = g(\lambda)/(\lambda^2-\mu^2) \qquad (3.5)$$

would the Schrodinger equation be separable in prolate spheroidal co-ordinates. One could of course take functions of the form (3.5), as Fisk[68] has done for studies of elastic scattering of slow electrons by diatomic molecules, with adjustable parameters. Such a method is not used in the present calculations but it is likely that such an approach will be useful in future work (see Ch. 8). We have chosen Flannery and Opik's final state model for the continuum states throughout these calculations.

This model is based on effective screening of the ejected electron from the nuclei by the remaining bound electrons in the ion. We expect of course that this screening will be most effective for electrons ejected from the most loosely bound states. Further, the use of this model also means that the continuum waves should be most reliable at large distances from the nuclei and hence we use the dipole length form of the matrix elements in preference to their velocity and acceleration forms for the reasons given in Ch. 1.

3.2 THE SCHRODINGER EQUATION IN PROLATE SPHEROIDAL CO-ORDINATES.

The Schrodinger eigenvalue equation

$$H\Psi = E\Psi \tag{3.6}$$

for an electron moving in the field of 2 half elementary positive charges whose separation is $|\underline{R}| = R$ can be easily found. The potential term is simply

$$V = -e^2/2r_1 - e^2/2r_2 + e^2/4R \tag{3.7}$$

where r_1 and r_2 are the distances of the electron from the positive charges. The kinetic energy operator is $-(\hbar^2/2m)\nabla^2$ so that, on noting that $a_0 = \hbar^2/me^2$, where a_0 is the Bohr radius, we obtain from (3.6,)

$$-\frac{e^2}{2}\left[a_0\nabla^2 + \frac{1}{r_1} + \frac{1}{r_2} - \frac{1}{2R}\right]\Psi = E\Psi \tag{3.8}$$

If we let the energy of the electron be E_e relative to the repulsive energy of the positive charges,

$$E_e = E - e^2/4R \tag{3.9}$$

and write

$$W = 2E_e/a_0e^2 \tag{3.10}$$

we obtain

$$\left[\nabla^2 + \frac{1}{a_0}\left(\frac{1}{r_1} + \frac{1}{r_2}\right) + W\right]\Psi = 0 \tag{3.11}$$

Using the relations

$$\left(\frac{1}{r_1}+\frac{1}{r_2}\right)=\frac{4\lambda}{R(\lambda^2-\mu^2)} \tag{3.12}$$

and

$$\nabla^2=\left(\frac{2}{R}\right)^2\frac{1}{\lambda^2-\mu^2}\left[\frac{\partial}{\partial\lambda}\left\{(\lambda^2-1)\frac{\partial}{\partial\lambda}\right\}+\frac{\partial}{\partial\mu}\left\{(1-\mu^2)\frac{\partial}{\partial\mu}\right\}+\frac{\lambda^2-\mu^2}{(\lambda^2-1)(1-\mu^2)}\frac{\partial^2}{\partial\phi^2}\right] \tag{3.13}$$

we obtain, using (1.42), the unseparated equation

$$\frac{\partial}{\partial\lambda}\left[(\lambda^2-1)\frac{\partial\Psi}{\partial\lambda}\right]+\frac{\partial}{\partial\mu}\left[(1-\mu^2)\frac{\partial M}{\partial\mu}\right]+\left[\frac{1}{\lambda^2-1}+\frac{1}{1-\mu^2}\right]\frac{\partial^2\Psi}{\partial\phi^2}+\left[\frac{R\lambda}{a_0}+\frac{R^2W}{4}(\lambda^2-\mu^2)\right]\Psi=0 \tag{3.14}$$

Noting that

$$\frac{\lambda^2-\mu^2}{(\lambda^2-1)(1-\mu^2)}=\frac{1}{\lambda^2-1}+\frac{1}{1-\mu^2} \tag{3.15}$$

and introducing the separation constants $-m^2$ and $-A$, we obtain the 3 ordinary differential equations

$$d^2\Phi/d\phi^2+m^2\Phi=0 \tag{3.16}$$

$$\frac{d}{d\mu}\left[(1-\mu^2)\frac{dM}{d\mu}\right]+\left[A-R^2\mu^2-\frac{m^2}{1-\mu^2}\right]M=0 \tag{3.17}$$

$$\frac{d}{d\lambda}\left[(\lambda^2-1)\frac{d\Lambda}{d\lambda}\right]+\left[-A+R\lambda+R^2\lambda^2-\frac{m^2}{\lambda^2-1}\right]\Lambda=0 \tag{3.18}$$

where $k^2 = R^2\mathcal{E}/4$, $\mathcal{E}$ being the kinetic energy of the electron in Rydbergs (1 Rydberg = I_H = 1st ionization potential of atomic hydrogen = $e^2/2a_o$).

The solutions of (3.16) and (3.17) have been much discussed (65, 69, 70) and in the next section a brief summary of their properties are given.

The solutions of (3.16) for Φ can be simply written

$$\Phi(\phi) = \begin{matrix}\cos \\ \sin\end{matrix}(m\phi) \qquad (3.19)$$

where the periodicity requirement makes m take only integer values. Clearly for $m \neq 0$ we have 2 - fold degeneracy because each solution $\cos(m\phi)$ and $\sin(m\phi)$ gives the same energy eigenvalue. Further, the usual notation is that m = 0 waves are called σ waves; m = 1, π waves; m = 2 δ waves; etc.

The solutions of (3.17) can be written as expansions in associated Legendre functions of the first or second kinds. Only those involving functions of the 1st kind are of physical interest. Further, these are obtained only for discrete values of the separation constant A which is thus labelled $A_\ell^m(h)$; with each (m,ℓ) one has a solution which is either odd or even in μ , the even solution being written

$$M_\ell^{m(1)}(h,\mu) = \sum_{n=0}^{\infty}{}' d_n(h|m,\ell) P_{n+m}^m(\mu), \qquad (3.20)$$

$$\ell = m, m+2, m+4, \ldots$$

and the odd solution,

$$M_\ell^{m(2)}(h,\mu) = \sum_{n=1}^{\infty}{}' d_n(h|m,\ell)\, P_{n+m}^m(\mu), \qquad (3.21).$$
$$\ell = m+1, m+3, m+5, \ldots .$$

We note that as $h \to 0$ (ie $R \to 0$), $A_\ell^m(h) \longrightarrow \ell(\ell+1)$, which is the separation constant for a central potential, and $M_\ell^m \to P_\ell^m$, so that as $h \to 0$ the angular solutions behave as spherical harmonics. In (3.20) and (3.21) the primes on the summations mean that only alternate values of n are taken into account. The $M_\ell^m(h,\mu)$ are normalized in the sense that $M_\ell^m(\mu,h) \to P_\ell^m(\mu)$ as $\mu \to 1$.

The values of the coefficients $d_n(h|m,\ell)$ in the expansions (3.20) and (3.21), for discrete values of h, can be obtained directly from the tables of reference 69. Further, in that reference, values of $t_\ell^m(h)$ are tabulated from which the separation constants can be found;

$$A_\ell^m(h) = \ell(\ell+1) + h^2\left[\frac{2\ell(\ell+1)-2m^2-1}{(2\ell-1)(2\ell+3)} + t_\ell^m(h)\right] \qquad (3.22).$$

3.4 THE RADIAL SOLUTIONS.

Analytic expressions for the solutions of the radial equation (3.18) cannot be found. Clearly there will be 2 linearly independent solutions Λ_1 , and Λ_2 , and their behaviour near $\lambda = 1$ can be obtained from the indicial equation to be,‡

$$\Lambda_1(\lambda) \underset{\lambda\to 1}{\sim} (\lambda-1)^{\frac{1}{2}m}\left(1+\sum_{n=1}^{\infty} a_n(\lambda-1)^n\right) \qquad (3.23)$$

$$\Lambda_2(\lambda) \underset{\lambda\to 1}{\sim} (\lambda-1)^{-\frac{1}{2}m}\left(1+\sum_{n=1}^{\infty} b_n(\lambda-1)^n\right) \qquad (3.24)\ .$$

Clearly (3.23) provides the solution of physical interest. Further we know the asymptotic forms of Λ_1 and Λ_2 must be the same as those of the free particle solutions together with a logarithmic term and a phase shift $\delta(k)$. It can be shown by the amplitude and phase method of Buckingham[71] that the asymptotic form at large λ for the solution Λ_1 which is regular at $\lambda = 1$ should therefore be

$$\Lambda^m_{1,l}(k,\lambda) \underset{\lambda\to\infty}{\sim} \frac{C(k)}{\lambda}\sin\left(k\lambda + \frac{R}{2k}\ln\lambda - \right.$$
$$\left. -\tfrac{1}{2}(l+m)\pi + \delta(k)\right) \qquad (3.25).$$

---

‡ If the recurrence relation for the coefficients b_n breaks down, a second solution can of course be found of the form $\Lambda_1 \log(\lambda-1) + (\lambda-1)^{-m/2}\left(1+\sum_{n=1}^{\infty} b_n(\lambda-1)^n\right)$ but such a solution is not needed here.

where $\delta(k)$ are the phase shifts and $C(k)$ is a normalization factor.

The method of numerical solution to (3.18) has been given by Bates[42] whose method will be briefly described. A few alterations are required because of the slightly different forms of the radial equations. Near $\lambda = 1$ a power series expansion is used; we write

$$\Lambda(\lambda) = (\lambda^2-1)^{m/2} F(\tau) \qquad (3.26)$$

with $\tau = \lambda - 1$. Then $F(\tau)$ satisfies the differential equation,

$$F''(\tau^2+2\tau) + 2(\tau+1)(m+1)F' + \\ + F\{R(\tau+1) - A + k^2(\tau^2+2\tau+1)\} + \\ + F(m(m+1)) = 0 \qquad (3.27)$$

We put

$$K = m(m+1) + R - A + k^2 \qquad (3.28)$$

$$H = R + 2k^2 \qquad (3.29)$$

$$F(\tau) = 1 + \sum_{n=1}^{\infty} a_n \tau^n \qquad (3.30)$$

and obtain for the coefficients

$$a_1 = -K/2(m+1) \qquad (3.31)$$

$$a_2 = -\left[H + a_1\{2(m+1)+K\}\right]/4(m+2) \qquad (3.32)$$

and for $k \geq 3$ we have the recurrence relation

$$a_{k+1} = \frac{-\left[h^2 a_{k-2} + H a_{k-1} + a_k\{k(k-1)+2(m+1)k+K\}\right]}{\left[2k(k+1)+2(m+1)(k+1)\right]} \qquad (3.33).$$

After the first few values of Λ have been thus obtained, the recurrence relation[71]

$$(1-\phi_1)G_1 = (2+10\phi_0)G_0 - (1-\phi_{-1})G_{-1} + \Delta \qquad (3.34)$$

$$\Delta = \{-(1/240)\delta^6 + (13/15120)\delta^8 - \cdots\}G_0 \qquad (3.35)$$

where

$$\phi(\lambda) = -\left[-A + R\lambda + h^2\lambda^2 - m^2/(\lambda^2-1)\right] \times \frac{\omega^2}{12} \qquad (3.36)$$

ω being the interval in λ and where

$$G(\lambda) = (\lambda^2-1)^{\frac{1}{2}}\Lambda(\lambda), \qquad (3.37)$$

is used to generate values of Λ at greater values of λ.

The normalization condition (1.10) when applied to the continuum waves $\Psi(\varepsilon|\lambda,\mu,\phi) = \Lambda(\varepsilon|\lambda)M(\varepsilon|\mu)\Phi(\phi)$ results in a specific value at a given energy for the asymptotic amplitudes of the normalized, radial functions. Bates[42] has shown that the values of C(h), the

asymptotic amplitudes of the $G_\ell^m(\lambda)$ defined in (3.37), are

$$C(\ell) = 2(\pi \hbar R Y_\ell^m)^{-1/2} \tag{3.38}$$

where

$$Y = \int_0^{2\pi} \bar{\Phi}(\phi)\Phi(\phi)\,d\phi \int_{-1}^{1} M(\mu)M(\mu)\,d\mu \tag{3.39}.$$

Furthermore, the asymptotic amplitudes of the unnormalized $G_\ell^m(\lambda)$ are

$$D(\ell) = (2\sqrt{\ell})^{-1} \times \left\{ [a(\lambda_1) + a(\lambda_2)]^2 \sec^2 \alpha(\lambda_1,\lambda_2) + [a(\lambda_1) - a(\lambda_2)]^2 \operatorname{cosec}^2 \alpha(\lambda_1,\lambda_2) \right\}^{1/2} \tag{3.40}$$

where

$$a(\lambda) = G(\lambda)\sqrt{U(\lambda)} \tag{3.41}$$

$$U(\lambda) = v(\lambda) + w(\lambda) \tag{3.42}$$

$$v(\lambda) = \frac{\hbar^2\lambda^2 + R\lambda - A}{\lambda^2 - 1} + \frac{1-m^2}{(\lambda^2-1)^2} \tag{3.43}$$

$$w(\lambda) = \frac{5}{16v^2}\left(\frac{dv}{d\lambda}\right)^2 - \frac{1}{4v}\frac{d^2v}{d\lambda^2} \tag{3.44}$$

$$\alpha(\lambda_1,\lambda_2) = \tfrac{1}{2}\int_{\lambda_1}^{\lambda_2} U(\lambda)\,d\lambda \tag{3.45}$$

and λ_1 and λ_2 are 2 values of λ so chosen that they make $w \ll v$.

The details of the application of the above

numerical methods will be discussed in Ch. 5. We note that the somewhat troublesome normalization of zero energy eigenfunctions for which a method had been given in the case of atoms by Hargreaves[72], is neatly performed by using (3.38) and (3.40) in the case of vanishingly small h, because C(h)/D(h) is always finite.

The determination of $v'(\lambda)$ and $v''(\lambda)$ is of course immediate from (3.43). We have in the present case

$$v'(\lambda) = \frac{(\lambda^2-1)(R+2R^2\lambda) + (-A+R\lambda+R^2\lambda^2)(2\lambda)}{(\lambda^2-1)^2} - \frac{4\lambda(1-m^2)}{(\lambda^2-1)^3} \tag{3.46}$$

$$v''(\lambda) = \frac{2(\lambda^2-1)(6R^2\lambda^2+3R\lambda-R^2-A) - 4\lambda(4R^2\lambda^3+3R\lambda^2-\lambda(2R^2+2A)-R)}{(\lambda^2-1)^3} + \frac{4(1-m^2)(5\lambda^2+1)}{(\lambda^2-1)^4} \tag{3.47}.$$

The application of (3.39) is straightforward from (3.20) or (3.21) together with the relation for associated Legendre functions

$$\int_{-1}^{1} \overline{P}_n^m(\mu) P_n^m(\mu) d\mu = \frac{2}{2n+1} \frac{(n+m)!}{(n-m)!} \qquad (3.48).$$

The resulting expressions Y for the various continuum waves which arise in the calculations for N_2 and O_2 will be given in Ch. 4.

To conclude this section we wish to point out that in calculating the continuum waves for the transitions of table 2.3, we have not included the phase shifts $\delta(l)$ in (3.25). Rough estimates of these could probably be made from the energy level data for the excited states of O_2^+ and N_2[64]. However, the quantum defect method which has been used to estimate phase shifts for continuum orbitals for atoms has not been rigorously developed for scattering by diatomic molecular ions. Flannery and Opik[52] have proposed a method of application without the theory. If E_ν° are the discrete eigenvalues for the 2 half elementary positive charge system, then put

$$E_\nu^\circ = -\frac{1}{2\nu^2}, \quad \nu = 1, 2 \ldots \qquad (3.49).$$

Further if E_ν are the corresponding eigenvalues for the diatomic molecule in question, then define the quantum

defects δ_ν by

$$E_\nu = \frac{-1}{2(n_\nu - \delta_\nu)^2} \qquad (3.50).$$

Then if the radial function for the 1st case is asymptotically

$$\Lambda^0(\lambda) \underset{\lambda \to \infty}{\cong} u(\lambda) \sin[\Theta(\lambda)] \qquad (3.51)$$

then in the second case we should have,

$$\Lambda(\lambda) \underset{\lambda \to \infty}{\cong} u(\lambda) \sin[\Theta(\lambda) + \pi\delta_\nu] \qquad (3.52).$$

Using the extrapolation method to find δ_ν for continuum waves, Flannery and Opik estimated the quantum defects for excited states of H_2. However, the functions used in evaluating the matrix elements were taken as the zero phase shift solutions (3.51), chiefly because of the uncertainties in the Q.D.M. phase shifts. Flannery and Opik also estimated that the error likely to be introduced in the cross sections by adopting (3.51) instead of (3.52) was 12%. We consider that the errors introduced in the present calculations by making this approximation, should not be significantly greater than this. Clearly more work could be done in developing the quantum defect method (though this name is slightly misleading) for diatomic ions and possibly some improvement achieved in the calculation of cross sections for H_2 as well as N_2 and O_2.

CHAPTER 4.

EVALUATION OF THE ELECTRONIC MATRIX ELEMENTS.

In this chapter we derive expressions for the dipole length matrix elements using the final state model we have discussed in Ch. 3 and the expressions for the L.C.A.O.-M.O.'s which occur in the electronic configurations of O_2 $(X^3\Sigma_g^-)$ and N_2 $(X^1\Sigma_g^+)$, for which expressions have been found in Ch. 2. We now bear in mind that the cross section depends on

$$|M|^2 = |(\pm)_f \underline{J}|^2 = |\mathcal{M}_x|^2 + |\mathcal{M}_y|^2 + |\mathcal{M}_z|^2 \qquad (4.1)$$

and that for a given photo-ionization process we must sum over degenerate final state waves. We have four basic bound orbital types to consider; π_g, π_u, σ_g and σ_u. It will be obvious that the results for $\bar{\pi}_g$ and $\bar{\pi}_u$ orbitals are equivalent to those for π_g and π_u respectively so we do not treat them separately. We devote one section to each of the above initial state functions.

4.1 π_g (or $\bar{\pi}_g$) INITIAL STATES.

Examination of (2.26), (3.19) and the relations for (x, y, z) in prolate spheroidal co-ordinates

$$\left.\begin{aligned} x &= (R/2)(\lambda^2-1)^{1/2}(1-\mu^2)^{\frac{1}{2}}\cos\phi \\ y &= (R/2)(\lambda^2-1)^{\frac{1}{2}}(1-\mu^2)^{\frac{1}{2}}\sin\phi \\ z &= (R/2)\lambda\mu \end{aligned}\right\} \qquad (4.2)$$

shows that for $(\mathcal{M}_x, \mathcal{M}_y, \mathcal{M}_z)$ the ϕ-dependences of the respective transition integrals are $(\cos\phi \sin\phi, \sin^2\phi, \sin\phi) \times \begin{Bmatrix}\cos\\ \sin\end{Bmatrix}(m\phi)$ or $(\frac{1}{2}\sin 2\phi, \frac{1}{2}(1-\cos 2\phi), \sin\phi) \times \begin{Bmatrix}\cos\\ \sin\end{Bmatrix}(m\phi)$.

Utilizing the general relations

$$\left.\begin{aligned} \int_0^{2\pi} \cos m\phi \cos n\phi \, d\phi &= \pi\delta_{mn} \\ \int_0^{2\pi} \sin m\phi \sin n\phi \, d\phi &= \pi\delta_{mn} \\ \int_0^{2\pi} \sin m\phi \cos n\phi \, d\phi &= 0 \end{aligned}\right\} \qquad (4.3)$$

we see that $\mathcal{M}_x$ and $\mathcal{M}_y$ have contributions from δ - waves, $\mathcal{M}_y$ also has contributions from σ - waves, and $\mathcal{M}_z$ only has contributions from π waves.

We can anticipate the <u>selection rules</u> on m for various initial state functions. If we let the initial state have a ϕ-dependence of $\begin{Bmatrix}\cos\\ \sin\end{Bmatrix}(n\phi)$, then via the integrals $\int_0^{2\pi} \begin{Bmatrix}\cos\\ \sin\end{Bmatrix}(n\phi)\cos\phi \begin{Bmatrix}\cos\\ \sin\end{Bmatrix}(m\phi)\, d\phi$, $\int_0^{2\pi} \begin{Bmatrix}\cos\\ \sin\end{Bmatrix}(n\phi)\sin\phi \begin{Bmatrix}\cos\\ \sin\end{Bmatrix}(m\phi)\, d\phi$, and $\int_0^{2\pi} \begin{Bmatrix}\cos\\ \sin\end{Bmatrix}(n\phi) \begin{Bmatrix}\cos\\ \sin\end{Bmatrix}(m\phi)\, d\phi$ we obtain

$$\Delta m = 0, \pm 1 \qquad (4.4)$$

where the first case always applies to the z component. For initial σ states clearly $\Delta m = -1$ does not apply.

Returning to the case of π_g orbitals, we decide on the notation $\mathcal{M}^x_{m,\ell}$ etc. for each contribution to the components of $\underline{M}$. Then we have

$$\mathcal{M}^x_{2,\ell} = \frac{c\pi R^5}{32}\int_1^\infty\int_{-1}^{1} (\lambda^2-1)(1-\mu^2)\, e^{-\alpha\lambda} \sinh(\beta\mu) M_{2,\ell}(\mu)\Lambda_{2,\ell}(\lambda) \times \times (\lambda^2-\mu^2)\, d\mu\, d\lambda \qquad (4.5)$$

$$\mathcal{M}^{y}_{2,\ell} = \mathcal{M}^{x}_{2,\ell} \tag{4.6}$$

$$\mathcal{M}^{y}_{0,\ell} = \frac{C\pi R^5}{16}\int_{1}^{\infty}\int_{-1}^{1}(\lambda^2-1)(1-\mu^2)e^{-\alpha\lambda}\sinh(\alpha\mu)M_{0,\ell}(\mu)\Lambda_{0,\ell}(\lambda)\times$$
$$\times(\lambda^2-\mu^2)\,d\mu\,d\lambda \tag{4.7}$$

$$\mathcal{M}^{z}_{1,\ell} = \frac{C\pi R^5}{16}\int_{1}^{\infty}\int_{-1}^{1}(\lambda^2-1)^{\frac{1}{2}}(1-\mu^2)^{\frac{1}{2}}e^{-\alpha\lambda}\sinh(\alpha\mu).\lambda\mu.M_{1,\ell}(\mu)\times$$
$$\times\Lambda_{1,\ell}(\lambda)(\lambda^2-\mu^2)\,d\mu\,d\lambda \tag{4.8}.$$

The integrands of (4.5), (4.7) and (4.8), excluding the functions $M_{m,\ell}(\mu)$ are odd, odd and even functions of μ respectively. Thus we have to use expansions of the form (3.21) for the first two and one of form (3.20) for the last for non vanishing contributions to the matrix elements. Then we have to find the sums,

$$|M_x|^2 = \sum_{\ell=3,5,\ldots}^{\infty}{}' |\mathcal{M}^{x}_{2,\ell}|^2 \tag{4.9}$$

$$|M_y|^2 = \sum_{\ell=3,5\ldots}^{\infty}{}' |\mathcal{M}^{y}_{2,\ell}|^2 + \sum_{\ell=1,3\ldots}^{\infty}{}' |\mathcal{M}^{y}_{0,\ell}|^2 \tag{4.10}$$

$$|M_z|^2 = \sum_{\ell=1,3\ldots}^{\infty}{}' |\mathcal{M}^{z}_{1,\ell}|^2 \tag{4.11}.$$

Our matrix elements for S - waves are now

$$\mathcal{M}^{x}_{2,\ell} = \frac{C\pi R^5}{32}\int_{1}^{\infty}\int_{-1}^{1}(\lambda^2-1)(1-\mu^2)e^{-\alpha\lambda}\sinh(\alpha\mu)\times$$
$$\times\Big[\sum_{n=1}^{\infty}{}' d_n(\ell|2,\ell)P^2_{n+2}(\mu)\Big]\Lambda_{2,\ell}(\lambda)(\lambda^2-\mu^2)\,d\mu\,d\lambda \tag{4.12}$$

which we write as

$$\mathcal{M}^{x}_{2,\ell} = \frac{c\pi R^5}{32}\int_1^\infty (\lambda^2-1)\, e^{-\alpha\lambda}\Lambda_{2,\ell}(\lambda) \times$$
$$\times\Big[\sum_{n=1}^{\infty}{}' d_n(\ell 12,\ell)\Big\{\lambda^2\big(G_n(\alpha)-H_n(\alpha)\big)+I_n(\alpha)-H_n(\alpha)\Big\}\Big]d\lambda \qquad (4.13)$$

where we have defined the angular integrals

$$G_n(\alpha), H_n(\alpha), I_n(\alpha) = \int_{-1}^{1} P^2_{n+2}(\mu)\sinh(\alpha\mu)\,(1,\mu^2,\mu^4)\,d\mu \qquad (4.14).$$

For the contributions from σ waves we have,

$$\mathcal{M}^{y}_{0,\ell} = \frac{c\pi R^5}{16}\int_1^\infty\int_{-1}^{1}(\lambda^2-1)(1-\mu^2)\,e^{-\alpha\lambda}\sinh(\alpha\mu)\times$$
$$\times\Big[\sum_{n=1}^{\infty}{}' d_n(\ell 10,\ell)\,P_n(\mu)\Big]\Lambda_{0,\ell}(\lambda)\,(\lambda^2-\mu^2)\,d\mu\,d\lambda \qquad (4.15)$$
$$= \frac{c\pi R^5}{16}\int_1^\infty(\lambda^2-1)\,e^{-\alpha\lambda}\Lambda_{0,\ell}(\lambda)\times$$
$$\times\Big[\sum_{n=1}^{\infty}{}' d_n(\ell 10,\ell)\Big\{\lambda^2\big(A_n(\alpha)-B_n(\alpha)\big)+C_n(\alpha)-B_n(\alpha)\Big\}\Big]d\lambda$$

where

$$A_n(\alpha), B_n(\alpha), C_n(\alpha) = \int_{-1}^{1} P_n(\mu)\sinh(\alpha\mu)\,(1,\mu^2,\mu^4)\,d\mu \qquad (4.16).$$

Finally for π continuum waves we have

$$\mathcal{M}^{z}_{1,\ell} = \frac{c\pi R^5}{16}\int_1^\infty\int_{-1}^{1}(\lambda^2-1)^{1/2}e^{-\alpha\lambda}(1-\mu^2)^{1/2}\sinh(\alpha\mu)\,\lambda\mu\times$$
$$\times\Big[\sum_{n\neq 0}^{\infty}{}' d_n(\ell 11,\ell)\,P'_{n+1}(\mu)\Big]\Lambda_{1,\ell}(\lambda)\,(\lambda^2-\mu^2)\,d\mu\,d\lambda \qquad (4.17)$$

$$= \frac{c\pi R^5}{16}\int_1^\infty (\lambda^2-1)^{\frac{1}{2}} e^{-\alpha\lambda}\lambda \Lambda_{1,\ell}(\lambda) \times$$
$$\times \left[\sum_{n=0}^{\infty}{}' d_n(k/1,\ell)\left\{\lambda^2 D_n(\alpha) - E_n(\alpha)\right\}\right] d\lambda \qquad (4.18)$$

where

$$D_n(\alpha), E_n(\alpha) = \int_{-1}^{1}(1-\mu^2)^{\frac{1}{2}} \sinh(\alpha\mu) P'_{n+1}(\mu)(\mu,\mu^2)\,d\mu \qquad (4.19).$$

We can evaluate the above angular integrals as follows. Define

$$\mathcal{J}_n(\alpha) = \int_0^1 \sinh(\alpha\mu)\mu^n\,d\mu = \frac{1}{\alpha^{n+1}}\int_0^\alpha \sinh x\, x^n\,dx \qquad (4.20)$$

and utilize the series form of Legendre polynomials

$$P_n(\mu) = \sum_{r=0}^{\frac{n-1}{2}} \frac{(-)^r(2n-r)!\,\mu^{n-2r}}{2^n r!(n-r)!(n-2r)!}, \quad n \text{ odd}, \qquad (4.21)$$

whence

$$A_n(\alpha), B_n(\alpha), C_n(\alpha) = \sum_{r=0}^{\frac{n-1}{2}} \frac{(-)^r(2n-r)!\,\mathcal{J}_{n-2r,\,n-2r+2,\,n-2r+4}(\alpha)}{r!\,2^{n-1}(n-r)!(n-2r)!} \qquad (4.22).$$

In Appendix 2 the coefficients in the above summations are evaluated explicitly for the first six values of n. Inspection of tables of the coefficients $d_n(k/m,\ell)$ shows that including only the first six values of n should be sufficiently accurate. Furthermore the $\mathcal{J}_n(\alpha)$ satisfy the recurrence relation

$$\mathcal{J}_n = \alpha^{-(n+1)}\left[\alpha^n\cosh\alpha - n\alpha^{n-1}\sinh\alpha + \right.$$
$$\left. + n(n-1)\alpha^{n-1}\mathcal{J}_{n-2}\right] \qquad (4.23)$$

which facilitates their machine computation.

To evaluate $D_n(\alpha)$ and $E_n(\alpha)$ we use the standard relations

$$P'_{n+1}(\mu) = (1-\mu^2)^{\frac{1}{2}} \frac{d}{d\mu} P_{n+1}(\mu) \tag{4.24}$$

$$(1-\mu^2)\frac{d}{d\mu} P_{n+1}(\mu) = (n+1)\left[P_n(\mu) - \mu P_{n+1}(\mu)\right] \tag{4.25}$$

so that

$$D_n(\alpha) = (n+1)\int_{-1}^{1}\left[P_n(\mu) - \mu P_{n+1}(\mu)\right]\sinh(\alpha\mu)\,\mu\,d\mu \tag{4.26}.$$

Utilizing (4.26) we obtain

$$\begin{aligned} D_n(\alpha) = (n+1)\int_{-1}^{1}\Bigg[\sum_{r=0}^{n/2}\frac{(-)^r(2n-r)!\,\mu^{n-2r}}{2^n r!(n-r)!(n-2r)!} - \\ - \sum_{r=0}^{n/2}\frac{(-)^r(2n+2-r)!\,\mu^{n+2-2r}}{2^{n+1}(n+1-r)!(n+1-2r)!}\Bigg]\sinh(\alpha\mu)\,\mu\,d\mu \end{aligned} \tag{4.27}$$

$$= (n+1)\sum_{r=0}^{n/2}\frac{(-)^r(2n-r)!}{2^{n-1}(n-r)!(n-2r)!} \times \left\{ J_{n+1-2r}(\alpha) - \left[\frac{(2n+2-r)(2n+1-r)}{2(n+1-r)(n+1-2r)} J_{n+3-2r}(\alpha)\right]\right\}$$

and a similar expression for $E_n(\alpha)$.

Finally, we can obtain $G_n(\alpha)$, $H_n(\alpha)$, $I_n(\alpha)$ by using

$$P^{2}_{n+2}(\mu) = (1-\mu^2)\frac{d^2}{d\mu^2}P_{n+2}(\mu) \tag{4.28}$$

so that

$$G_n(\alpha) = \sum_{r=0}^{\frac{n+1}{2}} \frac{(-)^r(2n-r+4)!}{2^{n+1}r!(n+2-r)!(n-2r)!}\left\{J_{n-2r}(\alpha) - J_{n-2r+2}(\alpha)\right\} \tag{4.29}$$

with similar expressions for $H_n(\alpha)$ and $I_n(\alpha)$.

To determine the cross section for a given final state wave there remains to find the asymptotic amplitudes of the normalized radial functions in accordance with (3.38). This means that we have to evaluate the Y(h) given by (3.39) for each type of continuum wave. We have for the σ - waves,

$$Y_{0,\ell}(k) = \int_0^{2\pi} d\phi \int_{-1}^{1} \overline{M}_{0,\ell}(k|\mu) M_{0,\ell}(k|\mu)\, d\mu \tag{4.30}$$

$$= 2\pi \int_{-1}^{1} \Big(\sum_{n'=1}^{\infty}{}' d_{n'}(k|0,\ell) P_{n'}(\mu) \Big) \Big(\sum_{n=1}^{\infty}{}' d_n(k|0,\ell) P_n(\mu) \Big) d\mu \tag{4.31}$$

$$= 4\pi \sum_{n=1}^{\infty}{}' \frac{d_n(k|0,\ell)^2}{(2n+1)} \tag{4.32}.$$

For π - continuum waves,

$$Y_{1,\ell}(k) = \pi \int_{-1}^{1} \overline{\Big(\sum_{n'=0}^{\infty}{}' d_{n'}(k|0,\ell) P'_{n'+1}(\mu) \Big) \Big(\sum_{n=0}^{\infty} d_n(k|1,\ell) P'_{n+1}(\mu) \Big)}\, d\mu \tag{4.33}$$

$$= 2\pi \sum_{n=0}^{\infty}{}' \frac{d_n(k|1,\ell)^2 (n+2)(n+1)}{(2n+3)} \qquad (4.34).$$

Finally, for δ - waves,

$$Y_{2,\ell}(k) = \int_0^{2\pi} \begin{matrix}\cos^2 \\ \sin^2\end{matrix}(2\phi)\, d\phi \int_{-1}^{1} \overline{M}_{2,\ell}(k|\mu)\, M_{2,\ell}(k|\mu)\, d\mu \qquad (4.35)$$

$$= \pi \int_{-1}^{1} \Big(\sum_{n'=1}^{\infty}{}' d_{n'}(k|2,\ell) P_{n'+2}^2(\mu) \Big) \Big(\sum_{n=1}^{\infty} d_n(k|2,\ell) P_{n+2}^2(\mu) \Big) d\mu \qquad (4.36)$$

$$= 2\pi \sum_{n=1}^{\infty}{}' \frac{d_n(k|2,\ell)^2 (n+4)(n+3)(n+2)(n+1)}{(2n+5)} \qquad (4.37).$$

We note that the unnormalized asymptotic amplitudes must be found numerically for a given final state wave.

4.2. π_u (or $\bar{\pi}_u$) INITIAL STATES.

We have noted in section 4.1 that the selection rule on m is $\Delta m = 0, \pm 1$. Since π orbitals have m = 1 we again find that σ, π and δ-waves contribute to the cross sections. We find for $\bar{\pi}_u$ orbitals, from (2.28) and the expressions for the angular solutions Φ and M, that equations (4.5) $\longrightarrow$ (4.8) for $\bar{\pi}_g$ orbitals are also applicable. In this case however when we consider the parity of the integrands we obtain

$$|M_x|^2 = \sum_{\ell=2,4..}^{\infty}{}' |\mathcal{M}^x_{2,\ell}|^2 \tag{4.38}$$

$$|M_y|^2 = \sum_{\ell=2,4...}^{\infty}{}' |\mathcal{M}^y_{2,\ell}|^2 + \sum_{\ell=0,2..}^{\infty}{}' |\mathcal{M}^y_{0,\ell}|^2 \tag{4.39}$$

$$|M_z|^2 = \sum_{\ell=2,4...}^{\infty}{}' |\mathcal{M}^z_{1,\ell}|^2 \tag{4.40}.$$

Following the same procedures as in the last section we find

$$\mathcal{M}^x_{2,\ell} = \frac{C\pi R^5}{32}\int_1^{\infty}(\lambda^2-1)e^{-\alpha\lambda}\Lambda_{2,\ell}(\lambda) \times$$
$$\times\Big[\sum_{n=0}^{\infty}{}' d_n(R|2,\ell)\Big\{\lambda^2\big(G_n'(\alpha)-H_n'(\alpha)\big)+I_n'(\alpha)-H_n'(\alpha)\Big\}\Big]d\lambda \tag{4.41}$$

where G_n', H_n', I_n' are defined by the expressions in (4.14) except that $\sinh(c\mu)$ is replaced by $\cosh(c\mu)$, and

$$\mathcal{M}^{y}_{0,\ell} = \frac{c\pi R^5}{16}\int_1^\infty (\lambda^2-1)e^{-\alpha\lambda}\Lambda_{0,\ell}(\lambda)\times$$

$$\times\Big[\sum_{n=0}^{\infty}{}'d_n(h|0,\ell)\left\{\lambda^2(A_n'(\alpha)-B_n'(\alpha))+C_n'(\alpha)-B_n'(\alpha)\right\}\Big]d\lambda \quad (4.42)$$

where A_n', B_n', C_n' are defined by (4.16) with $\sinh(\alpha\mu)$ replaced by $\cosh(\alpha\mu)$. Further

$$\mathcal{M}^{z}_{1,\ell} = \frac{c\pi R^5}{16}\int_1^\infty (\lambda^2-1)^{\frac{1}{2}}e^{-\alpha\lambda}\lambda\Lambda_{1,\ell}(\lambda)\times$$

$$\times\Big[\sum_{n=1}^{\infty}{}'d_n(h|1,\ell)\left[\lambda^2 D_n'(\alpha)-E_n'(\alpha)\right]\Big]d\lambda \quad (4.43)$$

where D_n' and E_n' are the same as D_n and E_n except for the replacement of $\sinh(\alpha\mu)$ by $\cosh(\alpha\mu)$. Equation (4.6) also applies for $\overline{\pi}_u$ orbitals.

To evaluate the angular integrals A_n', B_n' etc. we define

$$J_n(\alpha) = \int_0^1 \mu^n\cosh(\alpha\mu)\,d\mu = \frac{1}{\alpha^{n+1}}\int_0^\alpha \cosh x\, x^n dx \quad (4.44)$$

where the J_n satisfy the recurrence relation

$$J_n = \alpha^{-(n+1)}\left[\alpha^n\sinh\alpha - n\alpha^{n-1}\cosh\alpha + n(n-1)\alpha^{n-1}J_{n-2}\right] \quad (4.45).$$

We then have

$$A_n'(\alpha), B_n'(\alpha), C_n'(\alpha) = \sum_{r=0}^{n/2}\frac{(-)^r(2n-r)!\,J_{n-2r,n-2r+2,n-2r+4}(\alpha)}{2^{n-1}r!\,(n-r)!\,(n-2r)!} \quad (4.46)$$

$$D_n'(\alpha), E_n'(\alpha) = (n+1)\sum_{r=0}^{\frac{n-1}{2}} \frac{(-)^r(2n-r)!}{2^{n-1}(n-r)!(n-2r)!} \times$$

$$\times \left\{ J_{n+1-2r,\,n+3-2r}(\alpha) - \left[\frac{(2n+2-r)(2n+1-r)}{2(n+1-r)(n+1-2r)}\right] J_{n+3-2r,\,n+5-2r}(\alpha) \right\} \tag{4.47}$$

$$G_n'(\alpha) = \sum_{r=0}^{\frac{n}{2}+1} \frac{(-)^r(2n-r+1)!}{2^{n+1}r!(n+2-r)!(n-2r)!} \left\{ J_{n-2r}(\alpha) - J_{n-2r+2}(\alpha) \right\} \tag{4.48}$$

with similar expressions for $H_n'(\alpha)$ and $I_n'(\alpha)$.

For the functions Y(h) which are used in (3.38) to find the asymptotic amplitudes of the normalized functions $G_{ml}(R,\lambda)$ the expressions (4.32), (4.34) and (4.37) which were developed for the πg initial state can also be used for πu orbitals except that the summations commence with n = 0, 1, and 0 respectively.

4.3. σ_g INITIAL STATES.

Initial σ states can only give rise to continuum waves with m = 0 or 1. We find then that on performing the ϕ - integrations and considering the parities of the μ - dependent parts of the integrands, that the contributions to the matrix elements are, in the case of a σ_g bound state,

$$|M_x|^2 = \sum_{\ell=1}^{\infty}{}' |\mathcal{M}^x_{1,\ell}|^2 \tag{4.49}$$

$$|M_y|^2 = \sum_{\ell=1}^{\infty}{}' |\mathcal{M}^y_{1,\ell}|^2 \tag{4.50}$$

$$|M_z|^2 = \sum_{\ell=1}^{\infty}{}' |\mathcal{M}^z_{0,\ell}|^2 \tag{4.51}$$

and clearly $\mathcal{M}^x_{1,\ell} = \mathcal{M}^y_{1,\ell}$.

We find it convenient to write

$$\mathcal{M}^x_{1,\ell} = \frac{\pi R^4}{16}\left[2(c_1-c_3)\mathcal{M}_x^{\,I} + R\left\{\mathcal{M}_x^{\,II} - \mathcal{M}_x^{\,III}\right\}\right] \tag{4.52}$$

where

$$\mathcal{M}_x^{\,I} = \int_1^{\infty}\int_{-1}^{1} e^{-\beta\lambda}\cosh(\beta\mu)(\lambda^2-1)^{\frac{1}{2}}(1-\mu^2)^{\frac{1}{2}} \times \\ \times\, \Lambda_{1,\ell}(\lambda) M_{1,\ell}(\mu)(\lambda^2-\mu^2)\,d\mu\,d\lambda \tag{4.53}$$

$$= \int_1^\infty e^{-\beta\lambda}(\lambda^2-1)^{\frac{1}{2}}\Lambda_{1,\ell}(\lambda) \times \Big[\sum_{n=0}^{\infty}{}' d_n(k|1,\ell)\{\lambda^2 Q_n(\beta) - R_n(\beta)\}\Big] d\lambda \tag{4.54}$$

with

$$Q_n(\beta), R_n(\beta) = \int_{-1}^{1} \cosh(\beta\mu)(1-\mu^2)^{\frac{1}{2}} P'_{n+1}(\mu)(1,\mu^2)\, d\mu \tag{4.55}.$$

For the second "component" of $\mathcal{M}_x$ we obtain,

$$\mathcal{M}_x^{II} = \int_1^\infty \int_{-1}^{1} e^{-\alpha\lambda}\{C_2\lambda + C_4\}\cosh(\alpha\mu)(\lambda^2-1)^{1/2} \times \tag{4.56}$$

$$\times (1-\mu^2)^{\frac{1}{2}}\Lambda_{1,\ell}(\lambda) M_{1,\ell}(\mu)(\lambda^2-\mu^2)\, d\mu\, d\lambda$$

$$= \int_1^\infty e^{-\alpha\lambda}(\lambda^2-1)^{1/2}(C_2\lambda + C_4)\Lambda_{1,\ell}(\lambda) \times$$

$$\times \Big[\sum_{n=0}^{\infty}{}' d_n(k|1,\ell)\{\lambda^2 Q_n(\alpha) - R_n(\alpha)\}\Big] \tag{4.57}$$

and for the third component,

$$\mathcal{M}_x^{III} = \int_1^\infty \int_{-1}^{1} e^{-\alpha\lambda}\{C_2 + C_4\lambda\}\mu\sinh(\alpha\mu)(\lambda^2-1)^{1/2} \times \tag{4.58}$$

$$\times (1-\mu^2)^{1/2}\Lambda_{1,\ell}(\lambda) M_{1,\ell}(\mu)(\lambda^2-\mu^2)\, d\mu\, d\lambda$$

$$= \int_1^\infty e^{-\alpha\lambda}\{C_2 + C_4\lambda\}(\lambda^2-1)^{1/2}\Lambda_{1,\ell}(\lambda) \times$$

$$\times \Big[\sum_{n=0}^{\infty}{}' d_n(k|1,\ell)\{\lambda^2 D_n(\alpha) - E_n(\alpha)\}\Big] d\lambda \tag{4.59}.$$

Similarly for $\mathcal{M}^z_{0,\ell}$ we adopt the notation

$$\mathcal{M}^z_{0,\ell} = \frac{\pi R^4}{8}\Big[2(C_1 - C_3)\mathcal{M}_z^I + R\{\mathcal{M}_z^{II} - \mathcal{M}_z^{III}\}\Big] \tag{4.60}$$

with

$$\mathcal{M}_z^{I} = \int_{1}^{\infty}\int_{-1}^{1} e^{-\beta\lambda}\cosh(\beta\mu)\,\lambda\mu\,\Lambda_{0,\ell}(\lambda)\,M_{0,\ell}(\mu)(\lambda^2-\mu^2)\,d\mu\,d\lambda \qquad (4.61)'$$

$$= \int_{1}^{\infty} e^{-\beta\lambda}\lambda\,\Lambda_{0,\ell}(\lambda)\Big[\sum_{n=1}^{\infty}{}' d_n(k/0,\ell)\left\{\lambda^2 F_n(\beta) - K_n(\beta)\right\}\Big]\,d\lambda \qquad (4.62)$$

where

$$F_n(\beta), K_n(\beta) = \int_{-1}^{1}\cosh(\beta\mu)\,P_n(\mu)\,(\mu,\mu^3)\,d\mu \qquad (4.63).$$

For the second part of $\mathcal{M}_z$ we find

$$\mathcal{M}_z^{II} = \int_{1}^{\infty} e^{-\alpha\lambda}(c_2\lambda + c_4)\,\lambda\,\Lambda_{0,\ell}(\lambda)\Big[\sum_{n=1}^{\infty}{}' d_n(k/0,\ell)\left\{F_n(\alpha)\lambda^2 - K_n(\alpha)\right\}\Big]\,d\lambda \qquad (4.64)$$

and finally

$$\mathcal{M}_z^{III} = \int_{1}^{\infty} e^{-\alpha\lambda}(c_2+c_4\lambda)\,\lambda\,\Lambda_{0,\ell}(\lambda)\Big[\sum_{n=1}^{\infty}{}' d_n(k/0,\ell)\left\{\lambda^2 B_n(\alpha) - C_n(\alpha)\right\}\Big]\,d\lambda \qquad (4.65).$$

For the angular integrals we have

$$Q_n(\beta) = (n+1)\int_{-1}^{1}\cosh(\beta\mu)\left[P_n(\mu) - \mu P_{n+1}(\mu)\right]d\mu \qquad (4.66)$$

so that, by comparing this equation with (4.26) for $D_n(\alpha)$ we have immediately

$$P_n(\beta) = (n+1)\sum_{r=0}^{n/2} \frac{(-)^r(2n-r)!}{2^{n-1}(n-r)!(n-2r)!} \times \tag{4.67}$$

$$\times \left\{ J_{n-2r}(\beta) - \left[\frac{(2n+2-r)(2n+1-r)\, J_{n+2-2r}(\beta)}{2(n+1-r)(n+1-2r)} \right] \right\}$$

with a similar expression for $R_n(\beta)$. Further, by comparing the definitions of $F_n(\beta)$ and $A_n(\alpha)$ we find

$$F_n(\beta), K_n(\beta) = \sum_{r=0}^{\frac{n-1}{2}} \frac{(-)^r(2n-r)!\, J_{n-2r+1,\, n-2r+3}(\rho)}{r!\, 2^{n-1}(n-r)!(n-2r)!} \tag{4.68}$$

The normalization functions Y(h) in the case of transitions from σ_g states have already been given in section 4.1, because the final state functions for π and σ waves are identical to those for π_g orbitals. We now turn our attention to the bound state orbital, σ_u.

From (2.38) and the equations for continuum states we find, as in the case of σ_g orbitals, that only π and σ final state waves contribute for a σ_u bound state. The total cross section is obtained from

$$|M_x|^2 = \sum_{\ell=2}^{\infty}{}' |\mathcal{M}^x_{1,\ell}|^2. \tag{4.69}$$

$$|M_y|^2 = \sum_{\ell=2}^{\infty}{}' |\mathcal{M}^y_{1,\ell}|^2 \tag{4.70}$$

$$|M_z|^2 = \sum_{\ell=0}^{\infty}{}' |\mathcal{M}^z_{0,\ell}|^2 \tag{4.71}$$

where again $\mathcal{M}^x_{1,\ell} = \mathcal{M}^y_{1,\ell}$.

To evaluate the contributions from π - continuum waves we write

$$\mathcal{M}^x_{1,\ell} = \frac{\pi R^4}{16}\left[2(C_3 - C_1)\mathcal{M}_x{}^{I} + R\left\{\mathcal{M}_x{}^{II} - \mathcal{M}_x{}^{III}\right\}\right] \tag{4.72}$$

whence,

$$\mathcal{M}_x{}^{I} = \int_1^{\infty} e^{-\beta\lambda}(\lambda^2-1)^{\frac{1}{2}}\Lambda_{1,\ell}(\lambda) \times \times\left[\sum_{n=1}^{\infty}{}' d_n(\ell|1,\ell)\left\{\lambda^2 L_n'(\beta) - M_n(\beta)\right\}\right] d\lambda \tag{4.73}$$

with

$$L_n(\beta), M_n(\beta) = \int_{-1}^{1} \sinh(\beta\mu)(1-\mu^2)^{\frac{1}{2}} P'_{n+1}(\mu)(1,\mu^2)\,d\mu \tag{4.74}$$

$$\mathcal{M}_x^{II} = \int_1^\infty e^{-\alpha\lambda}(c_4\lambda + c_2)(\lambda^2-1)^{1/2}\Lambda_{1,\ell}(\lambda) \times \times \Big[\sum_{n=1}^{\infty}{}' d_n(k|1,\ell)\{\lambda^2 D_n'(\alpha) - E_n'(\alpha)\}\Big] d\lambda \tag{4.75}$$

$$\mathcal{M}_x^{III} = \int_1^\infty e^{-\alpha\lambda}(c_4 + c_2\lambda)(\lambda^2-1)^{1/2}\Lambda_{1,\ell}(\lambda) \times \times \Big[\sum_{n=1}^{\infty}{}' d_n(k|1,\ell)\{\lambda^2 L_n(\alpha) - M_n(\alpha)\}\Big] d\lambda \tag{4.76}.$$

Further we find for transitions to σ - continuum states, on letting

$$\mathcal{M}_{0,\ell}^{z} = \frac{\pi R^4}{8}\Big[2(c_3-c_1)\mathcal{M}_z^{I} + R\{\mathcal{M}_z^{II} - \mathcal{M}_z^{III}\}\Big] \tag{4.77}$$

that

$$\mathcal{M}_z^{I} = \int_1^\infty e^{-\beta\lambda}\lambda\Lambda_{0,\ell}(\lambda)\Big[\sum_{n=0}^{\infty}{}' d_n(k|0,\ell)\{\lambda^2 S_n(\beta) - T_n(\beta)\}\Big] \tag{4.78}$$

where

$$S_n(\beta), T_n(\beta) = \int_{-1}^{1} \sinh(\beta\mu) P_n(\mu)\,(\mu, \mu^3)\,d\mu \tag{4.79}.$$

Furthermore, we have for the second and third parts of $\mathcal{M}_{0,\ell}^{z}$

$$\mathcal{M}_z^{II} = \int_1^\infty e^{-\alpha\lambda}(c_4\lambda + c_2)\lambda\Lambda_{0,\ell}(\lambda)\Big[\sum_{n=0}^{\infty}{}' d_n(k|0,\ell)\{\lambda^2 B_n'(\alpha) - C_n'(\alpha)\}\Big] d\lambda \tag{4.80}$$

$$M_2^{III} = \int_1^\infty e^{-\alpha\lambda}(c_1+c_2\lambda)\lambda\Lambda_{0,\ell}(\lambda)\Big[\sum_{n=0}^{\infty}{}' d_n(\ell|0,\ell)\{\lambda^2 S_n(\alpha)-T_n(\alpha)\}\Big]d\lambda \qquad (4.81).$$

To evaluate the angular integrals we note that

$$L_n(\beta) = (n+1)\int_{-1}^{1}\sinh(\beta\mu)[P_n(\mu)-\mu P_{n+1}(\mu)]\,d\mu \qquad (4.82)$$

so that by comparison with $D_n(\alpha)$ we find

$$L_n(\beta) = (n+1)\sum_{r=0}^{\frac{n-1}{2}}\frac{(-)^r(2n-r)!}{2^{n-1}(n-r)!(n-2r)!}\times$$
$$\times\left\{\vartheta_{n-2r}(\beta)-\left[\frac{(2n+2-r)(2n+1-r)}{2(n+1-r)(n+1-2r)}\vartheta_{n-2r+2}(\beta)\right]\right\} \qquad (4.83)$$

and a similar expression for $M_n(\beta)$. Furthermore we find

$$S_n(\beta), T_n(\beta) = \sum_{r=0}^{n/2}\frac{(-)^r(2n-r)!\,\vartheta_{n-2r+1,\,n-2r+3}(\beta)}{r!\,2^{n-1}(n-r)!(n-2r)!} \qquad (4.84).$$

We also note that for transitions from σ_u states the values of Y(h) can be obtained from those for π_u initial states.

One final point on <u>selection rules</u> for dipole transitions concerns the symmetry (g or u) of the initial and final states. We have already seen that the selection rule on the azimuthal quantum number m is $\Delta m = 0, \pm 1$. In addition we find that the symmetry properties with respect to inversion must be different for the initial and final electronic states. Thus we have

$$g \longrightarrow u \,, \quad u \longrightarrow g \tag{4.85}$$

as a further requirement for allowed transitions. Combining the two selection rules (4.4) and (4.85) we find that the following transitions may occur for the different bound state orbitals.

$$\left.\begin{array}{l}
\sigma_g \longrightarrow \sigma_u \\
\qquad \longrightarrow \pi_u \\
\\
\sigma_u \longrightarrow \sigma_g \\
\qquad \longrightarrow \pi_g \\
\pi_u, \bar{\pi}_u \longrightarrow \sigma_g \\
\qquad \longrightarrow \pi_g \\
\qquad \longrightarrow \delta_g \\
\pi_g, \bar{\pi}_g \longrightarrow \sigma_u \\
\qquad \longrightarrow \pi_u \\
\qquad \longrightarrow \delta_u
\end{array}\right\} \quad \begin{array}{l}\text{ALLOWED ELECTRONIC} \\ \text{TRANSITIONS IN PHOTO-} \\ \text{IONIZATION OF HOMONUCLEAR} \\ \text{DIATOMIC MOLECULES}\end{array} \tag{4.86}.$$

4.5. HIGH ENERGY CALCULATION FOR Π_g ORBITALS.

In section 3.1 it was indicated that plane waves could be used to describe the ejected electrons at high energies and that such a formulation had the advantage of being analytic by virtue of the expansion (3.1). Though we do not use this approach in finding numerical values for the cross section, it is interesting to see the form that the matrix elements take in this framework. We restrict our attention to photoionization from $1\Pi_g$ (or $1\bar{\Pi}_g$) orbitals.

From the formulae of section 1.2 we have for the total cross section

$$\sigma(\nu) = \frac{8\pi^3 m^2 e^2 \nu v}{3h^3 c} \sum_f |M_{fi}|^2 \qquad (4.87).$$

It is clear that the selection rule on m still applies. Then, with the notation of section 4.1 we have‡, from (2.26) and (3.1),

$$\mathcal{M}_x^{2,\ell}(k,\theta_0,\phi_0) = -\frac{c\pi R^5 (-)^\ell i^\ell M_{2\ell}(k,\cos\theta_0)}{8 N_{2\ell}(k)} \times \sin 2\phi_0 \, \chi^{2,\ell}(k,\alpha) \qquad (4.88)$$

with

$$\chi^{2,\ell}(k,\alpha) = \int_1^\infty \sum_{n=1}^{\infty}{}' d_n(k|2,\ell) \left[\lambda^2 \{G_n(\alpha) - H_n(\alpha)\} + I_n(\alpha) - H_n(\alpha)\right] \times e^{-\alpha\lambda}(\lambda^2-1) j_{2\ell}(k,\lambda)\, d\lambda. \qquad (4.89)$$

---

‡ The angular functions $M_{m\ell}$ are equivalent to the $S_{m\ell}$ of (3.1).

$$\mathcal{M}_y^{2,\ell}(k,\theta_0,\phi_0) = \mathcal{M}_x^{2,\ell}(k,\theta_0,\phi_0) \tag{4.90}$$

$$\mathcal{M}_y^{0,\ell}(k,\theta_0,\phi_0) = -\frac{C\pi R^5 (-)^\ell i^\ell M_{0,\ell}(k,\cos\theta_0)\chi^{0,\ell}(k,\alpha)}{8 N_{0\ell}(k)} \tag{4.91}$$

where

$$\chi^{0,\ell}(k,\alpha) = \int_1^\infty (\lambda^2-1) e^{-\alpha\lambda} j_{e0\ell}(k,\lambda)\Big[\sum_{n=1}^{\infty}{}' d_n(k|0,\ell)\Big\{\lambda^2(A_n(\alpha) - B_n(\alpha)) + C_n(\alpha) - B_n(\alpha)\Big\}\Big] d\lambda \tag{4.92}$$

and finally,

$$\mathcal{M}_z^{1,\ell}(k,\theta_0,\phi_0) = -\frac{CR^5\pi(-)^\ell i^\ell M_{1\ell}(k,\cos\theta_0)\sin\phi_0}{4 N_{1\ell}(k)} \times \chi^{1,\ell}(k,\alpha) \tag{4.93}$$

$$\chi^{1,\ell}(k,\alpha) = \int_1^\infty e^{-\alpha\lambda} j_{e1\ell}(k,\lambda)\lambda(\lambda^2-1)^{\frac{1}{2}} \sum_{n=0}^{\infty}{}' d_n(k|1,\ell) \times \{\lambda^2 D_n(\alpha) - E_n(\alpha)\} d\lambda \tag{4.94}.$$

Integrations over (θ_0, ϕ_0) can be easily performed to give for the total cross section

$$\sigma(\nu) = \frac{C^2 R^{10}\pi^6 m^2 e^2 \nu v}{6k^3 c}\left[\sum_{\ell=1}^{\infty}{}' |\chi^{1,\ell}(k,\alpha)|^2 + \frac{1}{2}\sum_{\ell=1}^{\infty}{}' |\chi^{0,\ell}(k,\alpha)|^2 + \frac{1}{2}\sum_{\ell=3}^{\infty}{}' |\chi^{2,\ell}(k,\alpha)|^2\right] \tag{4.95}.$$

It can be seen from (3.4) and the above expressions for the matrix elements that the evaulation of the latter will involve integrals of the types

$$\int_1^\infty \lambda^p (\lambda^2-1)^{1/2} e^{-\alpha\lambda} j_n(k\lambda)\, d\lambda \qquad (4.96)$$

$$\int_1^\infty \lambda^p e^{-\alpha\lambda} j_n(k\lambda)\, d\lambda \qquad (4.97).$$

For these the asymptotic relation

$$j_n(k\lambda) \sim \frac{(k\lambda)^n}{1.3.5\ldots(2n+1)} \qquad (4.98)$$

was found to be not valid in the important range of λ. Furthermore, although integrals of the above type may be evaluated analytically it would probably be more efficient to use numerical methods for them if the results of this section were employed to calculate the cross section.

CHAPTER 5.

RESULTS AND DISCUSSION FOR FIXED NUCLEI.

We have noted in Ch. 1 that the vibrational and rotational eigenfunctions should be taken into account in accurate calculations of transition probabilities for molecular processes. In this chapter we give results for the cross sections obtained by the formulae developed in Ch. 4 where the nuclei were assumed fixed in the transitions so that the integrands of the various matrix elements have only been regarded as functions of $\underline{r}$, the electron co-ordinate. In most cases where the equilibrium internuclear separations of the ground electronic states of the molecule and the ion are not very much different we expect that including the effects of the different vibrational states of the ion (assuming a zeroth vibrational level for the molecule) will only affect the transition probabilities near the thresholds for photo-ionization. Studying the variation of the cross section curves with energy for fixed nuclei is expected to reveal their important overall features. This chapter divides into five parts, the first of which is concerned with details of the numerical procedures, the remainder being concerned with specific results.

5.1. DETAILS OF THE NUMERICAL METHODS.

For fixed nuclei calculations four programmes, one for each kind of initial state orbital, were written for a C.D.C. 6400 computer. Listings of these are given in appendix 3 together with brief explanatory notes.

The parameter $k = (R^2\varepsilon/4)^{1/2}$ is the basic energy variable. Values of the coefficients $d_n(k/m,\ell)$ in (3.20) and (3.21) and the $t_{m\ell}(k)$ in (3.22) are given only for discrete values of k. The values employed were h = 0(·1)1; h = 1(·2)2·2 ; h = 3(1)5 , which gives energies above the thresholds 19·2 I_H for O_2 and 23·4 I_H for N_2, if we use the equilibrium internuclear separations of $2{\cdot}282a_o$ and $2{\cdot}067a_o$ respectively as given by Herzberg[44].

The normalized radial functions $\Lambda_{m\ell}(k,\lambda)$ were evaluated at intervals of ·1 in λ from $\lambda = 1$ to $\lambda = 11$, at which latter value the bound state radial functions have become negligible. The power series expansion (3.30) was used to find unnormalized $\Lambda_{m\ell}(k,\lambda)$ at λ = 1, 1·1, 1·2 and then the recurrence relation (3.34) was employed to extend the corresponding $G_{m\ell}(k,\lambda)$ to $\lambda = 11$. Correction terms as given by (3.35) were found to be

negligible in the cases tried. The application of the normalization procedure as described in section 3.4 was carried out by means of a subroutine (AMP) which generated $G_{me}(R,\lambda)$ to $\lambda = 40{\cdot}7$, so that the function $U(\lambda)$ could be determined in the interval $[\,39{\cdot}7,\ 40{\cdot}7\,]$. This latter step was found necessary in order to make $\omega \ll \nu$.

The various continuum waves which were taken into account for the various orbitals are given in table 5.1.

TABLE 5.1.

Initial State.	Continuum Waves.
σ_g	$p\sigma_u, f\sigma_u, h\sigma_u$; $p\pi_u, f\pi_u, h\pi_u$
σ_u	$s\sigma_g, d\sigma_g, g\sigma_g$; $s\pi_g, d\pi_g, g\pi_g$
π_g	$p\sigma_u, f\sigma_u, h\sigma_u$; $p\pi_u, f\pi_u, h\pi_u$; $f\delta_u, h\delta_u$
π_u	$s\sigma_g, d\sigma_g, g\sigma_g$; $d\pi_g, g\pi_g, i\pi_g$; $g\delta_g, d\delta_g, i\delta_g$

Because $\ell = 5$ and $\ell = 6$ waves only play a minor role in the total cross sections the inclusion of states with higher angular momentum than those in table 5.1 was not necessary. In the evaluation of the radial transition integrals a subroutine for Simpson's rule (SIMP2) was employed, whose accuracy had been tested on certain standard integrals.

5.2 PARTIAL CROSS SECTIONS FOR INDIVIDUAL ORBITALS AND THEIR BEHAVIOUR NEAR THRESHOLDS.

Cross sections for the nine transitions from O_2 and for the four transitions in N_2 indicated in table 2, were calculated using Sahni and Lorenzo's initial state L.C.A.O.-M.O.'s. As mentioned in Ch. 2 transitions from pairs of M.S.O.'s in O_2 which have the same spatial wave functions in the restricted treatment have very similar cross section curves. We note that all results quoted in this section are for the photo-ejection of one electron.

The results for individual orbitals are presented in figs. 5.1 to 5.9 where the independant variable is taken as the incident photon wavelength. For $1\pi_g$ (or $1\bar{\pi}_g$) orbitals there is only one transition i.e. $O_2(X^3\Sigma_g^-) \rightarrow O_2^+(X^2\Pi_g)$. (See fig. 5.1). The chief contributions for this process near threshold come from $p\pi_u$ and $p\sigma_u$ waves, the transition probabilities to which both decrease rapidly as the energy increases. The declines can be explained by reference to figs. 5.10 and 5.11, where there are shown the most important final state radial functions for selected values of h, together with the bound state radial function. The first nodes of the continuum waves occur at relatively small values of $\lambda (\simeq \psi)$ for $h = 0$ ($\varepsilon = 0$, spectral head). As h increases the node

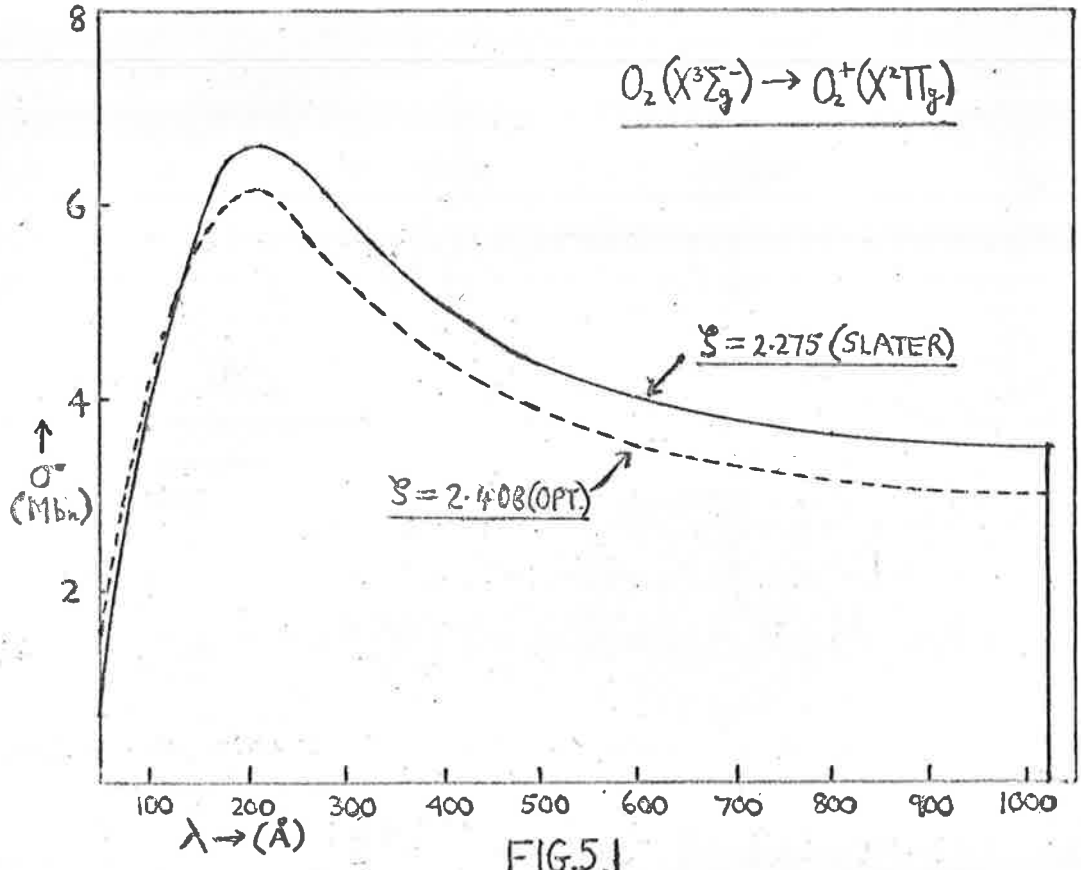
$O_2(X^3\Sigma_g^-) \rightarrow O_2^+(X^2\Pi_g)$
$S = 2.275$ (SLATER)
$S = 2.408$ (OPT.)
σ (Mb)
$\lambda \rightarrow$ (Å)
8
6
4
2
100
200
300
400
500
600
700
800
900
1000

FIG.5.1

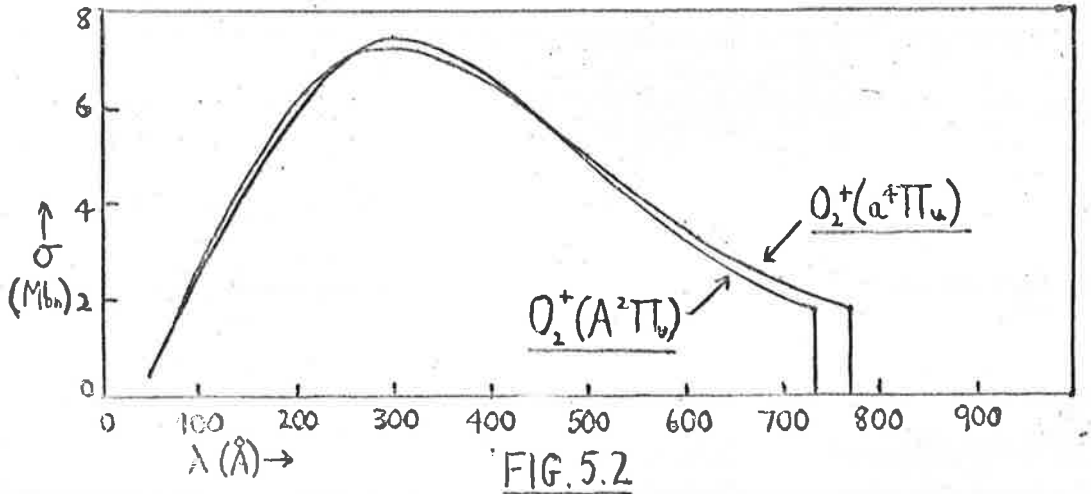
$O_2^+(a^4\Pi_u)$
$O_2^+(A^2\Pi_u)$
σ (Mb)
λ (Å)$\rightarrow$
8
6
4
2
0
0
100
200
300
400
500
600
700
800
900

FIG. 5.2

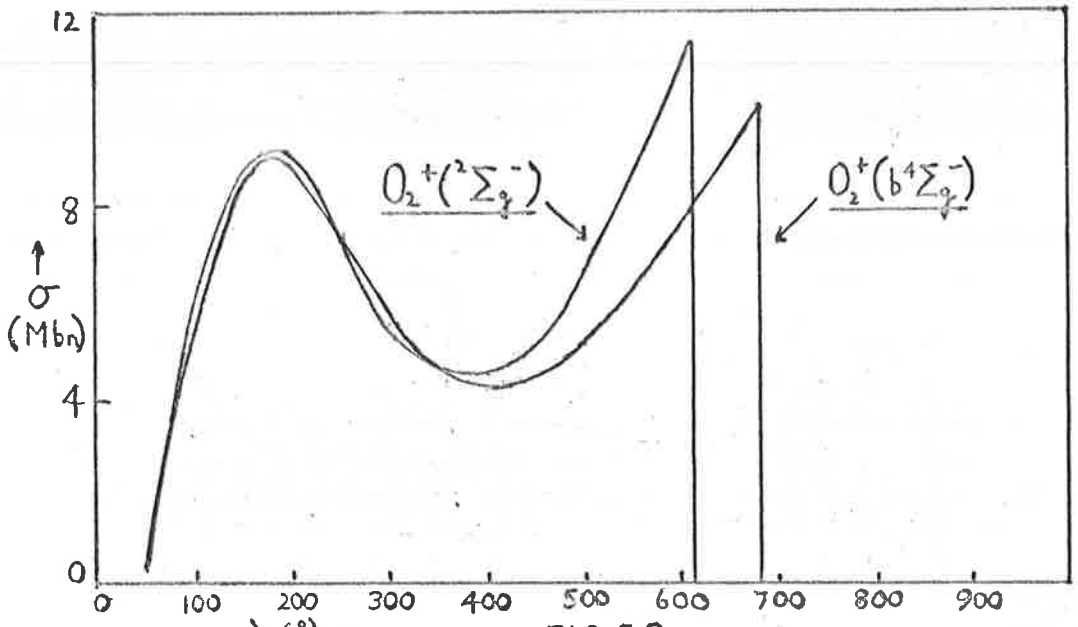
12
8
4
0
σ
(Mb)
$O_2^+(^2\Sigma_g^-)$
$O_2^+(b^4\Sigma_g^-)$
0
100
200
300
400
500
600
700
800
900
λ (Å)→

FIG. 5.3

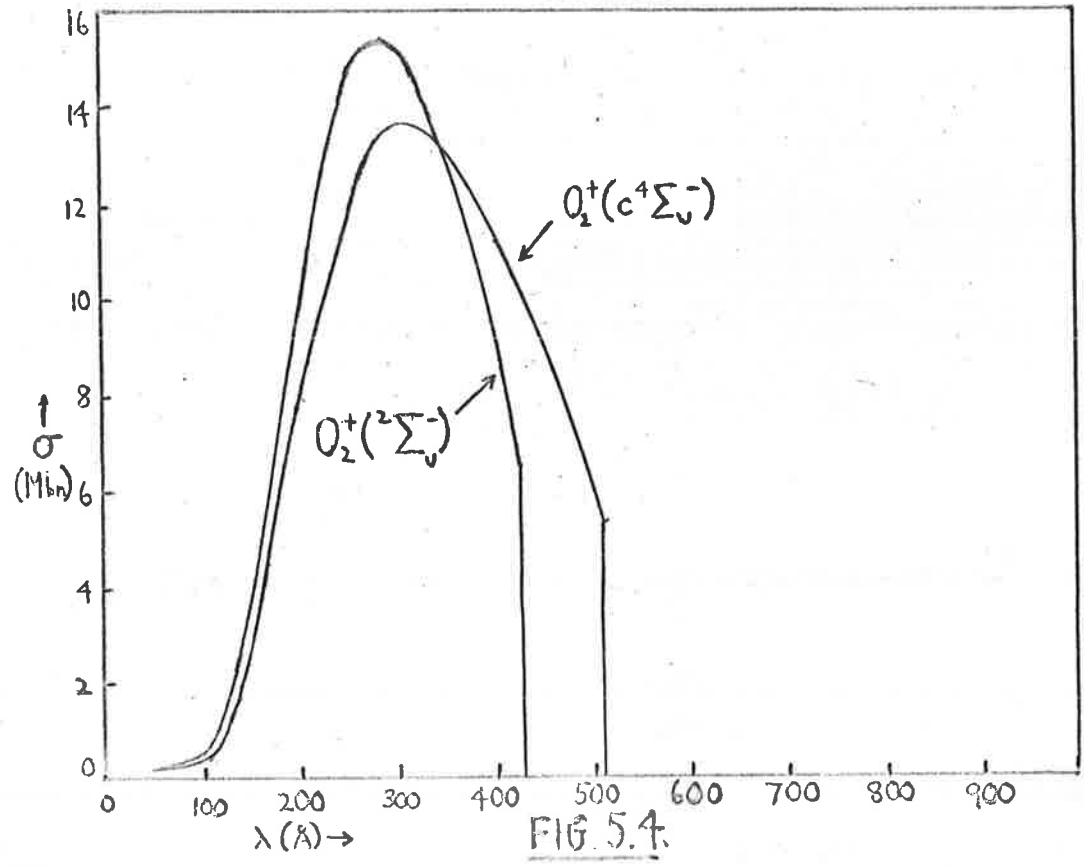
16
14
12
10
8
6
4
2
0
σ
(Mb)
$O_2^+(c^4\Sigma_u^-)$
$O_2^+(^2\Sigma_u^-)$
0
100
200
300
400
500
600
700
800
900
λ (Å)→

FIG. 5.4.

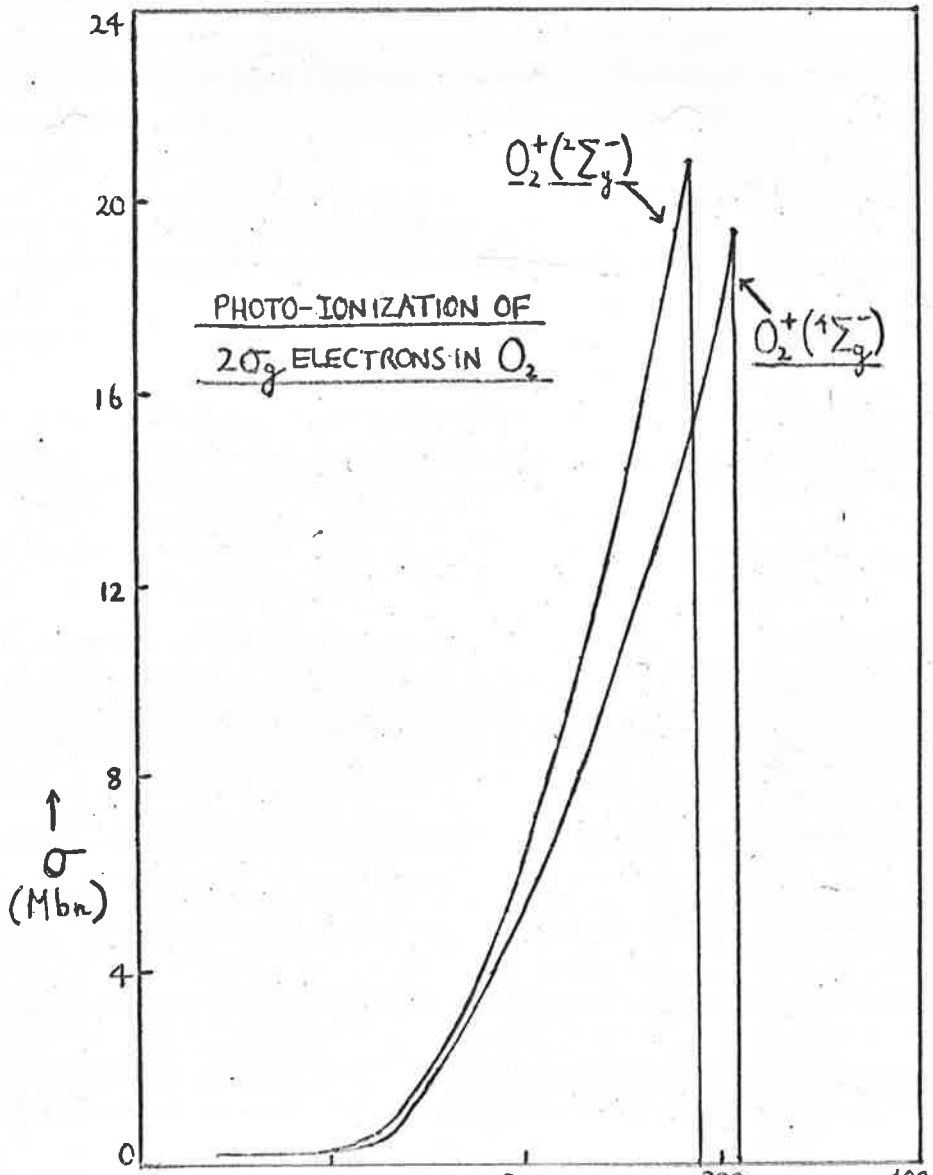
24
20
16
12
8
4
0
$O_2^+(^2\Sigma_g^-)$
$O_2^+(^4\Sigma_g^-)$
PHOTO-IONIZATION OF
$2\sigma_g$ ELECTRONS IN O_2
σ (Mbn)
100
200
300
400
$\lambda \rightarrow$ (Å)

FIG 5.5

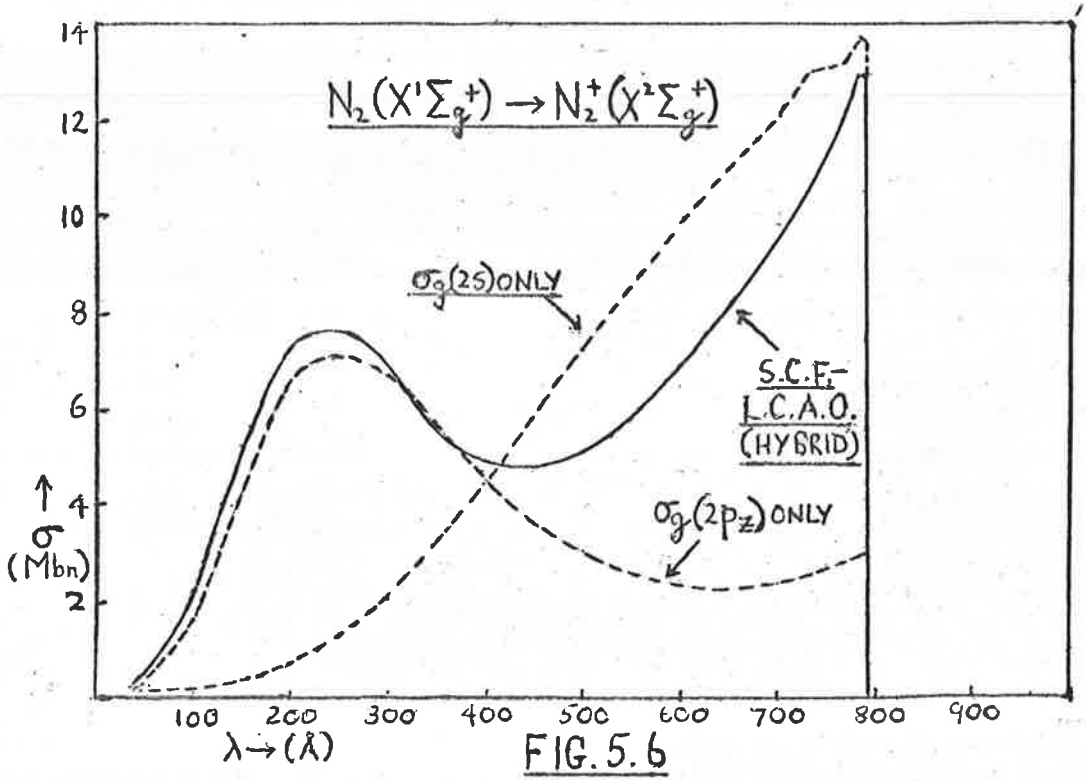
$N_2(X^1\Sigma_g^+) \rightarrow N_2^+(X^2\Sigma_g^+)$
$\sigma_g(2s)$ ONLY
S.C.F.-L.C.A.O. (HYBRID)
$\sigma_g(2p_z)$ ONLY
σ (Mbn)
λ → (Å)
14
12
10
8
6
4
2
100
200
300
400
500
600
700
800
900

FIG. 5.6

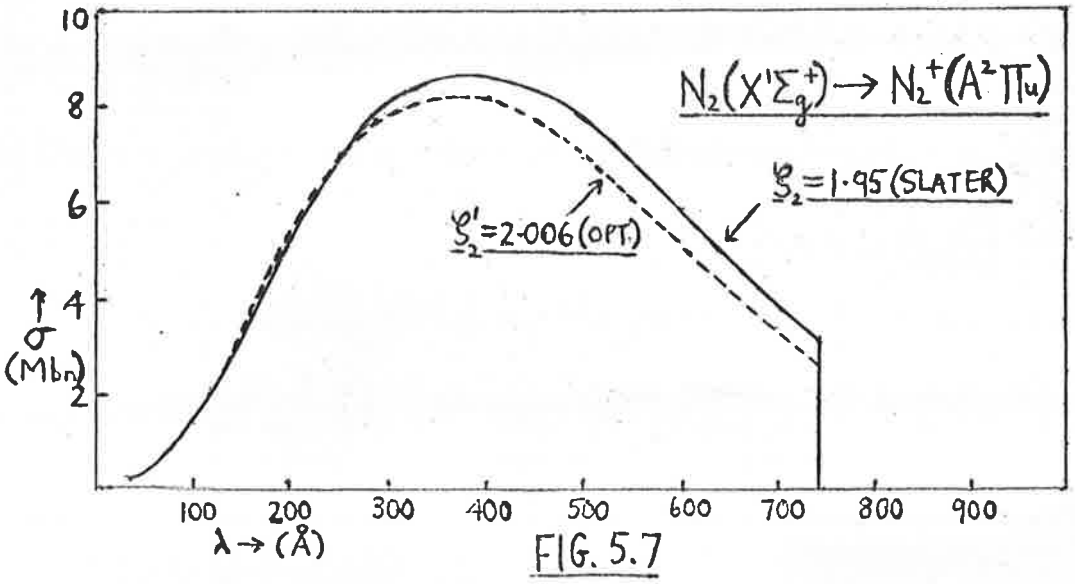
$N_2(X^1\Sigma_g^+) \rightarrow N_2^+(A^2\Pi_u)$
$\zeta_2 = 1.95$ (SLATER)
$\zeta_2' = 2.006$ (OPT.)
σ (Mbn)
λ → (Å)
10
8
6
4
2
100
200
300
400
500
600
700
800
900

FIG. 5.7

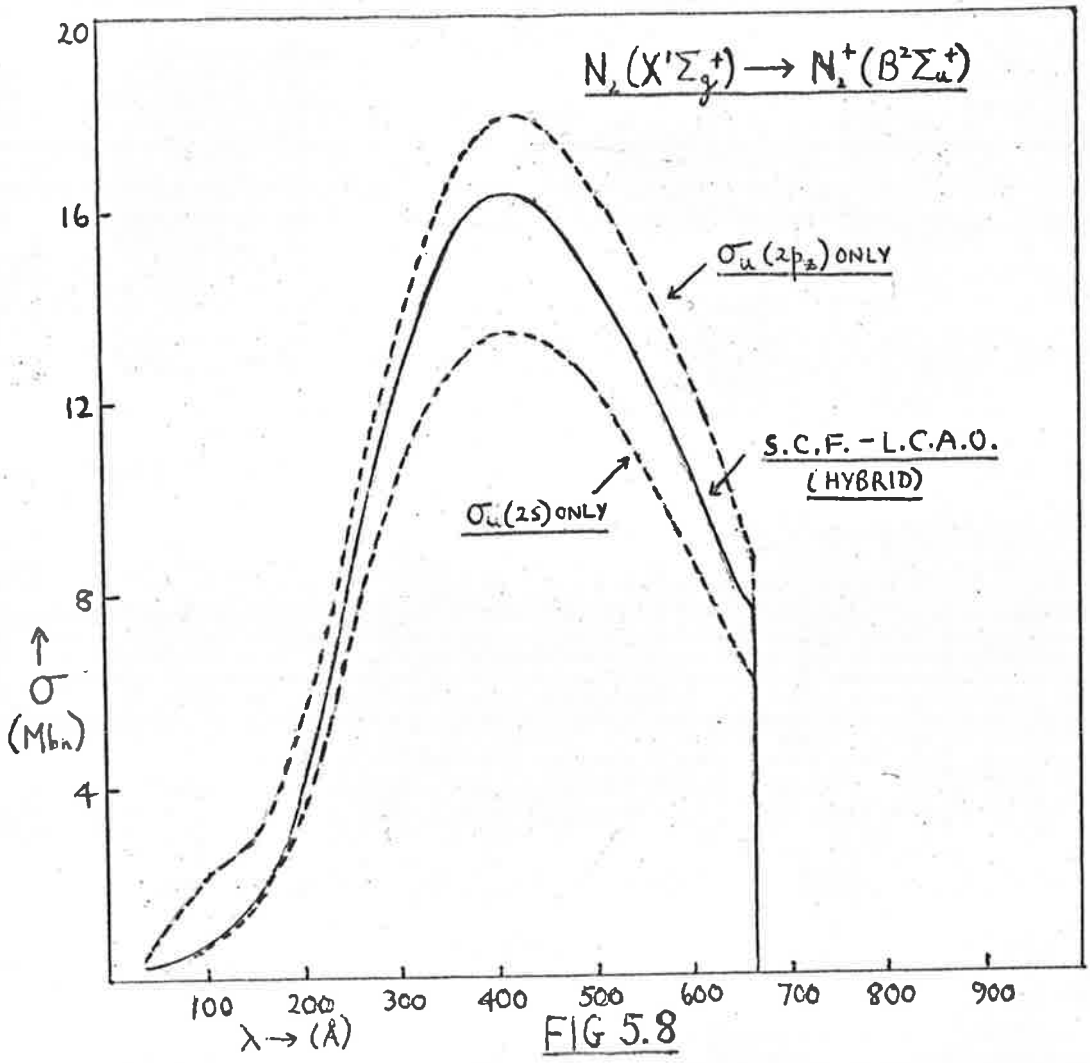
$N_2(X'\Sigma_g^+) \longrightarrow N_2^+(B^2\Sigma_u^+)$
$\sigma_u(2p_z)$ ONLY
S.C.F. - L.C.A.O.
(HYBRID)
$\sigma_u(2s)$ ONLY
20
16
12
8
4
σ (Mbn)
100
200
300
400
500
600
700
800
900
λ → (Å)

FIG 5.8

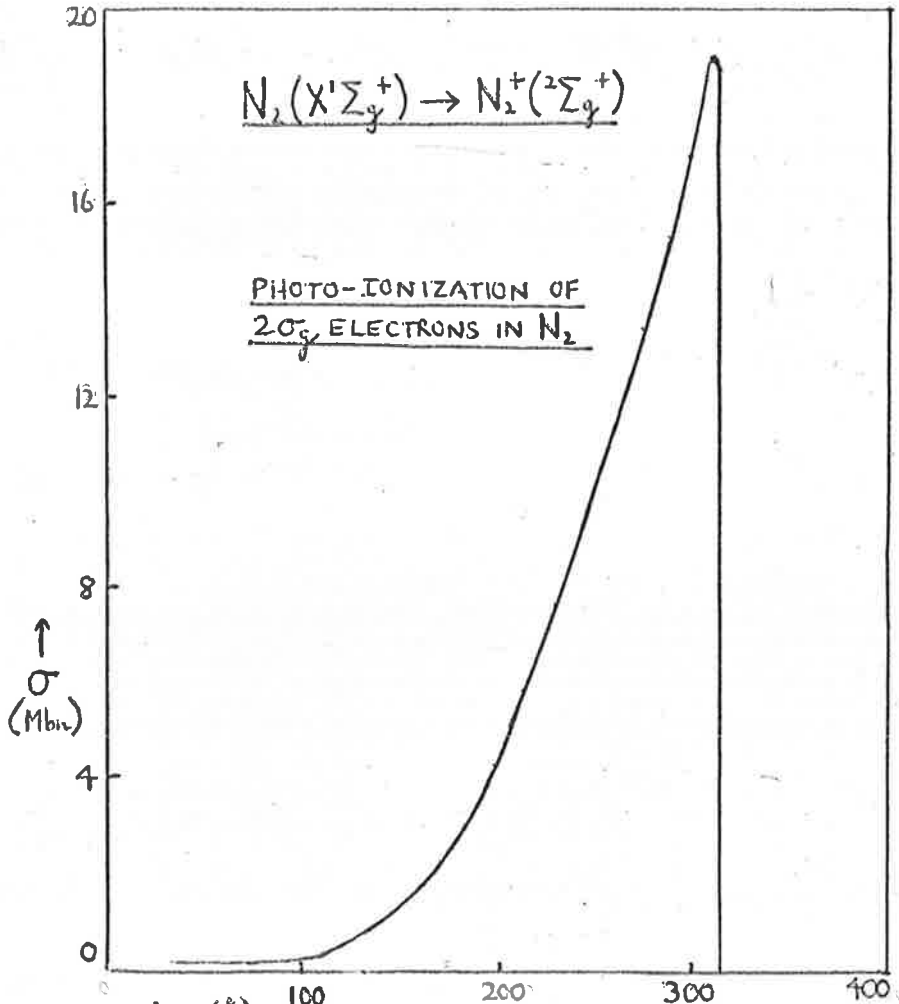
$N_2(X^1\Sigma_g^+) \rightarrow N_2^+(^2\Sigma_g^+)$
PHOTO-IONIZATION OF
$2\sigma_g$ ELECTRONS IN N_2
20
16
12
8
4
0
σ
(Mbn)
100
200
300
400
λ → (Å)

FIG. 5.9.

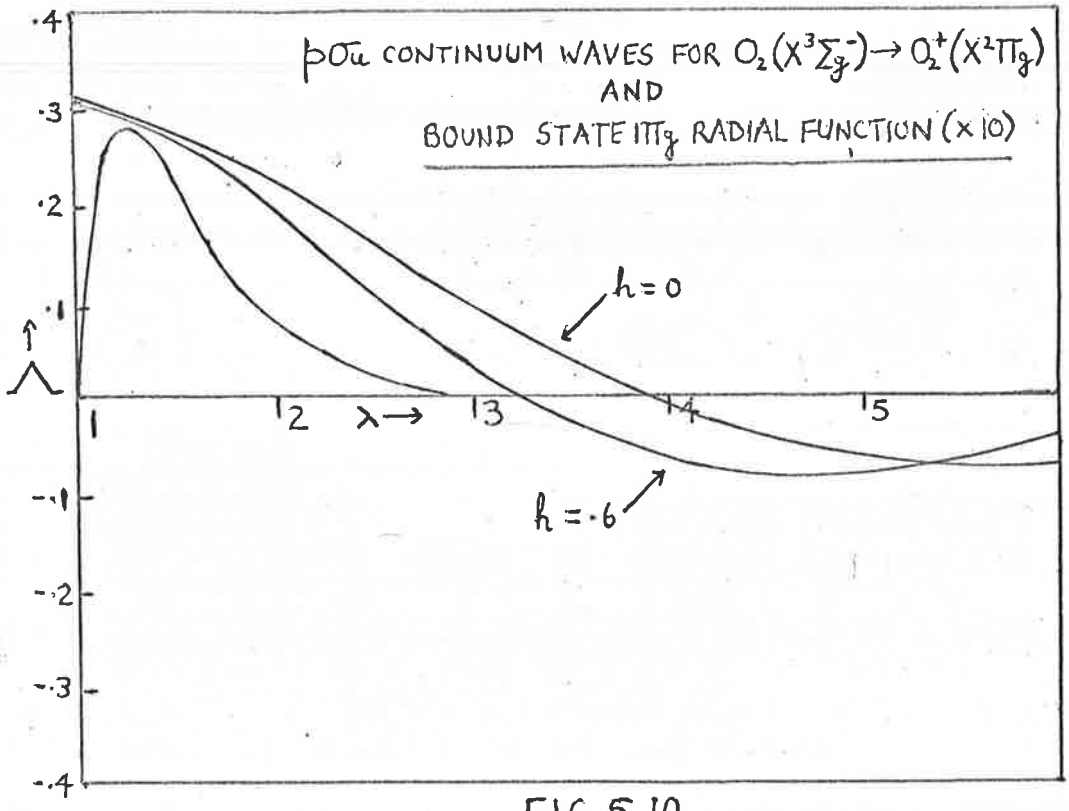

FIG 5.10

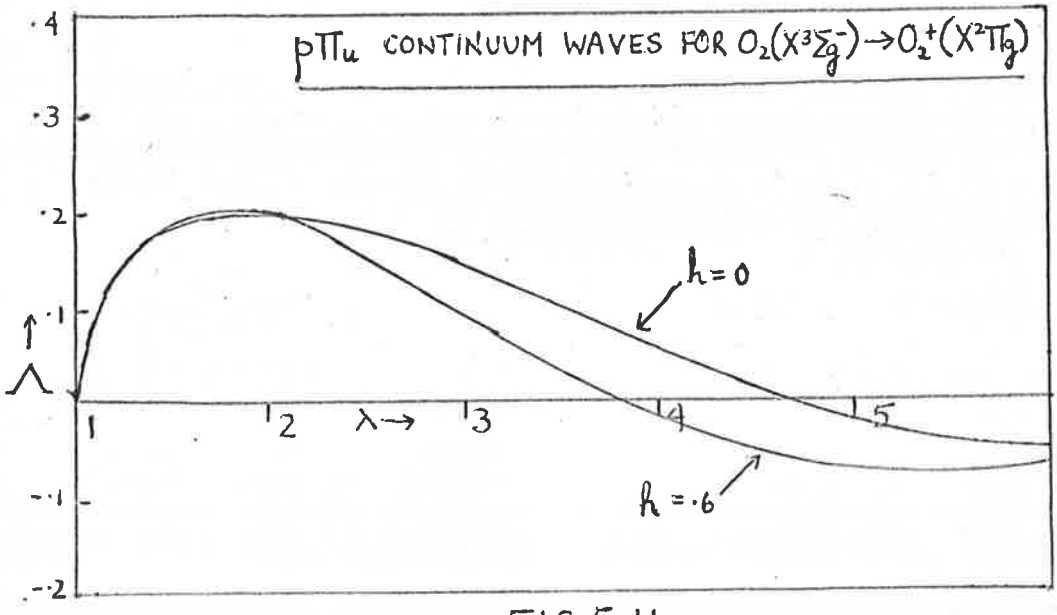

FIG 5.11

moves inward causing the negative contributions to the transition integrals $\int_1^\infty (\lambda^2-1) e^{-\alpha\lambda} \Lambda_{0,\ell}\, d\lambda$ and $\int_1^\infty (\lambda^2-1)^{\frac{1}{2}} e^{-\alpha\lambda} \lambda \Lambda_{1,\ell}\, d\lambda$ to increase with a consequent decrease in the corresponding matrix elements. The fact that the cross section remains almost steady (see fig.5.1) is due to the increasing value of $\mathcal{E}$ in the term $(E_i + \mathcal{E})$ in (1.7), which compensates the above decrease, as well as growing contributions from higher angular momentum states. (See section 5.5).

For σ_g orbitals, as the curves in figs. 5.3, 5.5, 5.6 and 5.9 indicate, the cross sections are high at the spectral head and decrease rapidly as the energy increases. This behaviour is attributable to the decreasing matrix elements for the most important continuum waves, $p\sigma_u$ and $p\pi_u$. The fact that the bound state function has a node near the nodes of the continuum waves enhances the possibility of a rapid decrease. We note that a factor which makes the cross section decrease (in contrast with π_g) is that $\Delta\mathcal{E}/E_i$ is small so there is little chance of the increase of $\mathcal{E}$ seriously compensating the decreasing transition integrals. The chief reason for a decrease, however, is that the $p\sigma_u$ waves completely dominate the low energy cross section so that despite their increases, contributions from higher angular

momentum states have no effect until much higher energies where the $p\sigma_u$ contributions are negligible. In section 5.4 we will discuss the relative importances of the various atomic orbitals in the σ_g L.C.A.O. wave functions in connection with this near threshold behaviour.

The cross sections for orbitals of u-symmetry behave in the opposite fashion to those of g-symmetry near threshold. In figures 5.2 and 5.7 are shown the cross sections for processes to $O_2^+ (a^4\pi_u, A^2\pi_u)$ and $N_2^+ (A^2\pi_u)$. The curves steadily increase because of the increasing matrix elements involving $d\pi_g$ and $d\delta_g$ continuum waves near threshold. We seek an explanation in terms of the positions of the nodes of the final state waves and to this end we have plotted these for the cases h = 0 and h = ·6 in figures 5.12 and 5.13 for O_2. (The bound state radial function is the same as the $1\pi_g$ function which is shown in fig. 5.10). For the waves concerned the first nodes at h = 0 are at relatively large values of λ. The negative parts of the important transition integrals, $\int_1^\infty (\lambda^2-1)^{\frac{1}{2}} e^{-\alpha\lambda} \lambda \Lambda_{1,2}\, d\lambda$ and $\int_1^\infty (\lambda^2-1)\, e^{-\alpha\lambda} \Lambda_{2,2}\, d\lambda$ are thus very small. As h increases the nodes move inwards but the negative parts of the integrals, still occurring at large λ and hence very small $e^{-\alpha\lambda}$, are small; further the positive parts of the integrals increase,

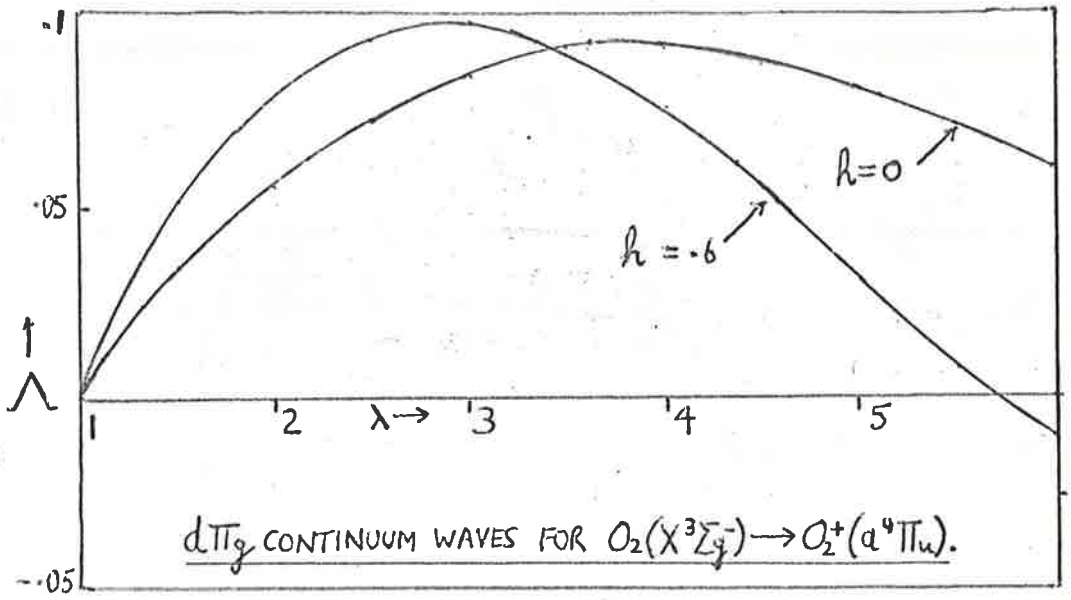

FIG. 5.12

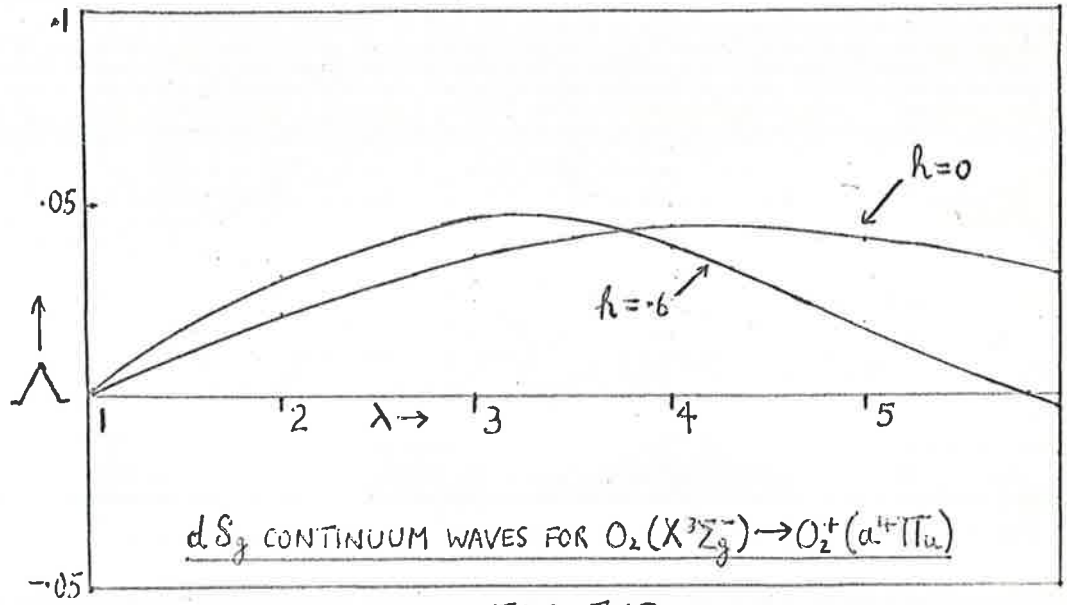

FIG. 5.13

as can be seen by comparing the waves $\Lambda_{1,2}$ (h = ·6), $\Lambda_{2,2}$ (h =·6) with $\Lambda_{1,2}$ (h = 0), $\Lambda_{2,2}$ (h = 0) in the region $1 < \lambda < 2.5$ where the bound function is greatest. The net effect is an increase in the matrix elements with a subsequent rise in the cross section above threshold. Not until $k \simeq .7$ does cancellation become appreciable enough to cause the above transition integrals to decrease.

The remaining orbital type, σ_u, gives rise to cross section curves which increase even more rapidly from threshold than π_u orbitals as can be seen in figs. 5.4 and 5.8. In this case the major contributions are from $d\sigma_g$ and $d\pi_g$ states, the former providing the dominant influence. Since these states have relatively high angular momentum ($\ell = 2$), their first nodes occur at large λ and the near threshold behaviour can be explained by the same arguments as for the π_u case.

The angular integrals $A_n(\alpha)$, $B_n(\alpha)$.... etc. have little influence on the variation of the cross sections with energy but are important in determining their magnitudes at a given energy. Tables 5.2 to 5.8 show the computed values of these integrals.

TABLE 5.2 (62)

ANGULAR INTEGRALS FOR TRANSITIONS IN O_2 USING L.C.A.O.-M.O.'S

n	An(α)	Bn(α)	Cn(α)
1	3·213959	2·119753	1·593764
3	·478443	·804782	·810172
5	·029233	·111676	·220889
7	·000952	·006780	·027521
9	·000019	·000222	·001624
11	·000000	·000004	·000043

n	Gn(α)	Hn(α)	In(α)
1	16·413096	7·889823	4·701555
3	25·397306	21·751945	16·487217
5	26·585077	26·157581	24·608654
7	26·652262	26·629756	-
9	26·654338	-	-
11	-	-	-

n	Dn(α)	En(α)
0	1·094206	·525988
2	2·303602	1·561795
4	·586028	·994172
6	·050573	·193706
8	·002127	·015159
10	·000056	·000716

TABLE 5.3 (62)

ANGULAR INTEGRALS FOR TRANSITIONS IN O_2 USING L.C.A.O.-M.O.'S

n	An'(α)	Bn'(α)	Cn'(α)
0	5·134948	2·658280	1·867997
2	1·419946	1·472855	1·241746
4	·129542	·337789	·460740
6	·005646	·030058	·086361
8	·000142	·001312	·007268
10	·000002	·000033	·000312

n	Gn'(α)	Hn'(α)	In'(α)
0	7·430003	2·370849	1·252501
2	22·914853	15·991645	10·624575
4	26·631726	25·223583	21·855933
6	26·939926	26·833336	26·285141
8	26·952537	26·948424	26·911214
10	-	-	-

n	Dn'(α)	En'(α)
1	2·370849	1·252501
3	1·379133	1·454023
5	·191428	·501444
7	·011190	·059665
9	·000354	·003269
11	·000035	·001141

TABLE 5.4

(62)

ANGULAR INTEGRALS FOR TRANSITIONS IN N_2 USING L.C.A.O. -M.O.'S.

n	An'(α)	Bn'(α)	Cn'(α)
0	3·657634	1·697764	1·151296
2	·717829	·878062	·740581
4	·041917	·158304	·250269
6	·001135	·009370	·037998
8	·000018	·000258	·002188
10	·000000	·000004	·000062

n	Gn'(α)	Hn'(α)	In'(α)
0	5·879610	1·639404	·821429
2	13·990550	10·276494	6·705173
4	15·214000	14·744517	13·073304
6	15·276599	15·254777	15·078650
8	15·278166	15·277648	15·270005
	-	-	-

n	Dn'(α)	En'(α)
1	1·639404	·821429
3	·693158	·866010
5	·061815	·234415
7	·002248	·018576
9	·000043	·000622
11	-·000084	-·005090

(62)

TABLE 5.5

ANGULAR INTEGRALS FOR TRANSITIONS IN O_2 USING L.C.A.O.-M.O.'S

n	$Q_n(\alpha)$	$Q_n(\beta)$	$R_n(\alpha)$	$R_n(\beta)$
0	2·476668	150·014646	·790283	96·258580
2	2·212121	496·917378	1·945828	367·569674
4	·337898	442·266851	·839267	407·657827
6	·020547	198·357519	·107317	236·719568
8	·000664	54·083494	·006057	84·315469
10	·000014	9·891060	·000202	19·994730

n	$F_n(\alpha)$	$F_n(\beta)$	$K_n(\alpha)$	$K_n(\beta)$
1	2·658280	593·522208	1·867997	497·263629
3	·682572	352·875759	·824246	326·611114
5	·061962	140·193044	·169935	153·187130
7	·002711	38·145114	·014727	51·427078
9	·000069	7·341147	·000639	12·468746
11	·000001	1·033610	·000015	2·219497

TABLE 5.6

ANGULAR INTEGRALS FOR TRANSITIONS IN N_2 USING L.C.A.O.-M.O.'S. (62)

n	$Q_n(\alpha)$	$Q_n(\beta)$	$R_n(\alpha)$	$R_n(\beta)$
0	1·959870	36·321858	·546468	20·890733
2	1·158706	102·197713	1·233870	73·530971
4	·111223	70·273856	·406184	69·999438
6	·004173	22·853558	·003402	32·404576
8	·000082	4·333640	·001204	8·637391
10	·000000	·536057	−·000018	1·461522

n	$F_n(\alpha)$	$F_n(\beta)$	$K_n(\alpha)$	$K_n(\beta)$
1	1·697764	110·680416	1·151296	89·789682
3	·331594	58·453582	·466772	54·833992
5	·019673	18·849383	·077067	22·451362
7	·000539	3·872279	·004510	6·155563
9	·000008	·534069	·000124	1·145281
11	·000000	·005197	·000006	·148677

TABLE 5.7

(62)

ANGULAR INTEGRALS FOR TRANSITIONS IN O_2 USING L.C.A.O.-M.O.'S.

n	Ln(α)	Ln(β)	Mn(α)	Mn(β)
1	3•282619	354•160899	1•577964	241•024510
3	•998246	520•574060	1•540236	426•792886
5	•091367	317•863647	•338895	332•506447
7	•003952	109•424783	•027775	149•281279
9	•000099	24•202890	•001141	43•032328
11	•000009	3•717894	•000253	8•513026

n	Sn(α)	Sn(β)	Tn(α)	Tn(β)
0	3•213959	658•893970	2•119753	540•840337
2	1•572649	481•813521	1•330770	420•328082
4	•228882	233•616373	•419723	233•288357
6	•014005	76•524286	•055194	92•512039
8	•000458	17•437096	•003308	26•350958
10	•000009	2•858497	•000108	5•460917

TABLE 5.8

(62)

ANGULAR INTEGRALS FOR TRANSITIONS IN N_2 USING L.C.A.O.-M.O.'S.

n	Ln(α)	Ln(β)	Mn(α)	Mn(β)
1	2•136729	80•153346	•987040	50•640685
3	•415909	95•020633	•882959	79•848596
5	•023658	43•281932	•133905	51•429704
7	•000628	10•558100	•006993	17•800805
9	•000011	1•599489	•000240	3•742464
11	•000268	•164460	•014170	•518599

n	Sn(α)	Sn(β)	Tn(α)	Tn(β)
0	1•975240	125•776895	1•262997	99•059113
2	•906875	85•700222	•769477	73•738771
4	•090655	35•227282	•219724	36•896393
6	•003530	9•009500	•020815	12•355057
8	•000072	1•506605	•000811	2•782856
10	•000001	•173534	•000010	•430742

5.3 EFFECTS OF VARYING THE BOUND STATE PARAMETER ζ_i FOR π ORBITALS.

The atomic orbitals used to synthesize the molecular orbitals in S.C.F.-L.C.A.O.-M.O.'s in most calculations done so far have been of the Slater type. These are chosen presumably because of their simplicity and convenience in the formulation of primitive M.O.'s. It has been pointed out by various authors that L.C.A.O.-M.O.'s are not as accurate in their description of molecular wave functions as Hartree-Fock M.O.'s. There is however, considerably uncertainty about the best A.O.'s to use in an L.C.A.O.-M.O. calculation; the S.C.F.-Hartree-Fock A.O.'s which are best for atoms, apparently have no claims to superiority in describing the electronic states of molecules which contain those atoms. Further, the accuracy of L.C.A.O.-M.O.'s can be tested only by comparing the two calculated quantities in the R.H.S. of equation (2.21). Thus even though the value of ε_i may be close to the experimental ionization potential there may be no reason for assuming that molecular wave functions themselves are accurate. For these reasons it seemed worthwhile to see the effects of varying the bound state parameter ζ_i which is basic in the formulation of π molecular orbitals. As mentioned before, the normalization condition (1.9)

completely determines these orbitals, and the application of this condition is straightforward from the formulae in Appendix 1.

We have used modified orbital exponents ζ_2' for the atomic orbitals, but rather than choose the new values in an arbitrary way, their values were found from

$$\zeta_2' = (E_e/E_t)^{1/2}\zeta_2 \qquad (5.1)$$

where E_e and E_t are the experimental and theoretical ionization potentials. The factor $(E_e/E_t)^{\frac{1}{2}}$ was chosen in a heuristic yet physically meaningful way, by considering the energy levels of a hydrogen like atom, $E_n \propto Z^2/n^2$, and then regarding the term $e^{-\alpha\lambda}$ in the M.O. wave function as analogous to the bound state radial factor $e^{-Zr/n}$ in atomic states.

For the $1\pi_g$ (or $1\bar{\pi}_g$) orbital in O_2, we obtain $\zeta_2' = 2{\cdot}408$ and the use of this value lowers the cross section by about ·6 Megabarns/electron from threshold to the maximum of the curve after which there is little difference. The results for this are shown by the dashed curve in fig. 5.1. For the $1\pi_u$ electron in N_2 $(X'\Sigma_g^+)$, ζ_2' =2·006 which effects a reduction of about 10% in the cross section from the threshold to the

peak of the curve; see fig. 5.7.

In the case of the $1\pi_u$ (or $1\bar{\pi}_u$) electrons of O_2 we consider the two final states $a^4\pi_u$ and $A^2\pi_u$ for which $\zeta_2' = 2.692$ and $\zeta_2' = 2.142$ respectively. The results for the quartet state are reduced by 40% and those for the doublet increased by 10% from the thresholds to the region of the maxima, which means a net reduction in cross section for most photon energies where both states are energetically possible.

It will be seen in Ch. 6 that the modified orbital exponents lead to cross sections which are in better agreement with experiment for the above orbitals. Further discussion of this point is postponed until section 6.3.

5.4 HIGH ENERGY BEHAVIOUR OF THE CROSS SECTIONS.

At very high energies the continuum waves described in Ch. 3 must approximate very closely to the plane wave solutions given by (3.1). Eventually, when the De Broglie wavelength of the ejected electrons is much smaller than the molecular dimensions, the positive and negative parts of the transition integrals will very nearly cancel each other and the cross sections become very small. Hence when the photon wavelength is 50Å, the cross sections are only of order 10^{-19} cm^2 and they usually diminish further for $\lambda < 50$Å.

The most interesting wavelength region, however is near $\lambda = 200$Å where for transitions to the well known excited states of O_2^+ and N_2^+ the photo-electrons have energies $\simeq$ 35eV. At such energies the cross sections for $1\pi_g$ (or $1\bar{\pi}_g$) and $3\sigma_g$ bound orbitals have peaks. We note that the maxima obtained (if any) in atomic cross sections (e.g. potassium) have been due to fluctuations in the transition integrals for a given pair of intitial and final states. The maxima observed in the above molecular cross sections, however, are of an entirely different origin.

The occurrence of such maxima has been anticipated by

Cohen and Fano[58], whose approach has already been discussed in section 1.5. Their prediction of shoulders due to increasing contributions from higher angular momentum final state waves is certainly borne out by our results for $3\sigma_g$ and $1\pi_g$ (or $1\bar{\pi}_g$) orbitals, as can be seen from figures 5.1, 5.3 and 5.6.

The origins of the maxima at high energies can be fully understood by reference to figures 5.14 and 5.15 where the partial cross sections are plotted for the more important (m,ℓ) contributions for the transitions to the states O_2^+ $(X^2\Pi_g)$ and N_2^+ $(X^2\Sigma_g^+)$. Figures 5.16 and 5.17 show the corresponding information for $1\pi_u$ (or $1\bar{\pi}_u$) and σ_u orbitals, the particular final states involved being N_2^+ $(A^2\Pi_u)$ and $N_2^+(B^2\Sigma_u^+)$.

We have already discussed, in section 5.2, the reasons for the different near threshold behaviours of the u and g symmetry orbitals, in terms of the relation between positions of nodes and angular momentum quantum numbers of the final state waves. We now seek an explanation of the difference in behaviour of the cross sections at high energies where we find again that the positions of the first nodes of the continuum waves play

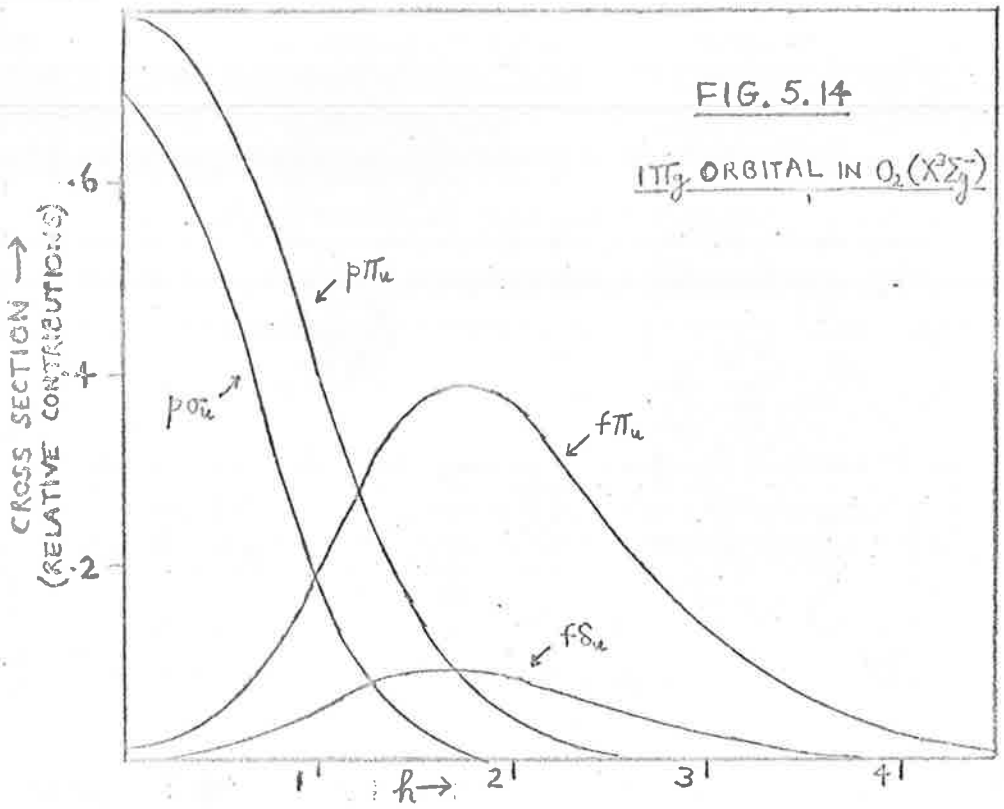

FIG. 5.14

$1\pi_g$ ORBITAL IN $O_2(X^3\Sigma_g^-)$

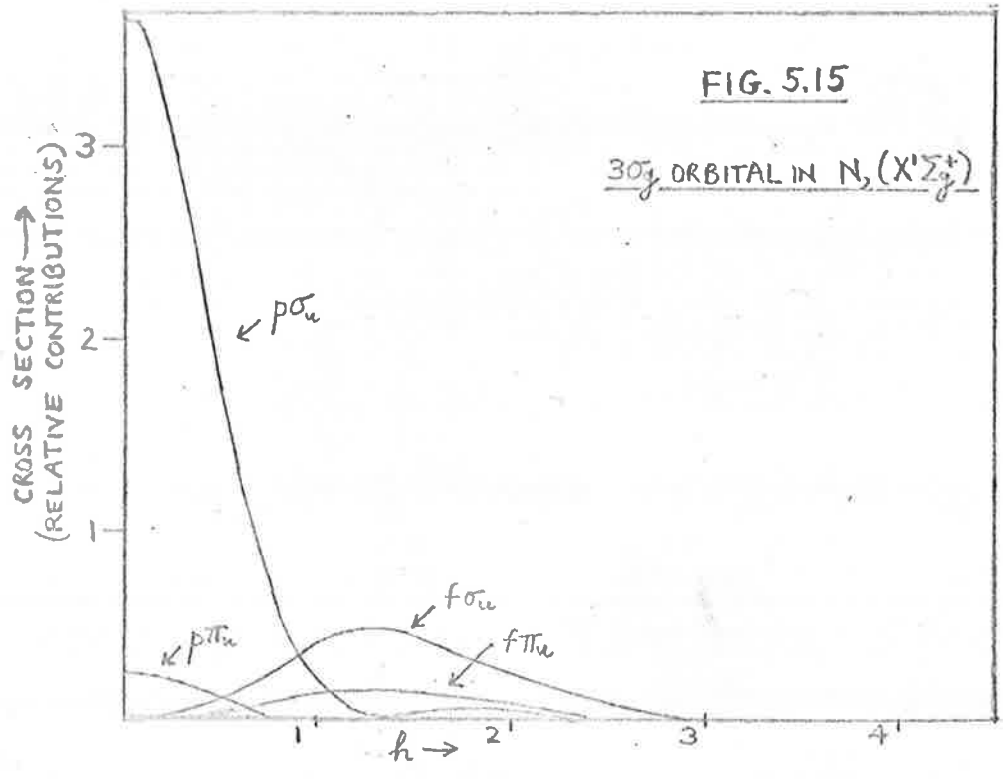

FIG. 5.15

$3\sigma_g$ ORBITAL IN $N_2(X^1\Sigma_g^+)$

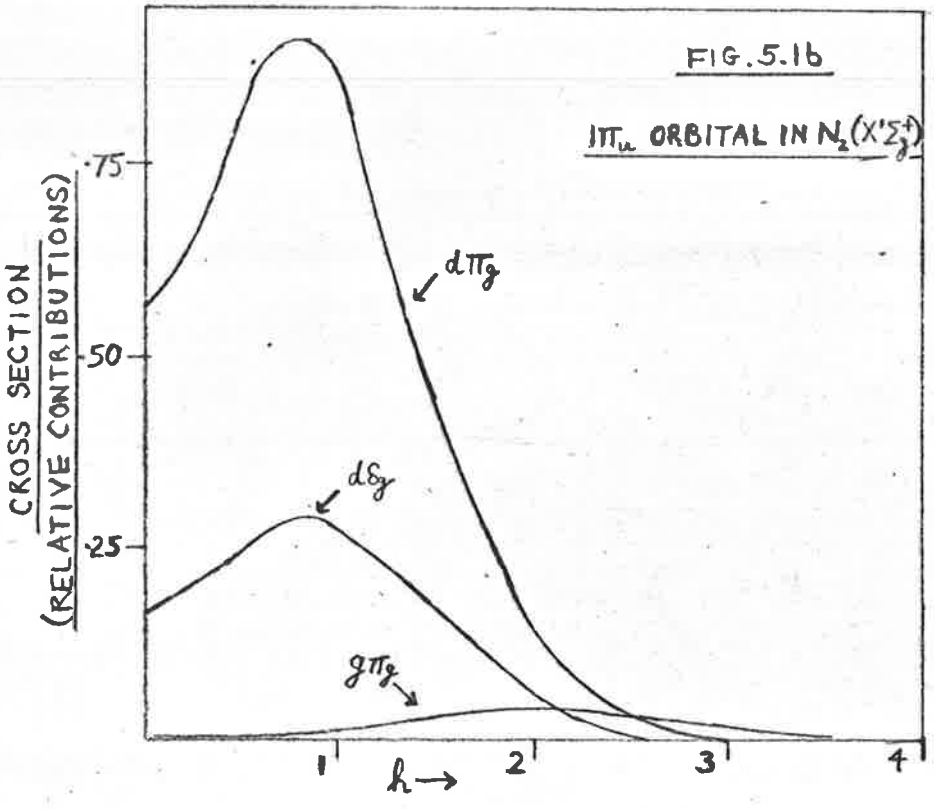
FIG. 5.16
$1\pi_u$ ORBITAL IN $N_2(X^1\Sigma_g^+)$
CROSS SECTION
(RELATIVE CONTRIBUTIONS)
·75
·50
·25
$d\pi_g$
$d\delta_g$
$g\pi_g$
1
2
3
4
h →

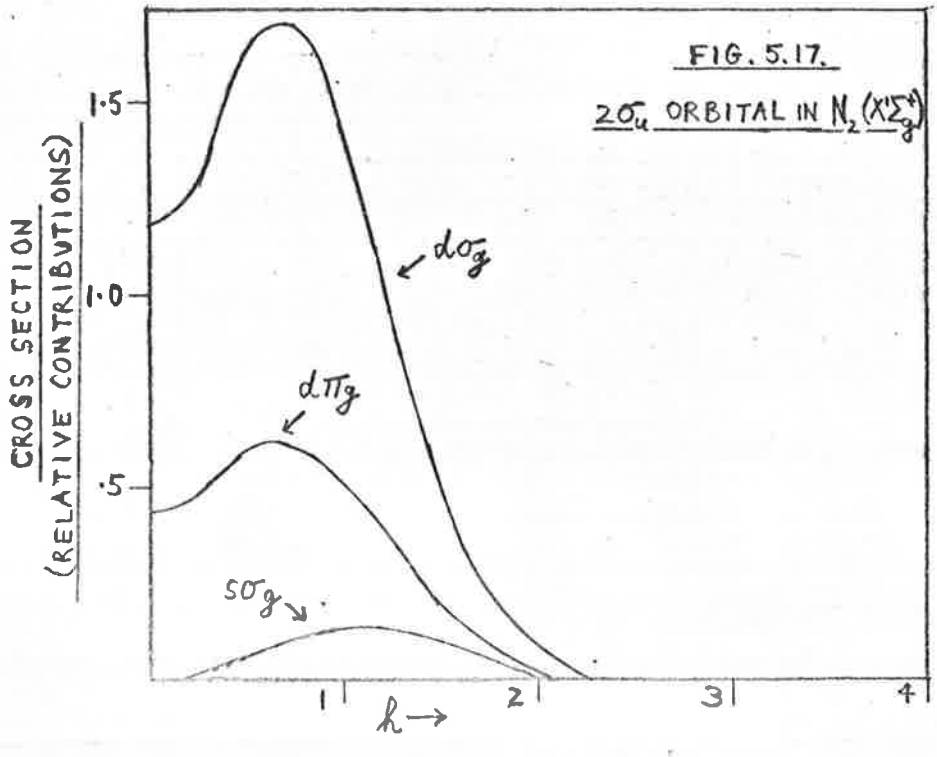
FIG. 5.17.
$2\sigma_u$ ORBITAL IN $N_2(X^1\Sigma_g^+)$
CROSS SECTION
(RELATIVE CONTRIBUTIONS)
1·5
1·0
·5
$d\sigma_g$
$d\pi_g$
$s\sigma_g$
1
2
3
4
h →

an important part.

In figures 5.18 and 5.19 are plotted the continuum waves $p\pi_u$ and $f\pi_u$ for the process to $O_2^+(X^2\Pi_g)$ and the $d\pi_g$ and $g\pi_g$ waves for transitions to $N_2^+(A^2\Pi_u)$, for energies corresponding to h = 1,2,3. We know from section 5.2 that the transition integrals involving $p\pi_u$ waves decrease from their threshold values, whereas those for $d\pi_g$ at first increase and then, at $k \simeq .9$ they too decrease. Compare the h = 1, $p\pi_u$ waves of figure 5.18 with the $f\pi_u$ waves of fig. 5.19, for the same energy, and bear in mind the bound state function of π orbitals of fig. 5.10. For the lower angular momentum p waves there is a good chance of cancellation in the transition integrals whereas for the f waves there is only a small chance of cancellation occurring. As h increases, the first nodes of both waves of course move inwards and when h = 2 cancellation is very strong for the $\ell = 1$ waves but is only slight for the $\ell = 3$ waves. Hence contributions from the latter dominate the cross section and a shoulder effect occurs. These remarks are also applicable to transitions involving electrons ejected from bound $3\sigma_g$ orbitals, for which, in our model, the m = 0 and m = 1 waves are the same as those for Π_g orbitals at a given energy of the electron.

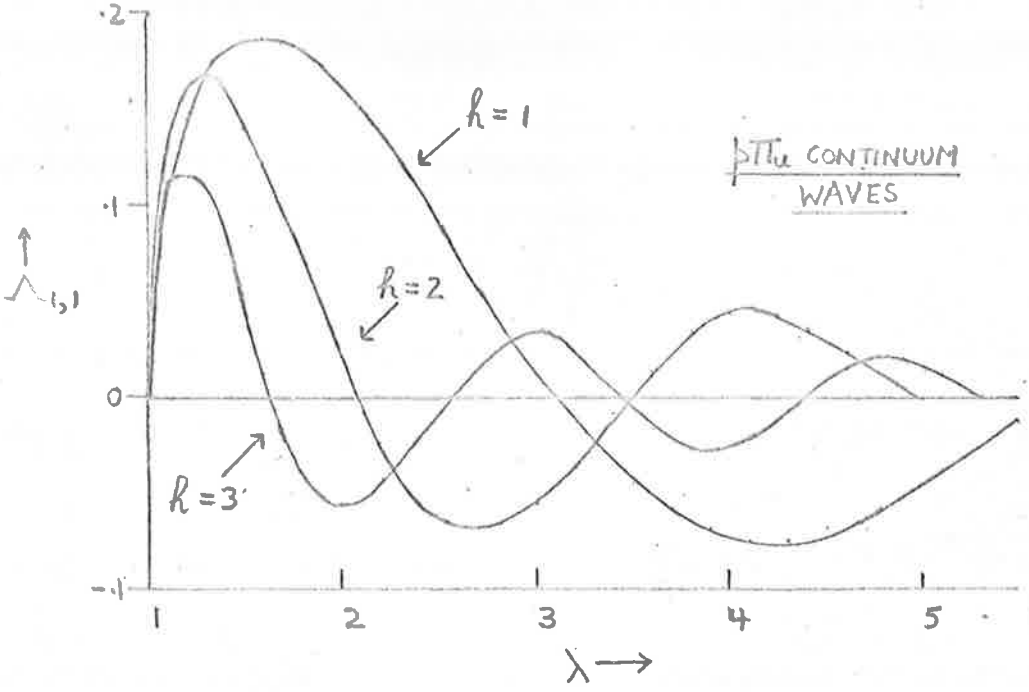

FIGURE 5.18.

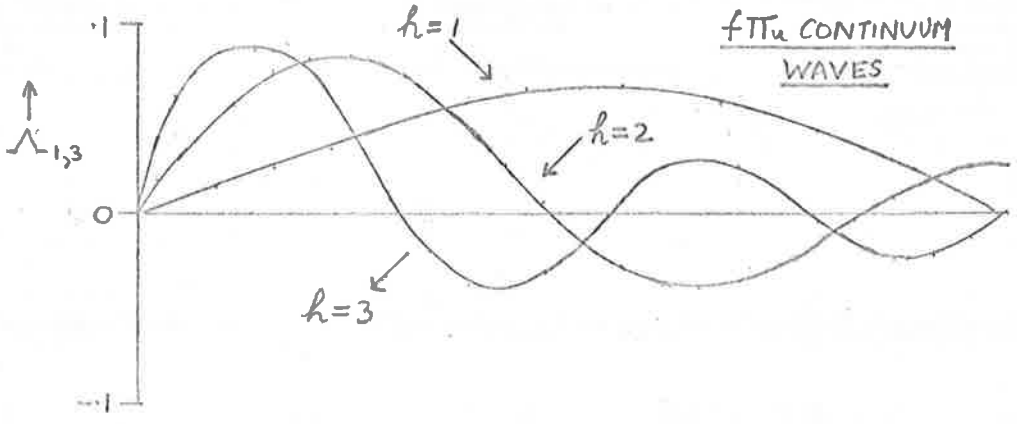

FIGURE 5.19

For the transitions involving bound orbitals of u-symmetry the situation is different. We consider figures 5.20 and 5.21 where the $d\pi_g$ and $g\pi_g$ continuum waves are plotted for h = 1,2,3. At h = 1 the first nodes of both d and g waves are beyond the region where the bound state function is greatest. Cancellation is thus not strong for either. As h increases the nodes again move inwards but at h = 2 they are still as far out as λ = 2.7 for the d - waves and λ = 3.7 for the g - waves. Examination of the π bound state radial function shows that the greatest contributions to the transition integrals should occur in the range of λ from 1.2 to 2.5 so cancellation is not strong for even the lower angular momentum waves. Since these have greater magnitudes than the $g\pi_g$ waves in the important range of λ , the latter cannot dominate the cross section. Most of the remarks for π_u bound states apply to σ_u bound states for which the m = 0, m = 1 continuum waves are the same.

We have seen that maxima in the cross sections occur at high energies for $1\pi_g$ (or $1\bar{\pi}_g$) and $3\sigma_g$ initial states. Since the expressions for $2\sigma_g$ orbitals (and $1\sigma_g$) orbitals are formally identical, except for the coefficients with

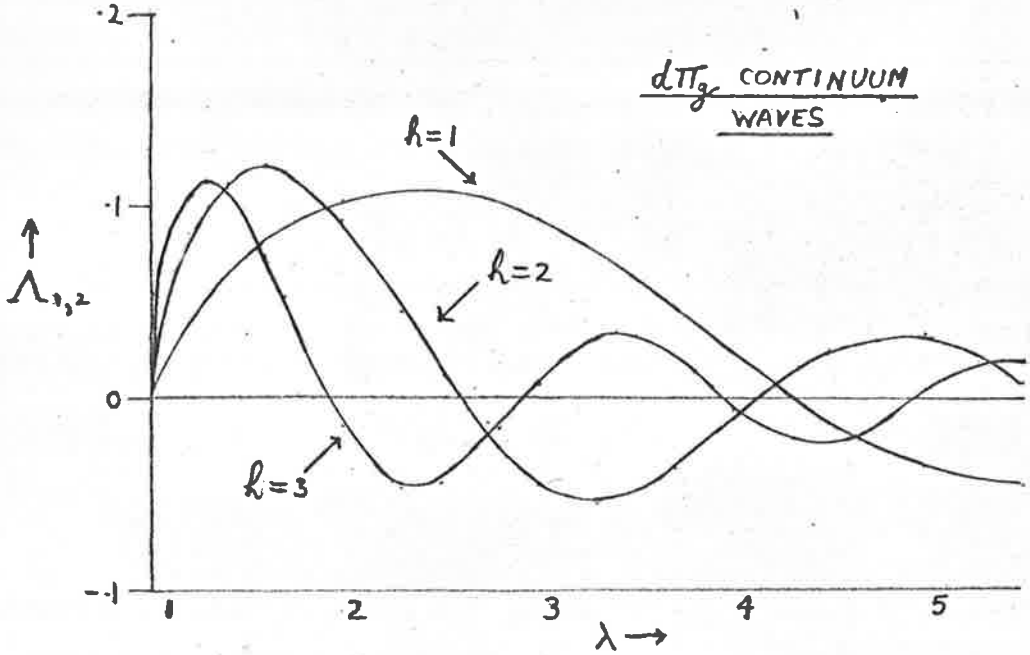

FIGURE 5.20

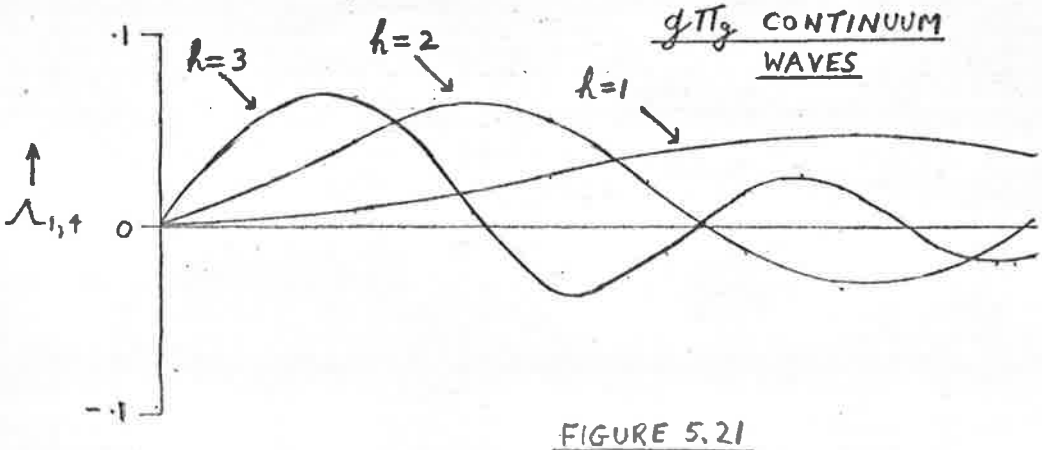

FIGURE 5.21

which the $1s\sigma_g$, $2s\sigma_g$ and $2p_z\sigma_g$ primitive orbitals enter into the expressions for the molecular orbital wave function, it might be expected that a similar effect should occur at high energies for the vacation of the $2\sigma_g$ and $1\sigma_g$ M.O.'s. The explanation of this apparent anomaly lies in the relative magnitudes of the L.C.A.O. coefficients. We defer discussion of this point until the next section where the effects of varying the L.C.A.O. coefficients for $3\sigma_g$ and $2\sigma_u$ orbitals is investigated.

Cohen and Fano's simple treatment of photo-ionization of diatomic molecules has yielded some of the general features of the results of our more detailed calculations. However they have taken a σ_g orbital containing only $1s$ atomic orbitals whereas the L.C.A.O.-M.O. wave functions used for $3\sigma_g$ orbitals in our calculations have $2s$ and $2p_z$ orbitals as well. In the next section, it will be seen why Cohen and Fano did not obtain an appreciable shoulder effect and that the reason may or may not be the rapidly declining $\sigma_H(Z^*)$ factor in (1.46), but is more than likely due to the nature of the initial state wave function. Furthermore, their prediction that the interference effects should result in a shoulder at longer photon wavelengths in O_2 than in N_2 is not borne out by the present results.

In the case of a $3\sigma_g$ bound orbital where a comparison is possible between the two molecules, we have obtained peaks in the partial cross sections and thus the possibility of a shoulder effect in the total cross section, at 185Å for O_2 and 230Å for N_2.

5.5 THE EFFECTS OF CHANGING THE L.C.A.O. COEFFICIENTS OF σ ORBITALS.

Thus far the results have been given for the case of S.C.F.-L.C.A.O.-M.O.'s for initial states where the σ orbitals consist of combinations of $1s$, $2s$ and $2p_z$ atomic orbitals. Besides the coefficients for the molecular orbitals of N_2 $(X^1\Sigma_g^+)$ and $O_2(X^3\Sigma_g^-)$ which were obtained by Sahni and Lorenzo (see Ch. 2) we have tried the extreme sets of coefficients which ignore the presence of $1s$ orbitals and take either linear combinations of $2s$ orbitals only or $2p_z$ orbitals only, i.e. we remove hybridization and consider pure $3\sigma_g$ and $2\sigma_u$ functions. The new ψ_i were normalized which involves somewhat lengthy formulae whose details are given in Appendix 1, and the same values for the internuclear separations and orbital exponents for atomic orbitals as before were used.

In figures 5.6 and 5.8 the results are shown for the non hybrid orbitals in the processes leading to N_2^+ $(X^2\Sigma_g^+)$ and $N_2^+(B^2\Sigma_u^+)$. The results for the former case, involving a $3\sigma_g$ bound state, are of much interest. It can be seen that high threshold cross

section is due almost entirely to the $2s\sigma_g$ component and that contributions from this component diminish steadily as the energy increases. Further, the cross section for the $2p_z\,\sigma_g$ function remains low until photon wavelengths of around 400Å where it commences on a high energy maximum. Thus the peaks in the cross sections at high energies for $3\sigma_g$ orbitals in our calculations which were discussed in the last section, can be attributed to the $2p_z$ component of the L.C.A.O. function. There is thus no discrepancy between Bate's results for H_2^+ at high energies and ours for O_2, N_2 because the bound state functions in the H_2^+ calculations were composed of pure S states and these do not give rise to substantial peaks at high energies. It is also very interesting to note the similarity of the cross section curve in the case of a pure $3s\sigma_g$ orbital and the results of Bates and Opik[59] for the model complex molecule which has been mentioned in section 1.5. The similarity is noticeable in the shape of the curve as well as in the orders of magnitude. We would expect this to some extent but it is somewhat surprising that the agreement is good despite the fact that we are using positive charges of $\frac{1}{2}e$ whereas Bates and Opik's model had $+2e$.

We can now see why cross section curves for photo ejection from $2\sigma_g$ orbitals do not have peaks at higher energies. In the L.C.A.O.-M.O. formulation, the wave functions contain $1S$, $2S$ and $2p_z$ atomic orbitals but for these M.O.'s the coefficients of the $2p_z$ components are much smaller than those for the $3\sigma_g$ orbitals. The immediate consequence of this is the absence of the high energy peak for the reasons given above.

We offer a tentative explanation of the differences in behaviour of the cross sections for $\sigma_g 2S$ and $\sigma_g 2p_z$ initial states. At higher energies the "molecular" features of the orbitals are lost to the outgoing electron, so we can consider the effects of atomic selection rules. For bound p - states, of which the $\sigma_g 2p_z$ molecular orbitals are composed, $\ell = 0$ and $\ell = 2$ final state waves are allowed whereas only $\ell = 1$ waves are possible for bound S - states. The high energy peaks are due to transitions to $\ell = 3$ waves and these are more accessible to electrons ejected from $\sigma_g 2p_z$ states than those ejected from $\sigma_g 2S$ states. Thus the latter do not have a peak in their cross section curves at high energies.

Finally, we note that the effects of removing the

hybridization of the $2\sigma_u$ orbitals has a much less striking effect on the cross section curves for such states. The results for $2\sigma_u(2s)$ and $2\sigma_u(2p_z)$ "pure" molecular orbitals are shown in figure 5.8 for the transition to $N_2^+ (B^2\Sigma_u^+)$. The result for $2\sigma_u$ $(2p_z)$ is slightly higher and that for $2\sigma_u$ $(2s)$ slightly lower than that for the hybrid $2\sigma_u$ orbital. Clearly we do not expect to find a peak in the $2\sigma_u(2p_z)$ case at high energies by the arguments given in section 5.4, explaining the absence of peaks in the cross sections for hybrid orbitals of u symmetry.

Our discussion of the cross sections for the various orbitals by calculations in which it has been assumed that the internuclear separation is fixed has revealed many interesting features. A brief summary will be given in Chapter 8 where the general conclusions are presented. We now turn to the inclusion of the rotational and vibrational eigenfunctions and determine the effects they have on the cross sections for different ionization processes in N_2 and O_2.

CHAPTER 6.

INCLUSION OF THE VIBRATIONAL AND ROTATIONAL EIGENSTATES.

6.1. THE BORN-OPPENHEIMER APPROXIMATION.

The Schrodinger equation for a molecular system containing n electrons and N nuclei, the latter carrying charges of +Ze, can be easily written down

$$\left[-\frac{\hbar^2}{2m}\sum_{i=1}^{n}\nabla_i^2-\frac{\hbar^2}{2M}\sum_{j=1}^{N}\nabla_j^2-\sum_{i,j}\frac{(ze^2/2)}{|\underline{r}_i-\underline{R}_j|}+\sum_{i_1,i_2,i_1\neq i_2}\frac{(e^2/2)}{|\underline{r}_{i_1}-\underline{r}_{i_2}|}+\sum_{j_1,j_2,j_1\neq j_2}\frac{(z^2e^2/2)}{|\underline{R}_{j_1}-\underline{R}_{j_2}|}\right]\Psi(\underline{r}_i,\underline{R}_j)=E\Psi(\underline{r}_i,\underline{R}_j) \qquad (6.1)$$

where m and M are the electronic and nuclear masses. In the Born-Oppenheimer approximation[56], the nuclear and electronic motions are separated by writing

$$\Psi(r_i,\underline{R}_j)=\psi_{\underline{R}_j}(e/\underline{r}_i)\,\omega(\underline{R}_j) \qquad (6.2)$$

where the electronic wave function $\psi(e/\underline{r}_i)$ depends only parametrically on $\underline{R}_j$. If we let $U(\underline{R}_j)$ be the energy eigenvalue of the electronic state, according to

$$\left[-\frac{\hbar^2}{2m}\sum_{i=1}^{n}\nabla_i^2+V\right]\psi_{\underline{R}_j}(e/\underline{r}_i)=U(\underline{R}_j)\,\psi_{\underline{R}_j}(e/\underline{r}_i) \qquad (6.3)$$

then as $\underline{R}_j$ varies we can regard U as the potential energy

for the nuclear motion and write

$$\left[-\frac{\hbar^2}{2M}\sum_{j=1}^{N}\nabla_j^2 + U(R_j)\right]w(R_j) = E\,w(R_j) \qquad (6.4).$$

Solutions to (6.3) for the electronic states have been discussed in Chapter 2. Turning to the case of a diatomic molecule we find that (6.4) becomes, for the C.O.M. particle, similar to that for the electronic states of the hydrogen atom.

$$-\frac{\hbar^2}{2\mu}\nabla^2\psi(\underline{R}) + U(R)\psi(\underline{R}) = E\psi(\underline{R}) \qquad (6.5)$$

where $$\underline{R} = \underline{R}_1 - \underline{R}_2 \qquad (6.6)$$

and μ is the reduced mass.

The Solutions to (6.5) can be separated in the customary way

$$\psi(\underline{R}) = \psi^J(v/R)\psi(J/\Theta,\Phi) \qquad (6.7)$$

where R, Θ , Φ are the spherical polar co-ordinates for the C.O.M., and v and J indicate vibrational and rotational quantum numbers respectively. The angular dependence of $\psi(\underline{R})$ can be most simply represented by spherical harmonics

$$Y_J^{M_J}(\Theta,\Phi) = (-)^{M_J}\left[\frac{(2J+1)(J-M_J)!}{4\pi(J+M_J)!}\right]^{\frac{1}{2}} P_J^{M_J}(\cos\Theta)\, e^{iM_J\Phi} \tag{6.8}$$

$P_J^{M_J}$ being associated Legendre functions of the first kind. The radial functions $\psi^J(v/R)$ then satisfy

$$\frac{1}{R^2}\frac{d}{dR}\left(R^2\frac{d\psi}{dR}\right) + \left\{2\mu[E-U(R)] - \frac{J(J+1)}{R^2}\right\}\psi = 0 \tag{6.9}$$

whereupon on making the substitution $\psi = P/R$ we obtain

$$\frac{d^2P}{dR^2} - \frac{J(J+1)}{R^2}P + \frac{2\mu}{\hbar^2}[E-U(R)]P = 0 \tag{6.10}.$$

The potential energy function U(R) can be found by numerical methods such as the Rydberg-Klein-Rees-method (see reference 64 for a modified version) if the spectroscopic constants of the molecule are known. It has been found however, that potentials of the form

$$U(R) = E_{el} + D\left[1 - e^{-\alpha(R-R_e)}\right]^2 \tag{6.11}$$

where D = the dissociation energy, R_e = equilibrium internuclear separation, which were first proposed by Morse[74], provide excellent approximations to the actual potential energy curves calculated by numerical methods. We found that Morse potentials fit the potential energy curves for most of the electronic states of O_2^+ and N_2^+ with a fairly high degree of accuracy. Morse had given

solutions to (6.10) with U of the form (6.11) for the case $J = 0$ only and the more general case, $J \neq 0$ was considered in detail by Pekeris[75], using perturbation theory techniques. The solutions have been discussed by Learner[76] and also for the case $J = 0$ by Nicholls[77]. The general solution can be written, for $J = 0$

$$P(v|R) = N_v e^{-kz} z^{b/2} {}_1F_1(-v, b+1; z) \tag{6.12}$$

where

$$z = k e^{-\alpha(R-R_e)} \tag{6.13}$$

$$k = \omega_e / \omega_e x_e \tag{6.14}$$

ω_e, $\omega_e x_e$ being the standard spectroscopic constants,

$$b = k - 1 - 2v \tag{6.15}$$

and ${}_1F_1$ is the confluent hypergeometric function

$${}_1F_1(-v, b+1; z) = \sum_{r=0}^{v} \frac{(-v)_r z^r}{(b+1)_r \, r!} \tag{6.16}$$

which is of course a polynomial of degree v in z. The normalization factor N_v obtained from the condition $\int |P|^2 dR = 1$ is given by

$$N_v = \left[\frac{\alpha \binom{v+b}{v}}{\Gamma(b)} \right]^{1/2} \tag{6.17}.$$

Equations (6.8) and (6.12) provide us with analytic wave functions for the rotational and vibrational motion of the nuclei which are of sufficient accuracy to justify

their use in the study of photo-ionization processes. The rotational eigenfunctions could be improved upon by those of the symmetric top but since rotational effects are expected to be small the simpler rigid rotator eigenfunctions will be employed.

6.2 EXPRESSIONS FOR THE CROSS SECTION.

In Chapter 1 formulae were given for the cross section for transitions between electronic states only. We recall that the complete expression for the cross section is

$$\sigma(\nu) = \frac{8\pi^3\nu}{3c} \frac{\sum_i \sum_f |\underline{M}_{if}|^2}{d_i} \qquad (6.18)$$

where $\sum_i \sum_f$ indicates summation over all combinations of degenerate initial and final states, d_i is the number of degenerate initial states (statistical weight).

$$\underline{M}_{if} = \int \bar{\psi}_i \underline{M} \psi_f \, d\tau \qquad (6.19)$$

is the dipole length matrix element. For a diatomic molecule, the electric dipole moment $\underline{M} = \sum_k q_k \underline{\rho}_k$ obtained from all the charges of the system q_k and their position vectors $\underline{\rho}_k$. Following Herzberg[44] we can resolve $\underline{M}$ into an electronic component $\underline{M}_e$ and a nuclear component $\underline{M}_n$. If we write a general molecular wave function

$$\psi(v, J, e \,|\, \underline{r}, \underline{R}) = \psi(v|R)\, \psi(J|\Theta, \Phi)\, \psi(e|\underline{r}, \underline{R}) \qquad (6.20)$$

then

$$\underline{M}_{if} = \iint \bar{\psi}(v_i|R)\, \bar{\psi}(J_i|\Theta, \Phi)\, \bar{\psi}(e_i|\underline{r}, \underline{R})\, \underline{M}_e\, \psi(v_f|R)\, \psi(J_f|\Theta, \Phi)\, \psi(e_f|\underline{r}, \underline{R})\, d\underline{r}\, d\underline{R}$$

$+$

$$+\iint \bar{\psi}(v_i|R)\bar{\psi}(J_i|\Theta,\Phi)\bar{\psi}(e_i|r,R)\,\underline{M}_n\,\psi(v_f|R)\psi(J_f|\Theta,\Phi)$$
$$\times \psi(e_f|r,R)\,dr\,dR \qquad (6.21)$$

where the integrations are over all electronic and nuclear co-ordinates. We assume that $\underline{M}_n$ does not depend on the electronic co-ordinates so that since the initial and final electronic states are orthogonal the second term in (6.21) vanishes.

Let $E(v_f,J_f)$ be the energy level of the ion and $E(v_i,J_i)$ that of the molecule before photoionization, both measured with respect to their zero point energies and let I be the energy difference between the initial level (v_i,J_i) and the vibrationless-rotationless state of the ion. Consideration of figure 6.1, which is an energy level diagram for molecule and ion, shows that the kinetic energy $\mathcal{E}$ of an ejected electron is

$$\mathcal{E}(v_f,J_f) = h\nu - (I + E(v_f,J_f)) \qquad (6.22)$$

providing of course that a transition to the (v_f,J_f) level of the ion is energetically possible, i.e. that $\mathcal{E}(v_f,J_f) \geq 0$. The photoionization cross section at frequency ν for an initial state $\psi(v_i,J_i,e_i|r,R)$ is then

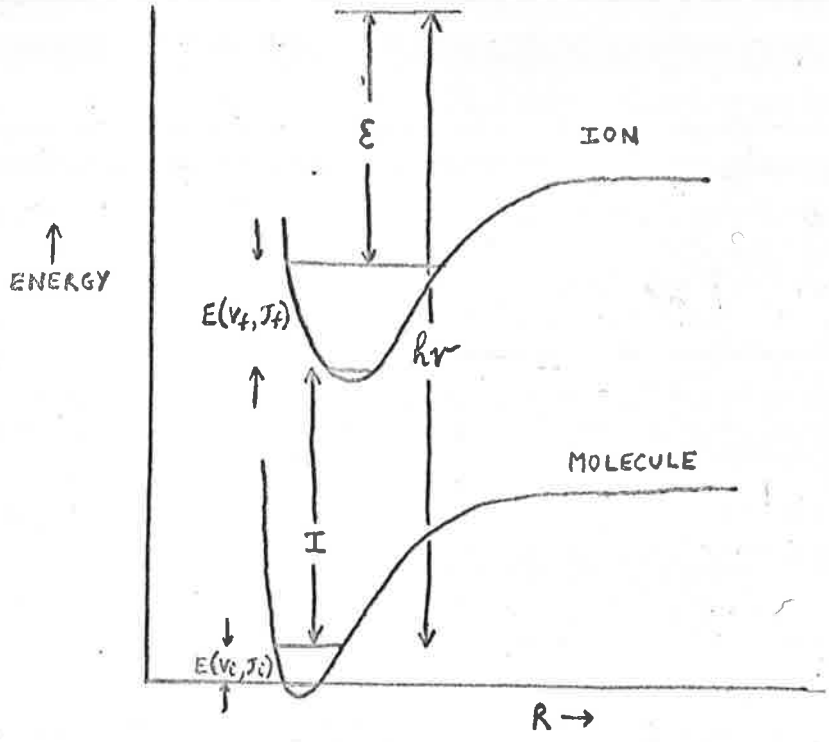

FIGURE 6.1

$$\sigma(\nu) = \frac{(4\pi\alpha a_0^2/3)}{(2J_i+1)} \sum_{M_{J_i}} \sum_{v_f, J_f, M_{J_f}} (I + \mathcal{E}(v_f, J_f)) \times \sum_{e_f} \left| \underline{M}(e_i, J_i, v_i, e_f, J_f, v_f, \epsilon) \right|^2 \qquad (6.23).$$

Consideration of Boltzmann factors for standard temperatures[44] shows that the $v_i = 0$ level is most probable for the initial vibrational states but that $J = 7$ and $J = 8$ are the most probable rotational states for N_2 and O_2 respectively. Assuming $J_i = 0$ is not

expected to have any significant effect on the calculated cross sections. Assuming $v_i = 0$, $J_i = 0$ we have

$$\underline{M}(e_i, e_f, v_f, J_f, \mathcal{E}) = \iint \overline{\Psi}(0,0,e_i|\underline{r},\underline{R}) \pm \phi(v_f, J_f, e_f, \mathcal{E}|\underline{r},\underline{R})\, d\underline{r}\, d\underline{R} \tag{6.24}$$

Performing the integrations over Θ, Φ gives a factor of unity and no change of the rotational quantum number by virtue of the orthonormality of the $Y_J^{M_J}(\Theta, \Phi)$. We note that the resultant selection rule on J is $\Delta J = 0$ in contrast with the case where symmetric top eigenfunctions are employed. $\underline{M}$ now takes the simple form

$$\underline{M}(e_i, e_f, v_f, \mathcal{E}) = \iint \bar{P}(0|R)\bar{\psi}(e_i|r,R) \pm P(v_f|R)\phi(\mathcal{E}_f, e_f|r,R)\, dr\, dR \tag{6.25}$$

The simplest approach to adopt in evaluating the matrix element (6.25) is to assume that the electronic wave functions do not depend on the nuclear radial variable R. Then we can write

$$|\underline{M}(e_i, e_f, v_f, \mathcal{E})|^2 = \left|\int \bar{P}(0|R) P(v_f|R) dR \int \bar{\psi}(e_i|r) \pm \phi(e_f, \mathcal{E}|r)\, dr\right|^2 \tag{6.26}$$

$$= q(v_f, 0) \left|\int \bar{\psi}(e_i|r) \pm \phi(e_f, \mathcal{E}|r)\, dr\right|^2 \tag{6.27}$$

where $q(v_f,0)$ is the Franck-Condon factor, introduced by Bates[78], for the zeroth vibrational level of the molecule and the v_f-th level of the ion. Franck-Condon factors are usually calculated for the case where U (in 6.10), is a Morse potential in which case the vibrational wave functions are given by (6.12). Such calculations have been performed for transitions to the ion states $O_2^+(X^2\Pi_g, a^4\Pi_u, A^2\Pi_u, b^4\Sigma_g^-)$ by Wacks[79], $O_2^+(^2\Sigma_g^-)$ by Bahr[80], and $N_2^+(X^2\Sigma_g^+, A^2\Pi_u, B^2\Sigma_u^+)$ by Nicholls[77].

With the above simplifications the cross section can be written

$$\sigma(\nu) = (4\pi^2 a_0^2/3) \sum_{v_f} (I + \varepsilon(v_f)) q(v_f,0) \times$$
$$\times \sum_{e_f} \left| \int \bar{\psi}(e_i|r) \pm \phi(e_f,\varepsilon|r)\, d\tau \right|^2 \qquad (6.28)$$

where $\sum_{v_f}$ means summation over the energetically possible vibrational levels of the ion. The use of Franck-Condon factors has the consequence that the <u>vibrational contribution</u> to the total transition probability is independent of the photon energy. This means that to find the total cross

section for all v_f one needs to determine from (6.22) at a given photon energy, subject to the condition $\mathcal{E}(v_f) \geq 0$, the value of the electron kinetic energies for all v_f. The corresponding values of $h(= R\mathcal{E}^{\frac{1}{2}}/2)$ can then be found and hence, by graphical methods the electronic matrix elements. Alternatively the known values of the electronic matrix elements at the tabulated values of h can be used to determine the cross sections for each v_f and then the corresponding values of the photon energy so that the variation of the total cross section with energy can be found by graphical methods. Both of these methods were used for the transitions to the states mentioned above for which Franck-Condon factors are known. The first method proved somewhat laborious, especially when up to 20 vibrational levels of the ion had appreciable Franck-Condon factors so a programme (included in Appendix 3) was written for the second method which provided a more efficient method of evaluating the total cross section.

6.3 RESULTS FOR PARTIAL CROSS SECTIONS CALCULATED WITH FRANCK-CONDON FACTORS AND COMPARISON WITH EXPERIMENT.

In figures 6.2 to 6.7 are shown the results obtained from (6.28) for the transitions from the ground electronic states of N_2 and O_2 to the ion electronic states $O_2^+(X^2\Pi_g)$, $O_2^+(a^4\Pi_u)$, $O_2^+(A^2\Pi_u)$, $O_2^+(b^4\Sigma_g^-)$, $O_2^+(\,^2\Sigma_g^-)$, $N_2^+(X^2\Sigma_g^+)$, $N_2^+(A^2\Pi_u)$, $N_2^+(B^2\Sigma_u^+)$. For all of these the partial cross sections have been found from photoelectron spectroscopy by Blake and Carver[81]. In Chapter 5 the cross sections obtained for fixed nuclei were discussed and comparisons between the curves for different electronic states were made and the differences in variation with energy explained. Those results would have been obtained by setting $\sum_{v_f} (q(v_f,0)) = 1$ independent of the photon energy and putting all $\varepsilon(v_f)=0$ in (6.28). Including the Franck-Condon factors has the most noticeable effect for those transitions in which the ground electronic state of the neutral molecule and the final state of the ion have appreciably different equilibrium internuclear separations. Under these circumstances, the Franck-Condon factors are small for small vibrational quantum numbers of the ion and increase slowly to achieve a maximum at a higher value of v_f. In figures 6.2 to

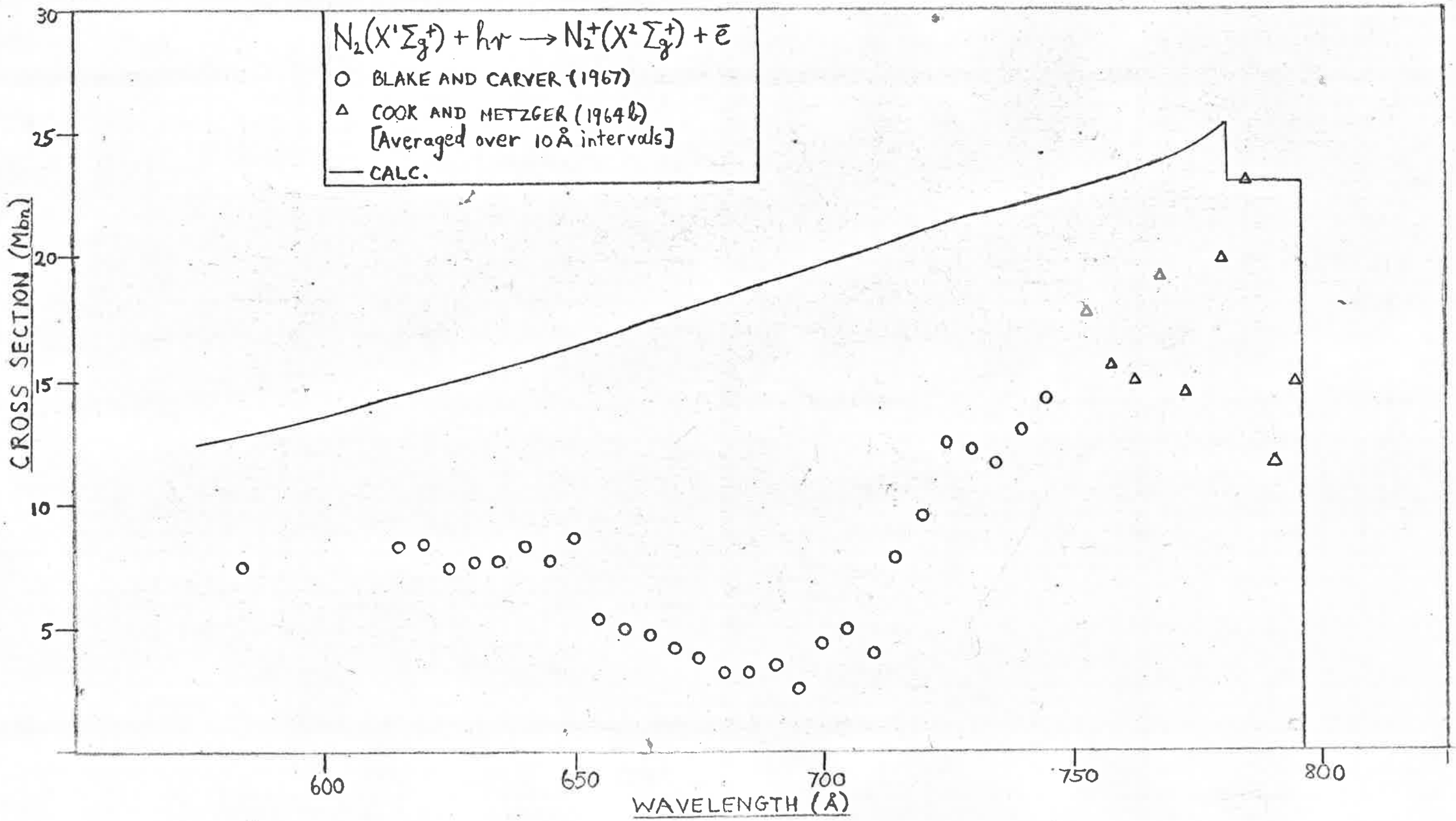
$N_2(X^1\Sigma_g^+) + h\nu \longrightarrow N_2^+(X^2\Sigma_g^+) + e$
O BLAKE AND CARVER (1967)
Δ COOK AND METZGER (1964b)
[Averaged over 10 Å intervals]
— CALC.
CROSS SECTION (Mbn)
30
25
20
15
10
5
600
650
700
750
800
WAVELENGTH (Å)

FIGURE 6.2

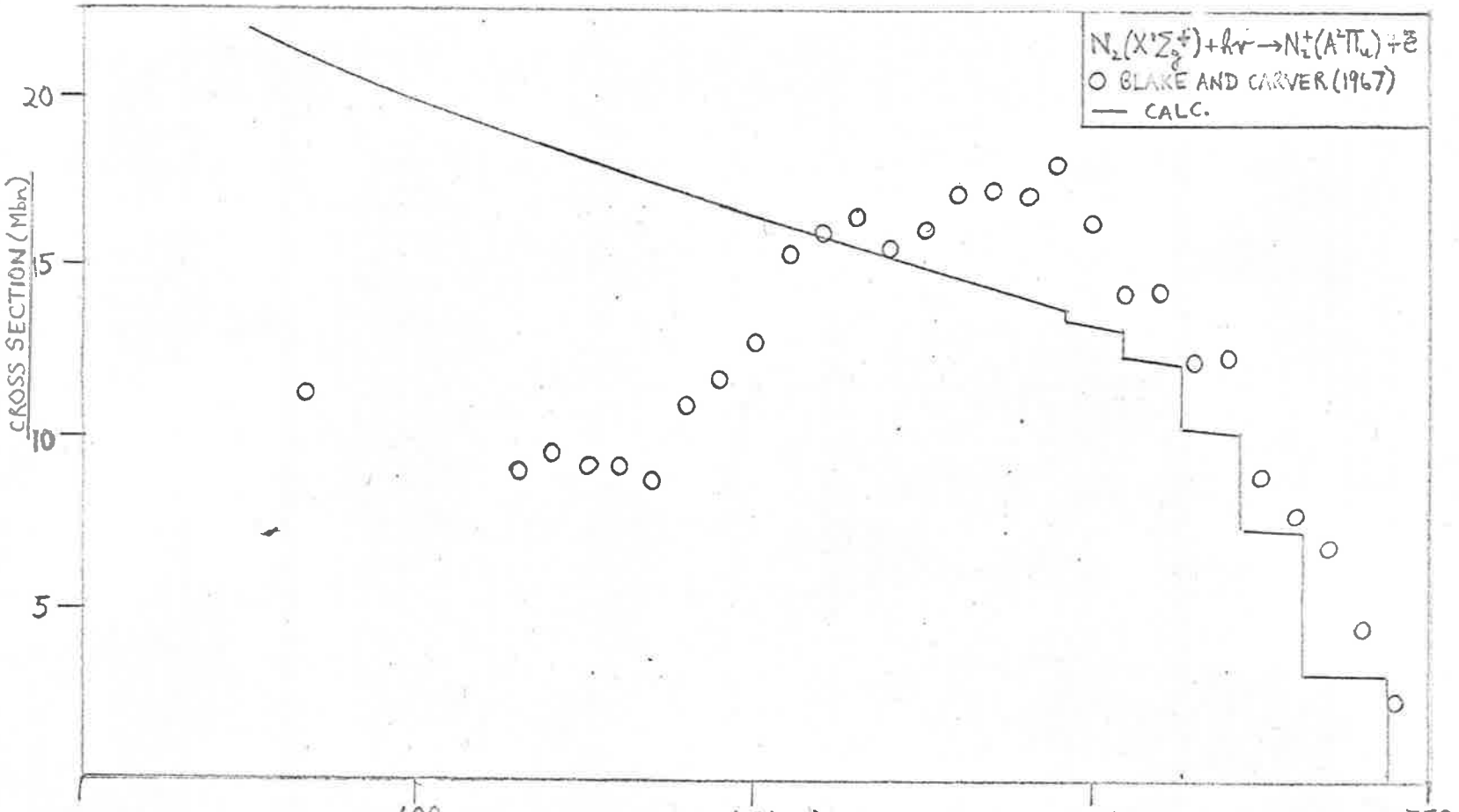
$N_2(X^1\Sigma_g^+) + h\nu \rightarrow N_2^+(A^2\Pi_u) + e$
BLAKE AND CARVER (1967)
CALC.
CROSS SECTION (Mbn)
20
15
10
5
600
650
700
750
WAVELENGTH (Å)

FIGURE 6.3

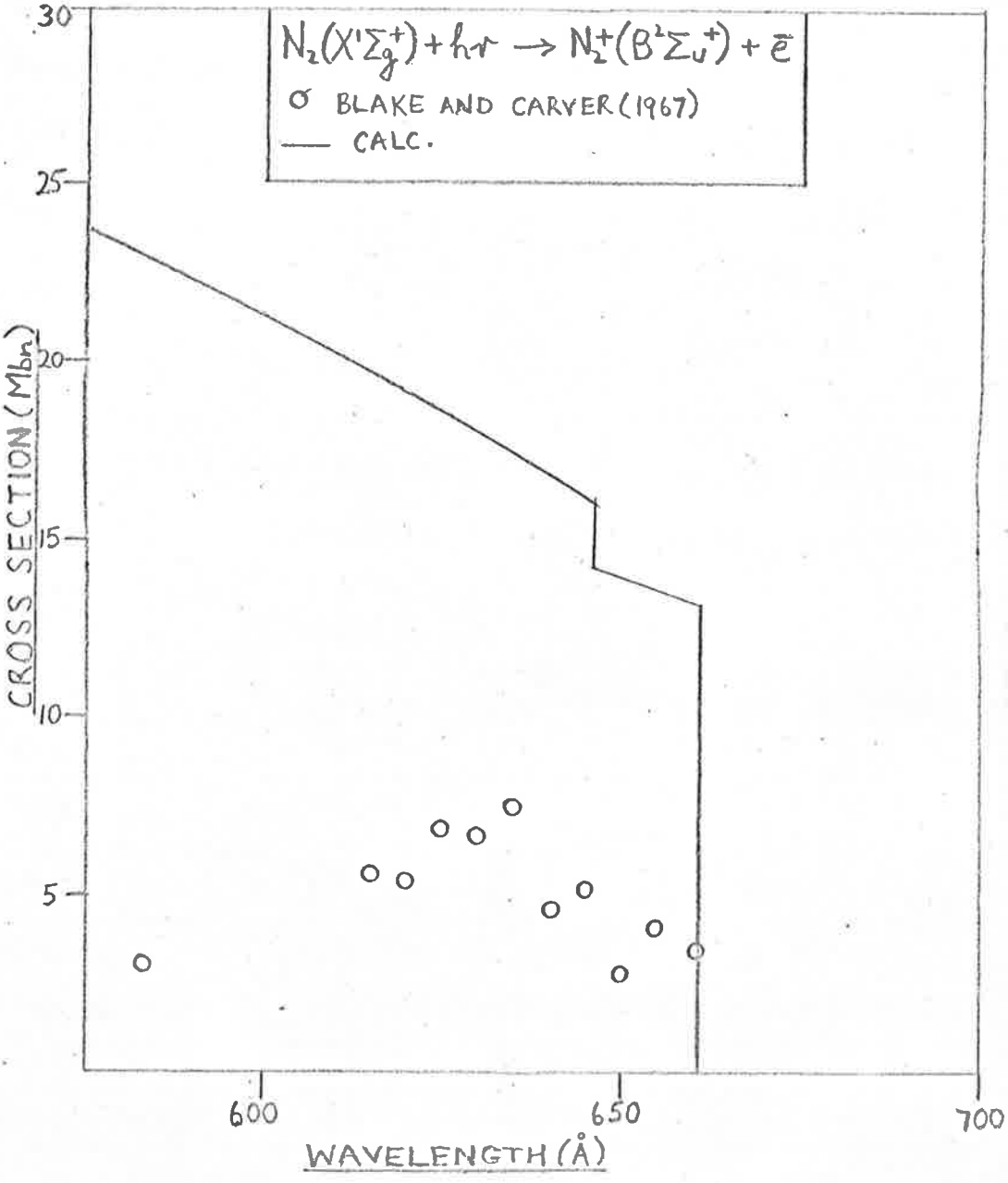
$N_2(X^1\Sigma_g^+) + h\nu \rightarrow N_2^+(B^2\Sigma_u^+) + e^-$
σ BLAKE AND CARVER (1967)
— CALC.
CROSS SECTION (Mbn)
30
25
20
15
10
5
600
650
700
WAVELENGTH (Å)

FIGURE 6.4

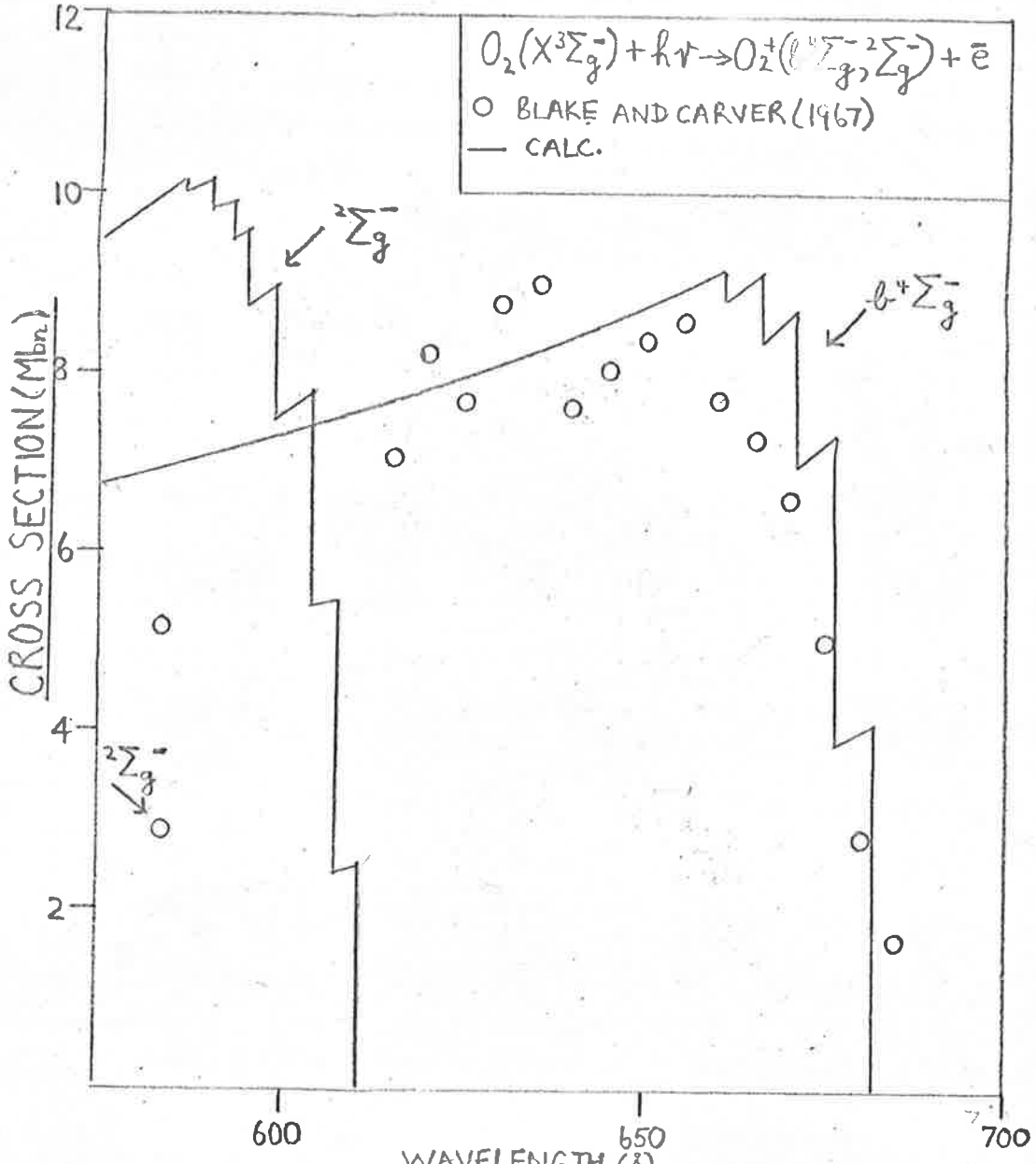
$O_2(X^3\Sigma_g^-) + h\nu \rightarrow O_2^+(\ell^4\Sigma_g^-, {}^2\Sigma_g^-) + \bar{e}$
O BLAKE AND CARVER (1967)
— CALC.
$^2\Sigma_g^-$
$b^4\Sigma_g^-$
$^2\Sigma_g^-$
CROSS SECTION (Mbn)
12
10
8
6
4
2
600
650
700
WAVELENGTH (Å)

FIGURE 6.5

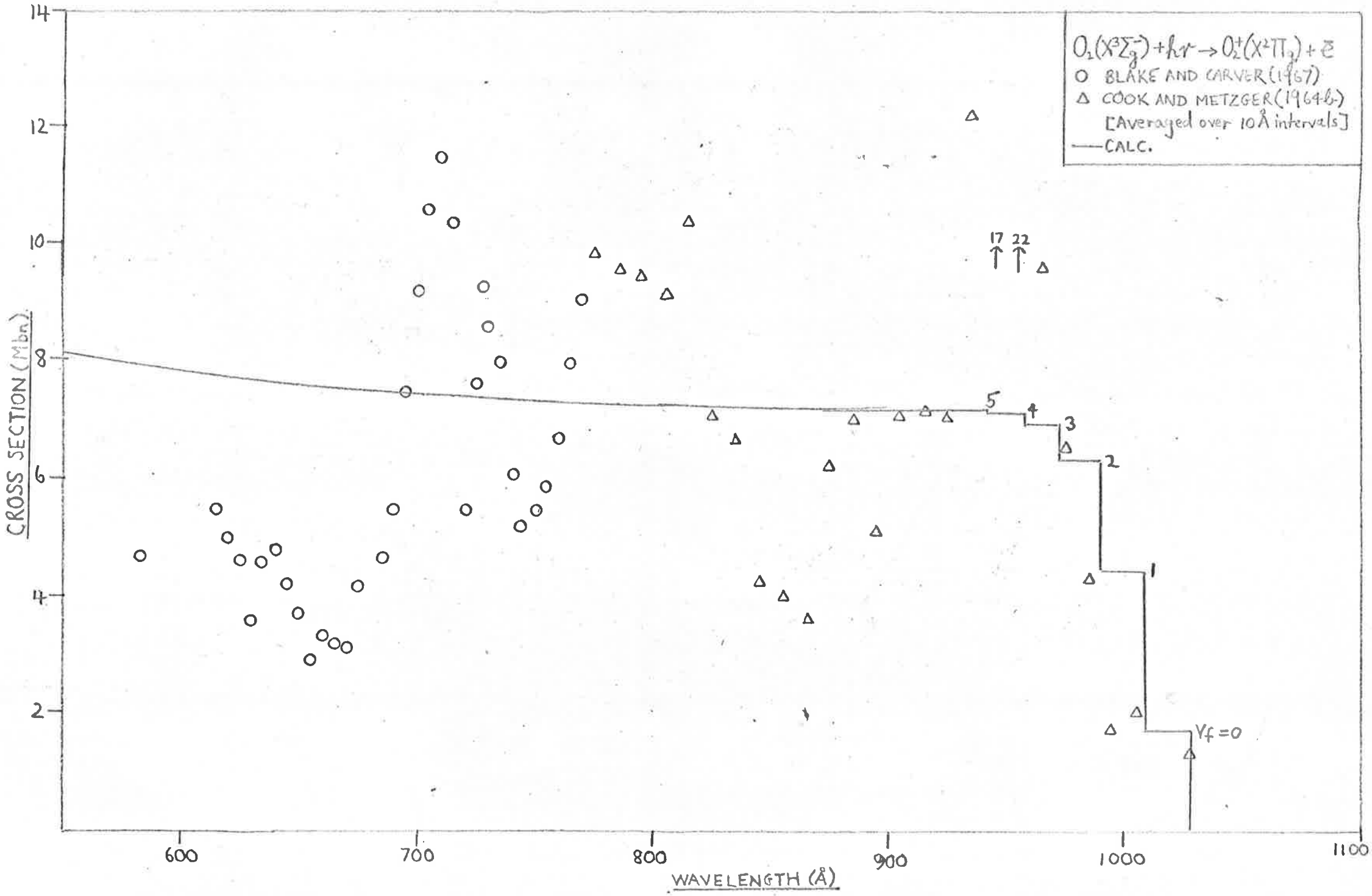
$O_2(X^3\Sigma_g^-) + h\nu \rightarrow O_2^+(X^2\Pi_g) + e$
BLAKE AND CARVER (1967)
COOK AND METZGER (1964b)
[Averaged over 10Å intervals]
CALC.
CROSS SECTION (Mbn)
WAVELENGTH (Å)
14
12
10
8
6
4
2
600
700
800
900
1000
1100
17
22
5
4
3
2
1
$V_f = 0$

FIGURE 6.6.

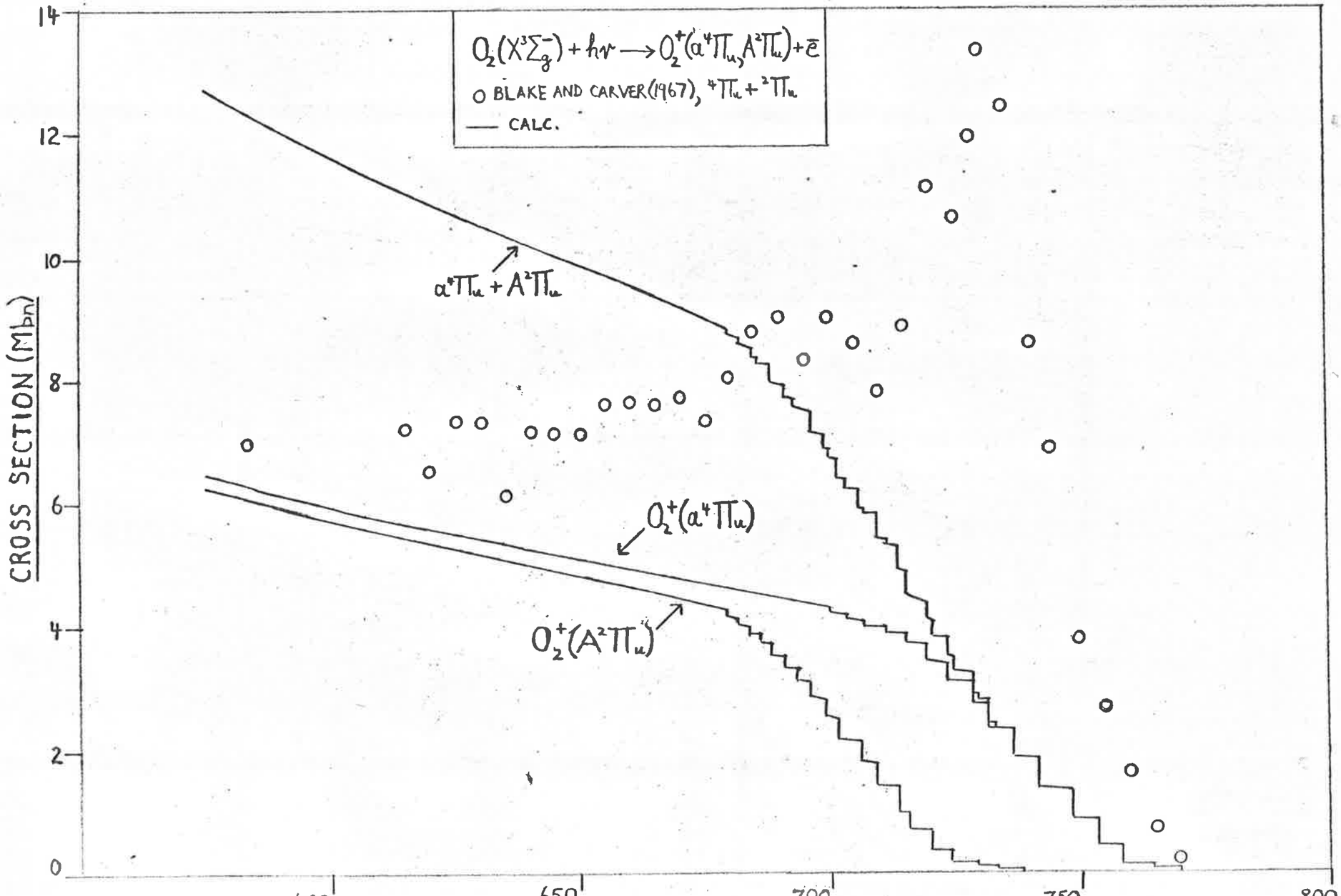
$O_2(X^3\Sigma_g^-) + h\nu \longrightarrow O_2^+(a^4\Pi_u, A^2\Pi_u) + e$
O BLAKE AND CARVER (1967), $^4\Pi_u + {}^2\Pi_u$
— CALC.
$a^4\Pi_u + A^2\Pi_u$
$O_2^+(a^4\Pi_u)$
$O_2^+(A^2\Pi_u)$
CROSS SECTION (Mbn)
0
2
4
6
8
10
12
14
600
650
700
750
800
WAVELENGTH (Å)

FIGURE 6.7.

6.7, the experimental points of Blake and Carver in the wavelength ranges from first threshold to 584Å are shown for the above transitions. It should be remembered that Blake and Carver applied their branching ratios to the total photoionization cross sections of Cook and Metzger[63]. Other reports of experimental total photoionization cross sections have tended to be somewhat higher than Cook and Metzger's results (see for instance the results of Wainfain et al[53], Matzanuga and Watanabe[83] (O_2 only)), and these would of course give rise to higher partial cross sections. In the wavelength ranges of 1027Å to 770Å for O_2 and 796Å to 743Å for N_2 the partial cross sections for transitions to the ion states $O_2^+(X^2\Pi_g)$ and $N_2^+(X^2\Sigma_g^+)$ are of course identical to the total cross sections. Further it is worth pointing out that there are two initial electron states to account for in the transitions to $O_2^+(X^2\Pi_g)$, $O_2^+(a^4\Pi_u)$, $O_2^+(A^2\Pi_u)$, $N_2^+(X^2\Sigma_g^+)$, $N_2^+(B^2\Sigma_u^+)$, and four in the transitions to $N_2^+(A^2\Pi_u)$. These multiplicative factors have been included in the final results.

For most of the transitions considered the calculated values agree well with the experimental results near the thresholds. We now discuss the results for each orbital type.

Π_g . The calculated cross section near threshold has large steps due to the large Franck-Condon factors for the small vibrational quantum numbers of the ion, $O_2^+(X^2\Pi_g)$. Cook and Metzger's readings seem to ascend in close agreement with the calculated values. Near 950Å however, the experimental points are up to three times the calculated values which may be attributable to autoionization lines which we have not taken into account. From 950Å to 584Å the experimental points tend to oscillate about a mean which is close to the almost steady value of the calculated cross section in this wavelength region.

Π_u . For the transition to $N_2^+(A^2\Pi_u)$ the agreement of calculated and experimental partial cross section is very good from 743Å to 660Å. At higher energies however, the calculated values increase steadily in contrast to the experimental results. This indicates that the critical first nodes of the important continuum waves are not occurring at sufficiently small values of the radial coordinate λ and so not causing the corresponding transition integrals to diminish at low enough energies. For the transitions to the Π_u states of O_2^+ the last remark also applies, but here the experimental results lie well above the calculated cross section from 770Å to 675Å. Since the

Franck-Condon factors are responsible for the sluggish increase of the calculated cross section just above the $a^4\Pi_u$ threshold, it is difficult to see why the experimental points should show such a rapid increase in this region. A tentative explanation would be that the electronic matrix element is sensitive to changes in internuclear separation so that the Franck-Condon factor approximation is no longer valid. Otherwise the threshold value of the cross section for the case of fixed nuclei would have to be several orders of magnitude greater than that calculated with our model and show an extremely rapid decrease for increasing energy. In the light of the good agreement for the corresponding orbital in N_2, however, we suspect that the calculated values cannot be too much in error.

$3\sigma_g$. There is insufficient experimental data for the transition to $O_2^+(\,^2\Sigma_g^-)$; the only available experimental point is about one third of the calculated value. The transitions to $O_2^+(b^4\Sigma_g^-)$ and $N_2^+(X^2\Sigma_g^+)$ show good agreement between experiment and theory near their thresholds. For the former the agreement remains to almost 600Å and again we see the Franck-Condon factors dominating the calculated cross section and probably the experimental readings as well. For $N_2^+(X^2\Sigma_g^+)$ the calculated and

experimental values depart considerably from 750Å to 650Å after which they approach one another. The drop in the experimental curve at energies above 750Å which is not noticeably in the computed results could possibly be explained by the above arguments for this phenomenon in the case of the π_u orbital in N_2.

$2\sigma_u$. The calculated results for the transition to $N_2^+(B^2\Sigma_u^+)$ are two to three times the experimental values from threshold to 615Å and the discrepancy may be even greater than this at higher energies. The final state waves are more likely to be seriously in error than the bound state functions for the following reasons. It is unrealistic that the continuum waves for electrons ejected from π_u and σ_u orbitals should be identical which is the case in our calculations for the σ_g and π_g continuum waves for processes involving these orbitals. Since the agreement between experiment and our approximate theory is good for the π_u bound states near threshold, we consider that the continuum waves for electrons ejected from the σ_u orbitals need to be greatly improved upon. Clearly we are testing Flannery and Opik's final state model to its limit when we use it for photoionization of inner shells because we cannot expect the screening of

the nuclei to be as effective as in the case of ejection from the more loosely bound π_u and π_g orbitals. It is somewhat surprising that the final state approximation has produced results which are of the correct orders of magnitude for photoionization from even $3\sigma_g$ orbitals.

6.4 INCLUSION OF THE DEPENDENCE OF THE ELECTRONIC TRANSITION MOMENT ON INTERNUCLEAR DISTANCE.

We recall that in the derivation of (6.28) the simplifying assumption was made that the electronic transition moment was independent of internuclear separation. Franck-Condon factors were used to account for the vibrational contribution to the transition probabilities. This approach has been generally adopted in the study of band intensities in emission and absorption[84]. For the latter we have

$$K_{v'v''} \sim N_{v''} \nu_{v'v''} \left| \int \psi_{v'} R_e(R) \psi_{v''}(R) dR \right|^2 \qquad (6.29)$$

where $N_{v''}$ is the relative population of the v'' level of the initial state, $\nu_{v'v''} = (E_{v'} - E_{v''})/h$ and $R_e(R)$ is the electronic transition moment. Because the dependence of R_e on the internuclear separation usually presents a difficult mathematical problem, the usual procedure is to write

$$K_{v'v''} \sim N_{v''} \nu_{v'v''} R_e^2(\bar{r}_{v'v''}) q_{v'v''} \qquad (6.30)$$

where $q_{v'v''} = \left| \int \bar{P}_{v''} P_{v'} dR \right|^2$ is the Franck-Condon factor and

$$\bar{r}_{v'v''} = \int P_{v'} R P_{v''} dR \Big/ \int P_{v''} P_{v'} dR \qquad (6.31)$$

is the r - centroid[85]. The justification for taking an average value for the transition moment has been the assumption that the variation of R_e with R is slow.

The above definition of the r - centroid and the inherent assumption is usually made in the context of bound-bound transitions but it has obvious application to bound-free transitions. We have therefore investigated the effects of including the dependence of the matrix elements of (6.24) on the internuclear distance R. At the time of writing we had only treated the single process

$$O_2(X^3\Sigma_g^-, v_i=0, J_i=0) + h\nu \rightarrow O_2^+(X^2\Pi_g)(v_f, J_f=0) + \bar{e} \tag{6.32}$$

and found the corresponding cross sections at the thresholds for each final vibrational level of the ion i.e. zero kinetic energy of the ejected electons.

For the process (6.32) the cross sections for each value of v_f are

$$\sigma(v_f|\varepsilon=0) = (4\pi\alpha a_0^2/3)\, I(\nu_f) \sum_{e_f} \left| \underline{M}(v_f, e_f, e_i, \varepsilon=0) \right|^2 \tag{6.33}$$

$$\underline{M}(v_f, e_f, e_i, \varepsilon=0) =$$

$$\iint \bar{\psi}(e_i|\pm, R)\,\bar{P}(0|R)\,\pm\,\phi(e_f, \varepsilon=0|\pm, R)\,P(v_f|R)\,d\pm\,dR \qquad (6.34).$$

The first stage of the calculation was the evaluation of the electronic transition moment as a function of R

$$R_e(R) = \int \bar{\psi}(e_i|\pm, R)\,\pm\,\phi(e_f, \varepsilon=0|\pm, R)\,d\pm \qquad (6.35).$$

The previous programme which we had used for the evaluation of the electronic matrix elements for fixed nuclei was extended to calculate these quantities in the range of R from 1·6 to 3·0 a_o in steps of ·02 a_o. The significant range of R was obtained by the method of Nicholls[77]. For the process (6.32) the chief contributions to the cross section come from $p\sigma_u$ and $p\pi_u$ continuum waves and in figure 6.8 are plotted the corresponding matrix elements for these final states as functions of the internuclear separation. It can be seen that the variation with R is indeed slow which lends support to the assumptions which have been previously made in the calculation of transition probabilities between molecular states. We feel that this result cannot be disregarded on the grounds that our final state model is only an approximate one. Our justification lies in the agreement of the magnitudes and variation

with energy of the cross sections near threshold as indicated in the last section.

To complete the calculations we have to multiply $R_e(R)$ by the initial and final state vibrational wave functions and integrate over R. The vibrational wave functions employed were those for the Morse potential for which the solutions have already been given in section 6.1. The relevant spectroscopic constants for $O_2^+(X^2\Pi_g)$ are[79] $\omega_e = 1876.9\,cm^{-1}$, $\omega_e x_e = 16.53\,cm^{-1}$, $r_e = 1.1227\,\text{Å}$, $\mu_a = 7.99986$. In figure 6.8 we have also plotted the normalized vibrational wave functions for the zeroth vibrational levels of $O_2(X^3\Sigma_g^-)$ and $O_2^+(X^2\Pi_g)$. It can be seen that in the region of appreciable contributions to the overlap integral which when squared gives the Franck-Condon factor, the electronic transition moment is varying so slowly with R that the cross sections obtained by the method of this section should not differ appreciably from those obtained by using the Franck-Condon factor approximation. This is certainly borne out by the computed result for the transition from the $v_i = 0$ state of $O_2(X^3\Sigma_g^-)$ to the $v_f = 0$ state of $O_2^+(X^2\Pi_g)$, which is given, together with the cross sections for all v_f at the corresponding thresholds,

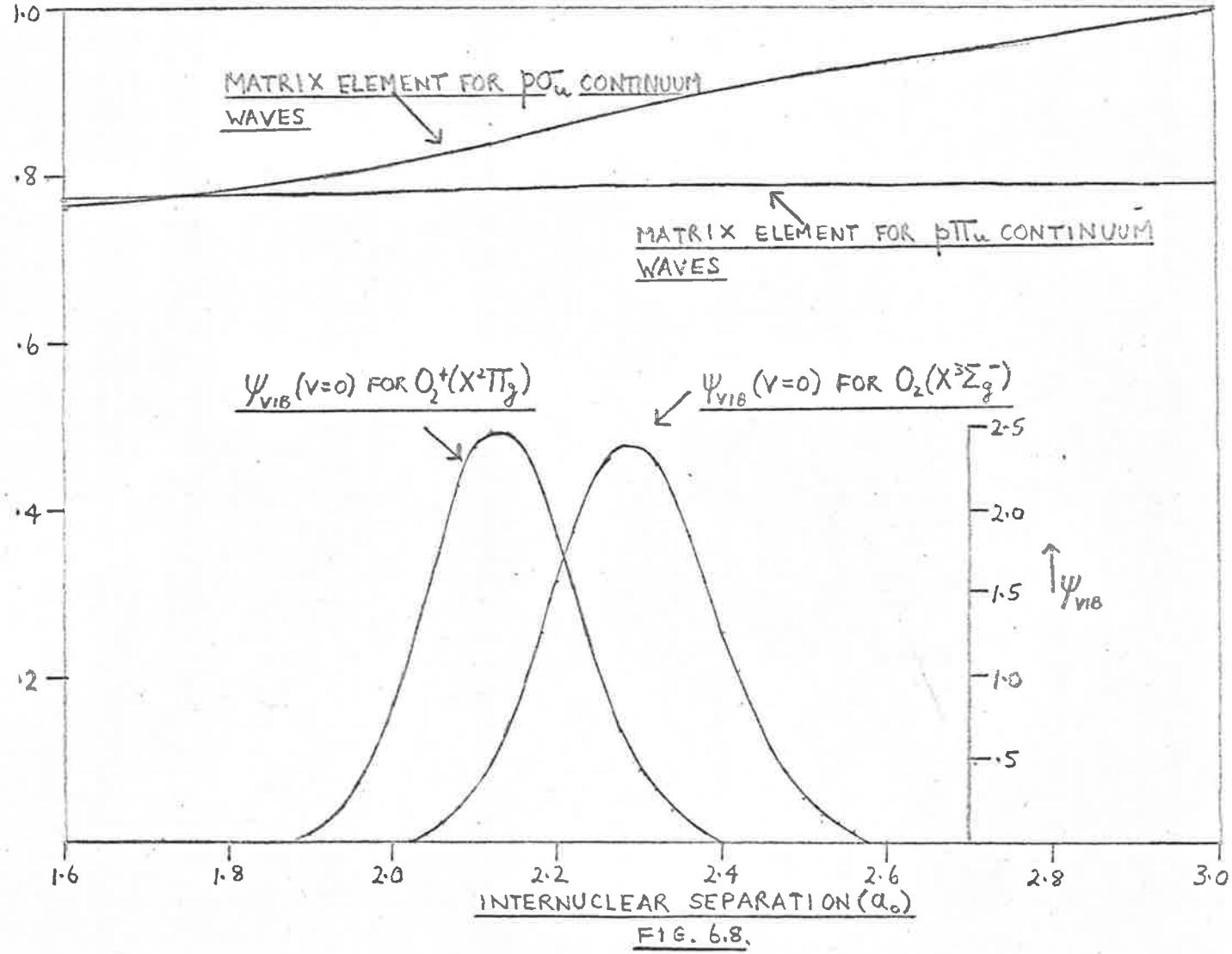
1·0
·8
·6
·4
·2
MATRIX ELEMENT FOR pσu CONTINUUM WAVES
MATRIX ELEMENT FOR pπu CONTINUUM WAVES
ψVIB (V=0) FOR O2+(X2Πg)
ψVIB (V=0) FOR O2(X3Σg−)
2·5
2·0
1·5
1·0
·5
ψVIB
1·6
1·8
2·0
2·2
2·4
2·6
2·8
3·0
INTERNUCLEAR SEPARATION (a0)

FIG. 6.8.

in table 6.1.

TABLE 6.1.

CROSS SECTIONS IN Mbn FOR PHOTOIONIZATION TO $O_2^+(X^2\Pi_g)$ FOR VARIOUS v_f AT THRESHOLDS ($\mathcal{E} = 0$)

v_f	CROSS SECTION USING FRANCK-CONDON FACTORS.	CROSS SECTION INCLUDING THE R - DEPENDENCE OF THE TRANSITION MOMENTS.
0	·83055	·80531
1	1·40248	1·39410
2	·96173	·97894
3	·34252	·35572
4	·06708	·07066
5	·00706	·00741
6	·00031	·00035
7	·00000	·00005
8	·00000	·00000
9	·00000	·00000

It can be seen that the difference in the results obtained by the two methods is only of the order of a few per cent for the most important contributions.

Our conclusion that the Franck-Condon factor

approximation is valid for photo-ionization calculations cannot at this stage be generalized. We have restricted our attention to a single process in O_2 and only considered the case of continuum waves for zero energy. We will be employing the methods of this section to investigate other transitions in O_2 as well as photoionization processes in N_2 in those cases where use of Flannery and Opik's final state model has given good agreement between experimental and calculated cross sections near threshold. We will then reach a more general conclusion concerning the Franck-Condon factor approximation, though the above results point to its validity.

6.5. TOTAL CROSS SECTIONS FOR N_2 AND O_2 FROM THRESHOLDS TO 50Å.

Most experimental reports on photo-ionization of N_2 and O_2 have given total cross sections or total absorption cross sections with or without photoionization efficiency data. The total absorption coefficient, k, defined by

$$I = I_0 e^{-kx} \tag{6.36}$$

has contributions from photoionization (above thresholds), pre-ionization, dissociation, dissociative ionization, band absorption etc. The processes of band absorption and pre-ionization are expected to have large cross sections at and near specific photon frequencies (for allowed transitions).

The early experimental work of Weissler and Lee[86] on O_2 was performed with line sources and results were given for the total absorption coefficient from 1306Å to 304Å. In 1955, Wainfain et al[53] determined absorption cross sections and photoionization cross sections for several gases including O_2 and N_2 from 473Å to 991Å. At certain frequencies measurements were made with large and small ion-chambers which usually give slightly different results. In figures 6.9 and 6.10 these results are shown. Averages

were taken for the two ion chambers if both were employed at a given frequency. Further, as is the case for the plotted results of Samson and Cairns[57,87], the measurements are averaged over 10Å intervals for the sake of clarity. That such an averaging procedure is necessary is unfortunate because some exceptionally high readings which are probably due to pre-ionization or discrete absorption, influence the photoionization results. There have been many other reports of absorption and photoionization cross sections [88,89,90,63,83], the reference list not being exhaustive. We have chosen not to include the more recent results of Cook and Metzger[63] and Matzanuga and Watanabe[83] because of the large fluctuations in the magnitudes of the cross sections. These arise when the experiments are performed with very accurate frequency measurement and are clearly not due to the transitions from the bound states of the ground electronic states of the molecules to the continuum. This explains why we only show the more smoothly varying (due to less accurate frequency measurement) results of Samson and Cairns and Wainfain et al. The results of Samson and Cairns[87] give the photoionization cross sections from threshold to 300Å. These experimentalists have also investigated the absorption cross sections from 550Å - 200Å and though no photoionization efficiencies

were given we have included this set of results in the absence of any other data in the above wavelength region. The results of our calculations for the total photoionization cross sections for N_2 and O_2 from first thresholds to 50Å are also shown in figures 6.9 and 6.10.

Results for O_2. (See fig. 6.9). We have already discussed the cross section from 1027Å to 796Å in section 6.3. At higher energies we must add the partial cross sections due to all energetically possible processes. It can be seen that the general trends of the calculated and experimental results are in concurrence from 796Å to 600Å. We note that whereas the onsets of the transitions to the Π_u states of O_2^+ result in fairly smooth increases in the cross section, those for the Σ_g states are sudden because of the large Franck-Condon factors. There is little agreement between calculated and observed cross sections above 600Å though the general trends remain similar to the onset of the transition to $O_2^+(c^4\Sigma_u^-)$ at 510Å. At higher energies the two curves depart radically indicating a general failure of the model we have employed in our calculations. More specifically the results where transitions only occur to the Π states, and to the $(b^4\Sigma_g^-, {}^2\Sigma_g^-)$ states are in reasonable agreement with experiment. When our model is used

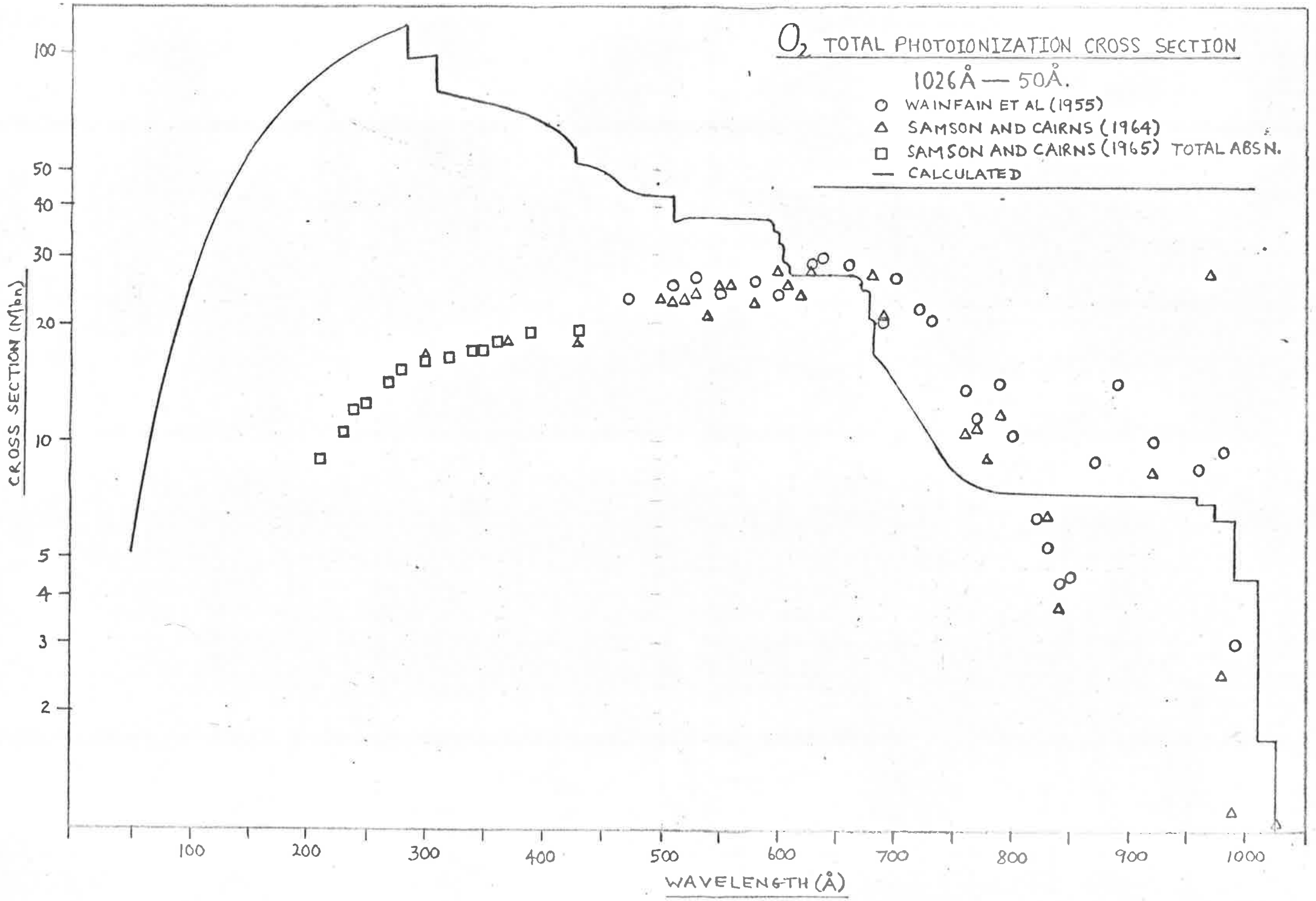
O_2 TOTAL PHOTOIONIZATION CROSS SECTION
1026Å — 50Å.
WAINFAIN ET AL (1955)
SAMSON AND CAIRNS (1964)
SAMSON AND CAIRNS (1965) TOTAL ABSN.
CALCULATED
CROSS SECTION (Mbn)
100
50
40
30
20
10
5
4
3
2
100
200
300
400
500
600
700
800
900
1000
WAVELENGTH (Å)

FIG. 6.9.

for $2\sigma_u$ and $2\sigma_g$ orbitals (see Ch. 5) the calculated values are much too large. Finally we note that the experimental absorption cross sections decrease at higher energies to a value of about 10Mbn near 200Å. The calculated cross sections also diminish at high energies but do not fall to 10Mbn until photon wavelengths of about 70Å.

Results for N_2. (See fig. 6.10). There are only four photoionization processes for $N_2(\ X^1\Sigma_g^+\ )$ in the wavelength range 796 $\longrightarrow$ 50Å. However, agreement between calculated and measured cross sections is found over a much narrower wavelength range for N_2 than for O_2. Only from the first ionization potential to the $N_2^+(\ B^2\Sigma_u^+\ )$ threshold do the two sets of results resemble one another. This disagreement was anticipated in section 6.3 where we saw that the transition involving the $2\sigma_u$ orbital gives calculated results which are nearly three times as large as the measured values. The partial cross sections for the $A^2\Pi_u$ and $B^2\Sigma_u^+$ final states increase from threshold to reach maxima at much shorter wavelengths and the diminishing contribution from the $X^2\Sigma_g^+$ final state cannot compensate these increases. Consequently, the calculated cross sections remain far too high even when

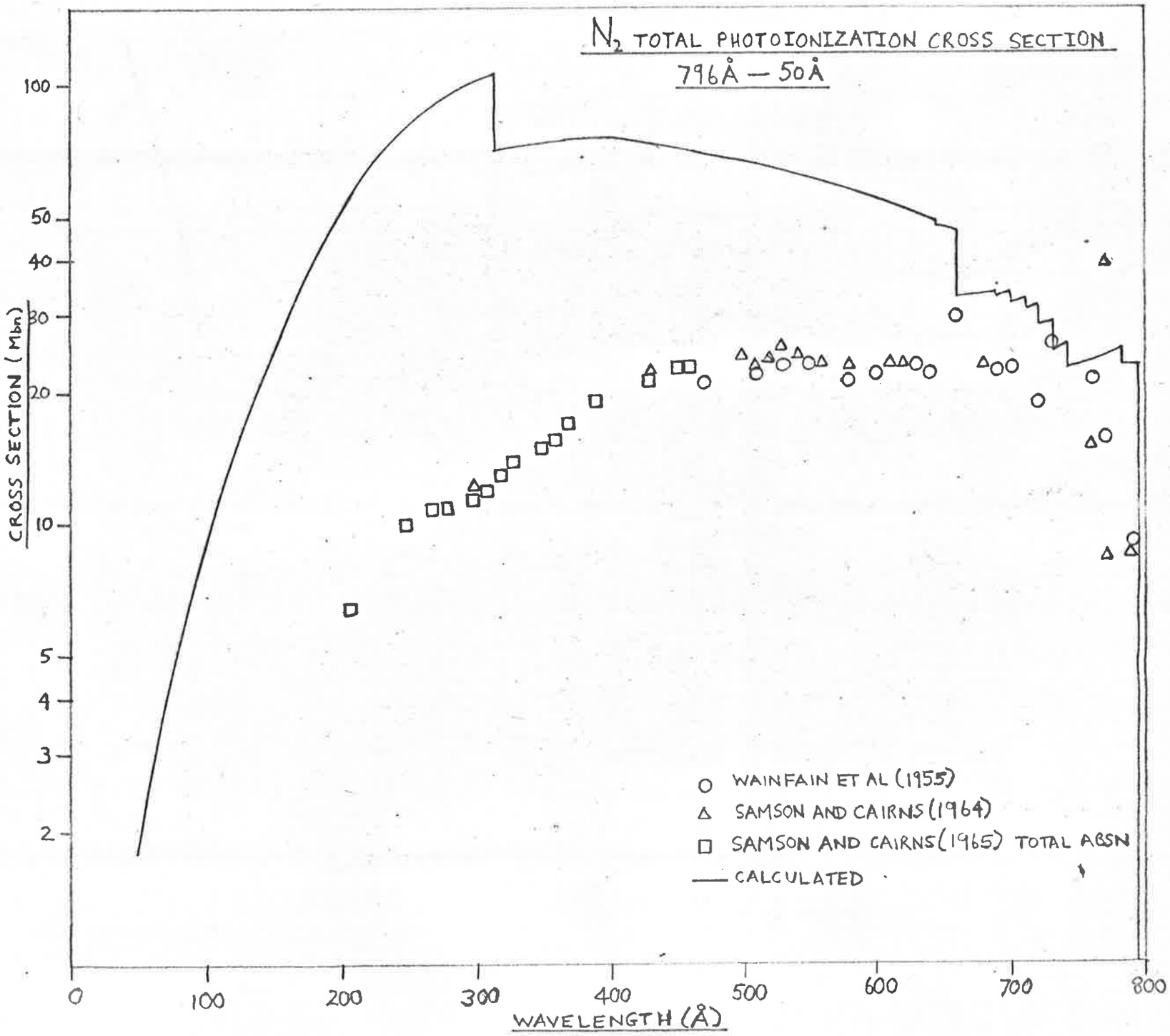
N_2 TOTAL PHOTOIONIZATION CROSS SECTION
796Å — 50Å
CROSS SECTION (Mbn)
100
50
40
30
20
10
5
4
3
2
0
100
200
300
400
500
600
700
800
WAVELENGTH (Å)
WAINFAIN ET AL (1955)
SAMSON AND CAIRNS (1964)
SAMSON AND CAIRNS (1965) TOTAL ABSN
CALCULATED

FIG. 6.10

the photon wavelength is of order 150Å. In Chapter 8 the failures and successes of our model for the various transitions will be discussed in greater detail.

CHAPTER 7.

PHOTOIONIZATION OF THE 2π ELECTRON OF NITRIC OXIDE.

7.1. BOUND STATE WAVE FUNCTION.

In heteronuclear diatomic molecules the molecular orbitals can not be ascribed g or u - symmetry on inversion because, in an L.C.A.O. framework, different atomic orbitals from which an M.O. is synthesised are employed for each centre. S.C.F.-L.C.A.O.-M.O. wave functions have been found for nitric oxide by Brion et al.[91,92] The electronic structure of NO was given as

$$NO(X^2\Pi_r) : (1\sigma)^2(2\sigma)^2(3\sigma)^2(4\sigma)^2(5\sigma)^2(1\pi)^4(2\pi) \qquad (7.1).$$

In this chapter we restrict our attention to the photoionization of the 2π electron which occurs at the first ionization potential of the molecule, and results in the production of the $X^1\Sigma^+$ state of NO^+.

Brion et al have employed real Slater type A.O.'s (with the orthogonal 2s function) which have been discussed in Ch. 2. Using subscripts O and N to denote orbitals on the oxygen and nitrogen centres respectively, the above workers found in their complete treatment that the coefficients a_1 and a_2 in the expression

$$\psi^{(2\pi)} = a_1 2p\pi_N + a_2 2p\pi_O \qquad (7.2)$$

should be $a_1 = \cdot 8781$, $a_2 = -\cdot 6936$. Denoting the orbital exponents of the oxygen and nitrogen Slater type $2p\pi$ orbitals by ζ_O and ζ_N respectively we have

$$\psi^{(2\pi)} = a_1' r_1 \sin\theta_1 \cos\phi_1 e^{-\zeta_N r_1} + a_2' r_2 \sin\theta_2 \cos\phi_2 e^{-\zeta_O r_2} \tag{7.3}$$

where $a_1' = a_1 (\zeta_N^5/\pi)^{1/2}$ and $a_2' = a_2 (\zeta_O^5/\pi)^{1/2}$.

We can write (7.3) in prolate spheroidal co-ordinates

$$\psi^{(2\pi)} = \frac{R}{2} (\lambda^2-1)^{1/2} (1-\mu^2)^{1/2} \cos\phi \left[a_1' e^{-\alpha_N \lambda} e^{-\alpha_N \mu} - a_2' e^{-\alpha_O \lambda} e^{\alpha_O \mu} \right] \tag{7.4}$$

with

$$\alpha_N = \zeta_N R/2 \qquad \alpha_O = \zeta_O R/2 \tag{7.5}.$$

Clearly (7.4) has no definite symmetry property under the inversion operation.

7.2. MATRIX ELEMENTS.

We have seen that Flannery and Opik's final state model has proved fairly reliable for the most loosely bound electrons in O_2 and N_2. We hence feel, that despite the obvious limitation of the model when applied to heteronuclear diatomic molecular ions in that the field of the latter will not be symmetric between the nuclei, we should be able to obtain fairly reliable continuum waves in such cases when the difference in atomic numbers of the two atoms in the molecule is not too large. With this latter condition certainly fulfilled in the case of NO, we now determine the expressions for the electronic matrix elements for photo-ejection from the 2π orbital given in (7.4).

Clearly by comparison with the case of ejection from $1\pi_{g,u}$ orbitals for which the electronic matrix elements have been evaluated in sections 4.1 and 4.2, we find that only σ, π and δ continuum waves contribute in the present case. Thus the selection rule on m is still satisfied. The analogous behaviour ceases when we consider the integrations over the angular co-ordinate μ. The expression (7.4) clearly admits mixtures of g and u symmetry waves in the

final states and further we expect that since both (3.20) and (3.21) will be valid for the functions $M(\mu)$ that the continuum waves will have both even and odd ℓ .

If we denote the components due to (3.20) and (3.21) by I and II respectively, then

$$\mathcal{M}^{0,\ell}_{x,I} = \frac{R^5\pi}{32}\int_1^\infty\int_{-1}^{1}(\lambda^2-1)(1-\mu^2)(\lambda^2-\mu^2)\times \tag{7.6}$$

$$\times\left[a_1' e^{-\alpha_N\lambda}e^{-\alpha_N\mu} - a_2' e^{-\alpha_0\lambda}e^{\alpha_0\mu}\right]\times\sum_{n=0}^{\infty}{}'(d_n(k|0,\ell))\times$$

$$\times P_n(\mu)\Lambda_{0,\ell}(\lambda)\,d\mu\,d\lambda\ ;\ \ell = 0,2,4\ldots.$$

$$= \frac{R^5\pi}{32}\sum_{n=0}^{\infty}{}'d_n(k|0,\ell)\int_1^\infty(\lambda^2-1)\Lambda_{0,\ell}(\lambda)\Big\{a_1' e^{-\alpha_N\lambda}\left[\lambda^2\left(A_n^N(\alpha_N)-B_n^N(\alpha_N)\right)\right.$$

$$\left.+C_n^N(\alpha_N)-B_n^N(\alpha_N)\right] - a_2' e^{-\alpha_0\lambda}\left[\lambda^2\left(A_n^0(\alpha_0)-B_n^0(\alpha_0)\right)+C_n^0(\alpha_0)-B_n^0(\alpha_0)\right]\Big\}d\lambda \tag{7.7}$$

where

$$A_n^N(\alpha_N), B_n^N(\alpha_N), C_n^N(\alpha_N) = \int_{-1}^{1}P_n(\mu)\,(1,\mu^2,\mu^4)\,e^{-\alpha_N\mu}\,d\mu \tag{7.8}$$

$$A_n^0(\alpha_0), B_n^0(\alpha_0), C_n^0(\alpha_0) = \int_{-1}^{1}P_n(\mu)\,(1,\mu^2,\mu^4)\,e^{\alpha_0\mu}\,d\mu \tag{7.9}$$

with n = 0, 2, 4.....

When we consider $\mathcal{M}^{0,\ell}_{x,II}$ we find that the expressions are identical to those for $\mathcal{M}^{0,\ell}_{x,I}$. However, the values of ℓ are now 1, 3, 5.... and those of n are 1, 3, 5....

We find for the contributions from δ - waves,

$$\mathcal{M}^{2,\ell}_{x,I} = \mathcal{M}^{2,\ell}_{y,I} = \frac{R^5\pi}{64}\sum_{n=0}^{\infty}{}' d_n(k|2,\ell)\int_1^{\infty}(\lambda^2-1)\Lambda_{2,\ell}(\lambda)\times$$

$$\times\left\{a_1' e^{-\alpha_N\lambda}\left[\lambda^2\left(G_n^N(\alpha_N) - H_n^N(\alpha_N)\right) + I_n^N(\alpha_N) - H_n^N(\alpha_N)\right] -\right.$$

$$\left. - a_2' e^{-\alpha_0\lambda}\left[\lambda^2\left(G_n^0(\alpha_0) - H_n^0(\alpha_0)\right) + I_n^0(\alpha_0) - H_n^0(\alpha_0)\right]\right\} d\lambda \qquad (7.10)$$

$\ell = 2, 4, 6\ldots$

where

$$G_n^N(\alpha_N), H_n^N(\alpha_N), I_n^N(\alpha_N) = \int_{-1}^{1} P_{n+2}^2(\mu)\, e^{-\alpha_N\mu}(1,\mu^2,\mu^4)\, d\mu \qquad (7.11)$$

$$G_n^0(\alpha_0), H_n^0(\alpha_0), I_n^0(\alpha_0) = \int_{-1}^{1} P_{n+2}^2(\mu)\, e^{\alpha_0\mu}(1,\mu^2,\mu^4)\, d\mu \qquad (7.12)$$

and for $\mathcal{M}^{2,\ell}_{x,II}$ the values of ℓ are 3, 5, 7.... and those of n are 1, 3, 5.... Finally we find for contributions from π- continuum waves,

$$\mathcal{M}^{1,\ell}_{z,I} = \frac{\pi R^5}{32}\sum_{n=0}^{\infty}{}' d_n(k|1,\ell)\int_1^{\infty}(\lambda^2-1)^{1/2}\Lambda_{1,\ell}(\lambda)\left\{a_1' e^{-\alpha_N\lambda}\left[\lambda^2 D_n^N(\alpha_N) -\right.\right.$$

$$\left.\left. - E_n^N(\alpha_N)\right] - a_2' e^{-\alpha_0\lambda}\left[\lambda^2 D_n^0(\alpha_0) - E_n^0(\alpha_0)\right]\right\} d\lambda \qquad (7.13)$$

$\ell = 1, 3, 5\ldots$; $\mathcal{M}^{1,\ell}_{z,II}$, $\ell = 2, 4, 6\ldots$, $n = 1, 3, 5\ldots$.

where

$$D_n^N(\alpha_N), E_n^N(\alpha_N) = \int_{-1}^{1}(1-\mu^2)^{\frac{1}{2}} e^{-\alpha_N\mu} P_{n+1}^1(\mu)(\mu,\mu^3)\, d\mu \qquad (7.14)$$

$$D_n^0(\alpha_0), E_n^0(\alpha_0) = \int_{-1}^{1}(1-\mu^2)^{\frac{1}{2}} e^{\alpha_0\mu} P_{n+1}^1(\mu)(\mu,\mu^3)\, d\mu$$

(7.15).

It can be seen that the labour involved in computing the cross sections for molecular orbitals in NO will be at least twice that for those of homonuclear diatomic molecules. The cross sections could indeed be found from the expressions we have developed in this section but we now turn to an approximate approach which we expect to yield reliable results.

7.3. APPROXIMATE CALCULATION OF THE CROSS SECTION FROM 1340 - 1022Å.

We have noted that the calculation of the cross section for ejection from even the 2π electron of NO by the methods of section 7.2 would involve much computational labour. Furthermore, since accurate methods have not yet been developed for finding continuum waves for electrons ejected from homonuclear diatomic molecules, it seems probable that accurate methods for finding wave functions for electrons ejected from heteronuclear diatomic molecules will not be found in the near future. We thus feel that some progress would be made in this field if a fairly reliable approximate method could be developed.

The most appealing simplification in the treatment of heteronuclear molecules in which the atomic numbers of the component atoms do not differ very much, is to regard the molecule as composed of two atoms whose properties represent the average properties of the two individual atoms.

In the case of NO the difference in atomic numbers is of course unity. Furthermore, NO is

isoelectronic with O_2^+, both having 15 electrons and ground electronic states denoted by $X^2\Pi$. We have constructed a Π_g orbital on two centres separated by the ground state equilibrium internuclear separation of NO, $r_e = 2{\cdot}17471a_o$ [79], using atomic Slater $^2p\pi$ orbitals whose orbital exponent is the average of the values for N and O atoms. This yields a value of $\zeta_2^{NO} = 2{\cdot}1125$. The only other parameter needed for the programme used in the evaluation of the cross section is the threshold energy, which, from Gilmore [64] is 9·25eV for transitions to the zeroth vibrational level of $NO^+(X'\Sigma^+)$. Furthermore, to account for transitions to different vibrational quantum levels of the ion, Franck-Condon factors are again employed and we expect from the discussion in section 6.4 that this approximation should be fairly reliable. Franck-Condon factors for the transition

$$NO(X^2\Pi_r) + h\nu \rightarrow NO^+(X'\Sigma^+) + \bar{e} \qquad (7.16)$$

have been calculated by Wacks [79] and these were employed in the present calculations according to the expression 6.28.

7.4. RESULTS AND DISCUSSION.

In figure 7.1 are shown the results for the cross section calculated by the method outlined in the previous section for photon wavelengths from 1340Å (threshold) to 1022Å. Experimental cross sections in this wavelength region have been obtained by Marmo[93], Watanabe et al[94], and Watanabe[95,96] and those of the last reference have been shown in figure 7.1 for the wavelength region from 1340Å to 1060Å.

Since the equilibrium internuclear separations of $NO(X^2\Pi_r)$ and $NO^+(X^1\Sigma^+)$ are not very much different, the Franck-Condon factors are large for small vibrational quantum numbers of the ion. As we have seen in section 6.4, this means that the cross section has large steps near the first ionization potential. Watanabe's experimental results show the onset of transitions to the various vibrational levels of NO^+ in a most striking manner, the $v_f = 0$, 1, 2 and 3 thresholds being most prominent. The general agreement between the calculated and experimental cross sections in the above wavelength region is surprisingly good, considering the approximate methods we have employed in determining the cross sections.

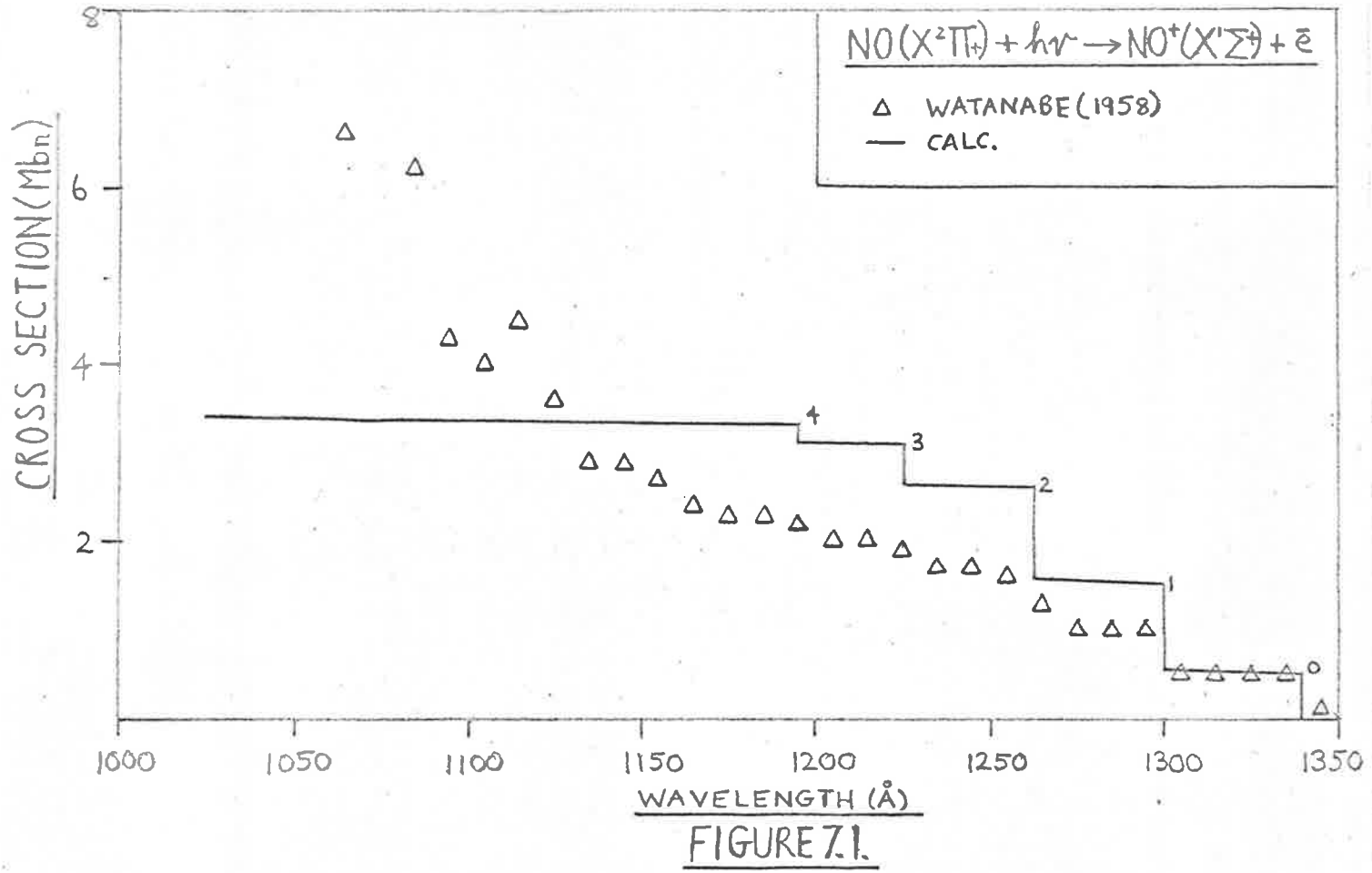
NO(X²Π) + hν → NO⁺(X¹Σ⁺) + e
WATANABE (1958)
CALC.
CROSS SECTION (Mbn)
8
6
4
2
1000
1050
1100
1150
1200
1250
1300
1350
WAVELENGTH (Å)
4
3
2
1
0

FIGURE 7.1.

These results are sufficiently encouraging to warrant the use of our method for determining the cross sections for the 1π and possibly the 5σ electrons of NO. We will also be able to investigate the reliability of our model for carbon monoxide. Furthermore, the results for the 2π electron in NO can be easily extended to higher energies and comparison will then be possible with the experimental partial cross section obtained for the process (7.16) by Kumar[97].

CHAPTER 8.

CONCLUSIONS.

We have seen in Ch. 1 that photo-ionization cross sections for any bound electronic system, whether atomic or molecular‡, can be reliably calculated if accurate one-electron initial and final state wave functions can be found. Further, for atomic calculations the problem of finding such wave functions can usually be solved by employing self consistent field methods, with or without exchange terms in the radial equations. That the problem can be solved in this manner is due to the high reliability of the central field approximation for atoms.

We are not suggesting that the problems concerned with atomic cross sections are at all finalized. Some systems have their special difficulties, especially when there is a strong chance of cancellation in the radial transition integrals. However such difficulties, though they may not be removable by exact methods, can at least be subject to a phenomenological approach and suitable mathematical models determined. We note that in atomic calculations the amount of labour involved in finding the variation of the cross section with the incident photon

‡ Assuming of course, for molecules, that accurate vibrational eigenfunctions are available.

energy is at least subject to an upper limit insofar as there are, for a given bound state orbital, at most two final state waves which need to be taken into account.

Turning our attention to molecules we see that cross sections for the simplest molecule, H_2^+, as is the case with the simplest atom, H, can be found exactly. The analogy is not complete however, for whereas in the case of H the final state waves can be expressed analytically (Coulomb scattered waves), in the case of H_2^+ the important radial equations must be solved numerically. Furthermore, whereas for the ground state of H(l=0), there is only one continuum wave, in the case of H_2^+ there are an infinite number. However, only those with angular momentum of order l = 1 will of course give rise to appreciable dipole length matrix elements. Nevertheless there is much more computational labour for H_2^+ than H.

In the history of atomic cross section calculations for more complex systems, it was found that the best simple approximation is to use Slater type A.O.'s and Coulomb scattered waves for the final states. This latter approximation has a physical foundation for electrons ejected from outer shells in that the remaining electrons

should screen the free electron from the nuclei, and a mathematical foundation in that the dipole length matrix elements rely most heavily on the form of the wave functions at large r where the continuum waves achieve their asymptotic forms. In a sense, our calculations for diatomic molecules, especially N_2 and O_2, have been of the same order of approximation as the above method for atoms. We expect that for electrons ejected from the most loosely bound molecular orbitals the effective field at large distances from the molecule will be approximately that of two half elementary positive charges placed at the nuclei. This approximation is justified for homonuclear diatomic molecules because such systems have no dipole moment. Further, the initial state electronic wave functions which were of the S.C.F.-L.C.A.O.-M.O. type in our calculations should be fairly reliable though as we have pointed out previously there is some uncertainty in the predicted ionization potentials which constitute one of the criteria for assessing their accuracy.

The inclusion of vibrational and rotational states for molecular calculations has no analogy in calculations for atoms. In Chapter 6 we developed a method for taking

the vibrational motion of the molecule into account, making use of the concept of Franck-Condon factors. With these three approximations i.e. S.C.F.-L.C.A.O.-M.O. initial electronic wave functions, Flannery and Opik's final state model and Franck-Condon factors we found that the calculated partial cross sections for the $1\pi_g$, $1\pi_u$, and $3\sigma_g$ electrons of N_2 and O_2 were in fair agreement with the experimental values. This agreement was very good near threshold for transitions to $O_2^+(X^2\Pi_g, b^4\Sigma_g^-)$ and $N_2^+(A^2\Pi_u)$, fair for the transition to $N_2^+(X^2\Sigma_g^+)$ and uncertain due to insufficient experimental data for $O_2^+(^2\Sigma_g^-)$. The calculated results for the transitions to $O_2^+(a^4\Pi_u, A^2\Pi_u)$ were somewhat lower than the experimental readings but it is difficult to find support for the latter if the Franck-Condon factor approximation is valid. The experimental results show an extremely rapid increase above threshold whereas the Franck-Condon factors indicate a slowly increasing cross section. If of course, the ground state equilibrium internuclear separations of $O_2^+(a^4\Pi_u, A^2\Pi_u)$ were revised so that they were closer to that of $O_2(X^3\Sigma_g^-)$, there would be a greater chance of agreement between the calculated and measured values for transitions to these states.‡

Furthermore the general trends of the calculated and

‡ Alternatively agreement would be better if the experimental thresholds were lower by about ·4eV.

experimental cross sections for these transitions are similar and the magnitudes of the same order. The major difference is that a given value of the cross section is attained at shorter photon wavelengths for the calculated results.

When we applied the above methods to the $2\sigma_u$ and $2\sigma_g$ electrons in N_2 and O_2 a radical failure of the model was encountered. For all such orbitals the calculated results were far too high. We could only compare calculated and experimental cross sections for the transition to $N_2^+(B^2\Sigma_u^+)$, experimental figures not being available for the other transitions involving 2σ orbitals. Nevertheless we can see that the calculated partial cross sections for these other transitions are far too high because the total cross sections show no noticeable increases near the expected thresholds.

The failure of the method in describing the processes involving the $2\sigma_u$ and $2\sigma_g$ orbitals can be traced primarily to the final state model though we cannot deem the bound state electronic wave functions beyond improvement by any means. We are led to suspect that the final state model is the cause of the break-down for physical and mathematical reasons. Physically, we expect that the screening

of the ejected electron from the nuclei by the outer electrons would not be as great for processes involving these orbitals. Mathematically, we see that with Flannery and Opik's final state model the continuum waves for a given (m, l, h) are the same for transitions involving $2\sigma_u$ and $2\sigma_g$ bound orbitals as for those involving $1\pi_u$ and $1\pi_g$ bound orbitals. For example, it is clearly unrealistic that the π and σ continuum waves for the $1\pi_g$ case be the same as the corresponding waves for the $2\sigma_g$ case. To further emphasize this point, consider the atomic case where continuum waves for $l = 1$ initial states have $l = 0$ and $l = 2$. For an $l = 0$ initial state there is only an $l = 1$ continuum wave which means different radial equations and hence solutions for the continuum waves in each case. Thus the final state model is most probably at fault. We have of course only explained why the results for the $2\sigma_u$ and $2\sigma_g$ orbitals are in error, not why they are too high. A full explanation is too difficult a task but tentatively it would seem that the inner orbital electrons which are not vacated may have a repulsive effect on the free electron and should therefore diminish the continuum waves in the region where the initial bound state functions for $2\sigma_u$ and $2\sigma_g$ are appreciable, thus lowering the values of the transition integrals and hence the cross sections for these orbitals.

With regard to final state waves for electrons moving in the field of a homonuclear diatomic molecular ion, our final conclusion is that Flannery and Opik's model is satisfactory, and is in fact quite good near threshold, for electrons ejected from $1\pi_g$, $1\bar{\pi}_g$, $1\pi_u$, $1\bar{\pi}_u$ and $3\sigma_g$ orbitals. Calculations for other molecules such as F_2 or Ne_2 would, if the experimental results were found, further substantiate or otherwise our claim which so far is based on Flannery and Opik's results for H_2 [50] and the results of this work for O_2 and N_2.

In Ch. 5 several results of interest were obtained. We had seen that in the calculations for fixed nuclei, the cross sections for $3\sigma_g$ and $1\pi_g$ electrons have pronounced peaks near 200Å where the contributions from higher angular momentum final state waves dominate the cross section. This effect was found to be absent for orbitals of u-symmetry and a tentative explanation of this difference was given in section 5.5. One of the most interesting phenomena was observed when we considered the effects of varying the degree of hybridization in the $3\sigma_g$ orbitals. It was found that when only 2s atomic orbitals were present the cross section steadily diminished from threshold to 50Å. In fact we found that high energy

peaks only arose when there were $2p_z$ atomic orbitals present in the initial state wave function. In addition we found that the effects of hybridization on the cross sections for $2\sigma_u$ orbitals were far less important than for $3\sigma_g$ orbitals. The use of $2p_z$ atomic orbitals only gave results which were higher at all energies than those for the hybrid (S.C.F.-L.C.A.O.-M.O.) orbital, whereas the use of 2s atomic orbitals only gave results which were lower at all energies.

The "shoulders" observed near 200Å in the absorption cross sections for N_2 and O_2 by Samson and Cairns[57] have been discussed recently by several workers [58],[59],[82]. Our high energy peaks in the cross sections for $3\sigma_g$ and $1\pi_g$ orbitals are pertinent to this subject. We feel that these peaks are definitely the effect that Cohen and Fano[58] discovered in their simple treatment of photoionization from a σ_g state. We suspect that the failure of Bates and Opik to find any appreciable shoulder effect for H_2^+ and for their model complex molecule was due to the absence of $2p_z$ orbitals in the bound states which as pointed out above are responsible for the high energy peaks. The locations of our peaks are at the right wavelengths to be considered as the cause of a

shoulder effect. However, in our total cross section curves for O_2 and N_2 these effects are masked because of the dominance of the partial cross sections for $2\sigma_u$ and $2\sigma_g$ states which we have noted are far too high.

In Chapter 6 we devoted a section to finding the effects of including the dependence of electronic dipole matrix elements on internuclear separation for the transition $O_2(X^3\Sigma_g^-) + h\nu \rightarrow O_2^+(X^2\Pi_g) + \bar{e}$. The r - centroid approximation which has been often used for describing band intensities in emission and absorption depends on the assumption that the electronic transition moment is a slowly varying function of internuclear separation. For the case we investigated we found that this variation was indeed slow. Furthermore, by performing the double integration over the electronic and nuclear co-ordinates we were able to investigate for the case of zero energy continuum waves, the reliability of the Franck-Condon factor approximation. We found that the results of the double integration method and the Franck-Condon factor approach gave results which agreed to within a few percent for those vibrational levels of the ion O_2^+ which have appreciable partial cross sections. Thus the results of this investigation pointed to the validity

of the Franck-Condon factor approximation though we could not at the time of writing generalize this conclusion. However, the fact that the shapes near threshold of the partial cross sections obtained by using Franck-Condon factors for those initial states where Flannery and Opik's model for the final electronic states should be reliable were similar to those of the experimental partial cross sections lends support to the validity of the Franck-Condon factor approximation for ionizing transitions in homonuclear diatomic molecules.

Our final investigation presented in Ch. 7 concerned photoionization cross sections for heteronuclear diatomic molecules. We only had space to investigate the transition from the ground state of NO to the ground state of NO^+. We found that since the initial states have no definite symmetry properties on inversion in the mid point between the nuclei, both g and u-symmetry final state continuum waves were allowed and further-more that both odd and even l continuum states contributed to the cross section. Since the computational work would then be at least twice as much as for a homonuclear molecule we pursued an approximate treatment where the molecule NO was replaced by a homonuclear molecule composed of

two atoms whose properties were, in the sense described in Ch. 7, the average of the properties of N and O. The results obtained with this approximation were sufficiently promising in the wavelength range 1340Å to 1022Å that we feel it will be worthwhile to apply the technique at higher energies for the transition considered, for other orbitals of NO and also for other heteronuclear diatomic molecules such as CO where the atomic numbers of the constituent atoms do not differ appreciably.

At present, calculations on molecular photoionization cross sections have reached the stage that atomic calculations had reached in the late 1930's when approximate methods were being sought in order to obtain results for many systems without too much computational labour. Modern computers make the numerical work much easier of course, but it is difficult to see exactly what form the next steps should take in estimating molecular cross sections. At present it does not seem that a method analogous to be the self consistent field approach for atoms will be found in the near future. Thus a phenomenological approach, though it would not incorporate rigorous methods and generalized formulations of the various problems, would perhaps be the best way of gaining insight into the nature of the

various effects involved. The greatest problem at present appears to be the determination of reliable continuum waves for electrons ejected from the inner shells $2\sigma_u$ and $2\sigma_g$. A phenomenological approach to this kind of problem has already been mentioned in Ch. 3, where the method of Fisk[68] for calculations on elastic scattering of slow electrons by diatomic molecules was mentioned. The basic approach would then be to try different $g(\lambda)$ in the potential $V(\lambda,\mu) = g(\lambda)/(\lambda^2-\mu^2)$. One could then work with a Schrodinger equation whose solutions are separable in prolate spheroidal co-ordinates which has the distinct advantage that since the S.C.F.-L.C.A.O.-M.O.'s can be written (as in Ch. 2) in analytic form if Slater type A.O.'s are used (not necessarily with the original Slater values for the orbital exponents), then the evaluation of the dipole length matrix elements can be performed for a great part by analytic methods.

Calculation of molecular photoionization cross sections presents difficult problems which have not been solved or to a large extent even tackled. In the light of the important astrophysical applications, it is clear that a vigorous research programme is needed in order to bring this field to a more advanced level, or at least

to the level that has been attained for calculations of atomic cross sections.

CHAPTER 9.

APPENDICES.

9.1. NORMALIZATION OF THE BOUND 'MOLECULAR ORBITALS OF CHAPTER 2.

Throughout this work we have employed L.C.A.O.-M.O. wave functions for the initial electronic states. In some of our calculations we employed the S.C.F.-L.C.A.O.-M.O.'s of Sahni and Lorenzo[62] but in several others, such as those described in sections 5.3, 5.5, 6.4 and 7.3, we employed modified forms of the wave functions. The algebra involved in the normalization procedures is presented below, and subroutines (XNORM) were employed for their evaluation. Further all these formulae were checked by using the L.C.A.O. coefficients of Sahni and Lorenzo and then verifying that the condition $\int |\psi|^2 d\tau = 1$ was in fact satisfied.

π_g (or $\bar{\pi}_g$) Orbitals.

From (2.26) and (1.9) we find on writing

$$\psi^{(\pi_g, \bar{\pi}_g)} = c(\alpha)(\lambda^2-1)^{\frac{1}{2}}(1-\mu^2)^{1/2} e^{-\alpha\lambda} \sinh(\alpha\mu)(\cos\phi, \sin\phi) \quad (9.1)$$

that

$$\left(\frac{R}{2}\right)^3 C(\alpha)^2 \int_1^\infty \int_{-1}^{1} (\lambda^2-1)(1-\mu^2) e^{-2\alpha\lambda} \sinh^2(\alpha\mu)(\lambda^2-\mu^2)\, d\mu\, d\lambda$$

$$= \left[(2/R)^3 C(\alpha)^{-2}\right]/\pi \qquad (9.2).$$

Eventually we find

$$C(\alpha) = 2\sqrt{2}\, R^{-1} \Big/ \left\{R\pi \left[I_1(J_3-J_2) + I_2(J_1-J_3) + I_3(J_2-J_1)\right]\right\}^{1/2} \qquad (9.3)$$

where

$$I_1, I_2, I_3 = \int_{-1}^{1} \sinh^2(\alpha\mu)(1, \mu^2, \mu^4)\, d\mu \qquad (9.4)$$

$$J_1, J_2, J_3 = \int_1^\infty e^{-2\alpha\lambda}(1, \lambda^2, \lambda^4)\, d\lambda \qquad (9.5).$$

Explicitly we have

$$I_1 = \alpha^{-1}\left[\sinh 2\alpha/2 - \alpha\right] \qquad (9.6)$$

$$I_2 = \alpha^{-3}\left[\sinh(2\alpha)\left[\alpha^2/2 + 1/4\right] - \tfrac{1}{2}\alpha\cosh(2\alpha) - \alpha^3/3\right] \qquad (9.7)$$

$$I_3 = \alpha^{-5}\left[\sinh(2\alpha)\left\{\alpha^4/2 + 3\alpha^2/2 + 3/4\right\} - \right. \qquad (9.8)$$

$$\left. - \tfrac{1}{4}\cosh(2\alpha)\left(4\alpha^3 + 6\alpha\right) - \alpha^5/5\right]$$

$$J_1 = \tfrac{1}{2}\alpha^{-1} e^{-2\alpha} \qquad (9.9)$$

$$J_2 = \tfrac{1}{2} e^{-2\alpha}\alpha^{-1}\left[1 + \alpha^{-1} + \tfrac{1}{2}\alpha^{-2}\right] \qquad (9.10)$$

$$J_3 = e^{-2\alpha}\alpha^{-1}\left[\tfrac{1}{2} + \alpha^{-1} + \tfrac{3}{2}\alpha^{-2} + \tfrac{3}{2}\alpha^{-3} + \tfrac{3}{4}\alpha^{-4}\right] \qquad (9.11).$$

π_u (or $\bar{\pi}_u$) Orbitals.

If we write

$$\psi(\pi_u, \bar{\pi}_u) = C(\alpha)(\lambda^2-1)^{\frac{1}{2}}(1-\mu^2)^{1/2} e^{-\alpha\lambda}\cosh(\alpha\mu)(\cos\phi, \sin\phi) \tag{9.12}$$

then using the above notation we find

$$C(\alpha) = 2\sqrt{2}R^{-1}/\left\{\left(\frac{4}{3}J_3 - \frac{8}{5}J_2 + \frac{4}{15}J_1\right) + I_1(J_3 - J_2) + \right.$$
$$\left. + I_2(J_1 - J_3) + I_3(J_2 - J_1)\right\}^{1/2} \tag{9.13}$$

σ_g Orbitals.

We have

$$\psi(\sigma_g) = C(\alpha,\beta)\left[2(C_1-C_3)e^{-\beta\lambda}\cosh(\beta\mu) + \right.$$
$$\left. + Re^{-\alpha\lambda}\{\cosh(\alpha\mu)(C_4+C_2\lambda) - (C_2+C_4\lambda)\mu\sinh(\alpha\mu)\}\right] \tag{9.14}$$

Applying the normalization condition (1.9) gives

$$C(\alpha,\beta) = 2/\left\{R^3\,\Pi\, I(\alpha,\beta)\right\}^{1/2} \tag{9.15}$$

where

$$I = C_5^2 I_1 + R^2 I_2 + 2C_5 R I_3 \quad , \quad C_5 = 2(C_1 - C_3) \tag{9.16}$$

$$I_1 = \int_1^\infty\int_{-1}^{1} e^{-2\beta\lambda}\cosh^2(\beta\mu)(\lambda^2-\mu^2)\,d\mu\,d\lambda \tag{9.17}$$

$$I_2 = \int_1^\infty \int_{-1}^{1} e^{-2\alpha\lambda} \left\{ \cosh(\alpha\mu)(C_4 + C_2\lambda) - (C_2 + C_4\lambda)\mu \sinh(\alpha\mu) \right\}^2 \times (\lambda^2 - \mu^2)\, d\mu\, d\lambda \tag{9.18}$$

$$I_3 = \int_1^\infty \int_{-1}^{1} e^{-(\alpha+\beta)\lambda} \cosh(\beta\mu) \left\{ \cosh(\alpha\mu)(C_4 + C_2\lambda) - (C_2 + C_4\lambda)\mu \sinh(\alpha\mu) \right\} \times (\lambda^2 - \mu^2)\, d\mu\, d\lambda \tag{9.19}.$$

We find we can write

$$I_1 = \tfrac{1}{2} e^{-2\beta} \beta^{-1} \left[I_4 (1 + \beta^{-1} + \tfrac{1}{2}\beta^{-2}) - I_5 \right] \tag{9.20}$$

where

$$I_4, I_5 = \int_{-1}^{1} \cosh^2(\beta\mu)\, (1, \mu^2)\, d\mu \tag{9.21}$$

which gives

$$I_4 = 2\beta^{-1} \left[\tfrac{1}{4} \sinh 2\beta + \beta/2 \right] \tag{9.22}$$

$$I_5 = 2\beta^{-3} \left[\beta^2 \left\{ \tfrac{1}{4} \sinh(2\beta) + \beta/2 \right\} - \beta^3/3 - \tfrac{1}{8} \left\{ 2\beta \cosh(2\beta) - \sinh(2\beta) \right\} \right] \tag{9.23}.$$

Further we find

$$\begin{aligned} I_2 = {} & J_0 \left[2 I_{11} C_2 C_4 - I_{10} C_2^2 - I_9 C_4^2 \right] \\ & + 2 J_1 \left[I_{11} (C_2^2 + C_4^2) - C_2 C_4 (I_9 + I_{10}) \right] \\ & + J_2 \left[C_2^2 (I_7 - I_9) + C_4^2 (I_6 - I_{10}) - 2 C_2 C_4 (I_8 - I_{11}) \right] \\ & + 2 J_3 \left[C_2 C_4 (I_6 + I_7) - I_8 (C_4^2 + C_2^2) \right] + J_4 \left[I_6 C_2^2 + I_7 C_4^2 - 2 I_8 C_2 C_4 \right] \end{aligned} \tag{9.24}$$

where

$$J_n = \int_1^\infty e^{-2\alpha\lambda} \lambda^n \, d\lambda \; ; n = 0, 1, 2, 3, 4. \tag{9.25}$$

so that

$$J_0 = e^{-2\alpha}/2\alpha \; ; \quad J_1 = e^{-2\alpha}\alpha^{-1}\left[\tfrac{1}{2} + \tfrac{1}{4}\alpha^{-1}\right] \tag{9.26}$$

$$J_2 = \tfrac{1}{2} e^{-2\alpha}\alpha^{-1}\left[1 + \alpha^{-1} + \tfrac{1}{2}\alpha^{-2}\right] \tag{9.27}$$

$$J_3 = \tfrac{1}{2}\alpha^{-1} e^{-2\alpha}\left[1 + \tfrac{3}{2}\alpha^{-1} + \tfrac{3}{2}\alpha^{-2} + \tfrac{3}{4}\alpha^{-3}\right] \tag{9.28}$$

$$J_4 = (e^{-2\alpha}/2\alpha) + 2\alpha^{-1} J_3 \tag{9.29}.$$

We have defined

$$I_6, I_9 = \int_{-1}^{1} \cosh^2(\alpha\mu)\,(1, \mu^2)\, d\mu \tag{9.30}$$

$$I_7, I_{10} = \int_{-1}^{1} \sinh^2(\alpha\mu)\,(\mu^2, \mu^4)\, d\mu \tag{9.31}$$

$$I_8, I_{11} = \int_{-1}^{1} \cosh(\alpha\mu)\sinh(\alpha\mu)\,(\mu, \mu^3)\, d\mu \tag{9.32}$$

I_6 and I_9 have been developed for argument β in I_4 and I_5 - see equations (9.22) and (9.23). I_7 can be easily seen to be

$$I_7 = 2\alpha^{-3}\left[\alpha^2\left\{\frac{\sinh 2\alpha}{4} - \alpha/2\right\} + \alpha^3/3 - \right.$$
$$\left. - \tfrac{1}{8}\left\{2\alpha\cosh(2\alpha) - \sinh(2\alpha)\right\}\right] \tag{9.33}$$

and we have $I_8 = \tfrac{1}{4}\alpha^{-2}\left[2\alpha\cosh 2\alpha - \sinh 2\alpha\right]$ (9.34)

$$I_7 = I_9 - 2/3 \tag{9.35}$$

$$I_{10} = \alpha^{-5}\left[\frac{\alpha^4 \sinh 2\alpha}{2} - \frac{1}{8}\left\{(8\alpha^3+12\alpha)\cosh 2\alpha - \right.\right.$$
$$\left.\left. - (12\alpha^2+6)\sinh(2\alpha)\right\} - \frac{\alpha^5}{5}\right] \tag{9.36}.$$

$$I_{11} = \frac{1}{16}\alpha^{-4}\left[(8\alpha^3+12\alpha)\cosh 2\alpha - \right.$$
$$\left. - (12\alpha^2+6)\sinh 2\alpha\right] \tag{9.37}.$$

We find we can write

$$I_3 = L_3\left\{K_1C_2 - K_3C_4\right\} + L_2\left\{K_1C_4 - K_3C_2\right\}$$
$$+ L_1\left\{K_4C_4 + K_2C_2\right\} + L_0\left\{K_4C_2 - K_2C_4\right\} \tag{9.38}$$

with $L_n = \int_{+1}^{\infty} e^{-(\alpha+\beta)}\lambda^n\, d\lambda$ (9.39)

so that

$$L_0 = e^{-(\alpha+\beta)}/(\alpha+\beta) \qquad L_1 = e^{-(\alpha+\beta)}\left[(\alpha+\beta)^{-1} + (\alpha+\beta)^{-2}\right] \tag{9.40}$$

$$L_2 = e^{-(\alpha+\beta)}\left[(\alpha+\beta)^{-1} + 2(\alpha+\beta)^{-2} + 2(\alpha+\beta)^{-3}\right] \tag{9.41}$$

$$L_3 = e^{-(\alpha+\beta)}\left[(\alpha+\beta)^{-1} + 3(\alpha+\beta)^{-2} + 6(\alpha+\beta)^{-3} + 6(\alpha+\beta)^{-4}\right] \tag{9.42}.$$

Further we have put

$$K_1, K_2 = \int_{-1}^{1} \cosh(\alpha\mu)\cosh(\beta\mu)(1,\mu^2)\, d\mu \tag{9.43}$$

$$K_3, K_4 = \int_{-1}^{1} \cosh(\beta\mu)\sinh(\alpha\mu)(\mu, \mu^3)\, d\mu \tag{9.44}$$

so that

$$K_1 = \frac{1}{\alpha+\beta}\left[\sinh(\alpha+\beta)\right] + \frac{1}{\beta-\alpha}\left[\sinh(\beta-\alpha)\right] \tag{9.45}$$

$$K_2 = \frac{1}{(\alpha+\beta)^3}\left[\{(\alpha+\beta)^2+2\}\sinh(\alpha+\beta) - 2(\alpha+\beta)\cosh(\alpha+\beta)\right]$$

$$+ \frac{1}{(\beta-\alpha)^3}\left[\{(\beta-\alpha)^2+2\}\sinh(\beta-\alpha) - 2(\beta-\alpha)\cosh(\beta-\alpha)\right] \tag{9.46}$$

$$K_3 = \frac{1}{(\alpha+\beta)^2}\left[(\alpha+\beta)\cosh(\alpha+\beta) - \sinh(\alpha+\beta)\right]$$

$$+ \frac{1}{(\alpha-\beta)^2}\left[(\alpha-\beta)\cosh(\alpha-\beta) - \sinh(\alpha-\beta)\right] \tag{9.47}$$

$$K_4 = \int_0^1 \left[\sinh(\alpha+\beta)\mu + \sinh(\alpha-\beta)\mu\right]\mu^3\, d\mu \tag{9.48}$$

$$= \frac{1}{(\alpha+\beta)^4}\left[\{(\alpha+\beta)^3 + 6(\alpha+\beta)\}\cosh(\alpha+\beta) - \{3(\alpha+\beta)^2+6\}\sinh(\alpha+\beta)\right]$$

$$+ \frac{1}{(\alpha-\beta)^4}\left[\{(\alpha-\beta)^3 + 6(\alpha-\beta)\}\cosh(\alpha-\beta) - \{3(\alpha-\beta)^2+6\}\sinh(\alpha-\beta)\right] \tag{9.49}$$

which completes the calculation.

σ_u Orbitals.

If we write

$$\psi^{(\sigma_u)} = c(\alpha,\beta)\left[C_5 e^{-\beta\lambda}\sinh(\beta\mu) + \right.$$
$$\left. + Re^{-\alpha\lambda}\left\{(C_2+C_4\lambda)\mu\cosh(\alpha\mu) - (C_4+C_2\lambda)\sinh(\alpha\mu)\right\}\right] \quad (9.50)$$

then equations (9.15) and (9.16) can be used to find $C(\alpha,\beta)$ but that the following definitions apply;

$$I_1 = \int_1^\infty\int_{-1}^{1} e^{-2\beta\lambda}\sinh^2(\beta\mu)(\lambda^2-\mu^2)\,d\mu\,d\lambda \quad (9.51)$$

$$I_2 = \int_1^\infty\int_{-1}^{1} e^{-2\alpha\lambda}\left\{(C_2+C_4\lambda)\mu\cosh(\alpha\mu) - (C_4+C_2\lambda)\sinh(\alpha\mu)\right\}^2 \times$$
$$\times (\lambda^2-\mu^2)\,d\mu\,d\lambda \quad (9.52)$$

$$I_3 = \int_1^\infty\int_{-1}^{1} e^{-(\alpha+\beta)\lambda}\left\{(C_2+C_4\lambda)\mu\cosh(\alpha\mu) - \right.$$
$$\left. -(C_4+C_2\lambda)\sinh(\alpha\mu)\right\}\sinh(\beta\mu)(\lambda^2-\mu^2)\,d\mu\,d\lambda \quad (9.53).$$

In order not to make the appendices unduly long we do not display the results for the evaluation of I_1, I_2 and I_3 in this case. They are very similar to those for σ_g orbitals.

9.2. ANGULAR INTEGRALS.

In sections 4.1 to 4.4, various definitions of angular integrals were given as well as expressions for evaluating them in series form. In most cases we evaluated these integrals for the first six values of n by using tables of coefficients of Legendre polynomials (73). In any group of two or three integrals, e.g. A_n, B_n, C_n, those whose integrands contain the higher powers of μ can be found from the expressions for the integral containing the lowest power of μ simply by adding two or four to the suffices on the angular integrals I_n or J_n in terms of which our expressions are written. Thus for example,

$$A_3(\alpha) = \int_{-1}^{1} P_n(\mu) \sin(\alpha\mu)\, d\mu = 5\vartheta_3 - 3\vartheta_1 \qquad (9.54)$$

whereupon $B_3(\alpha) = 5\vartheta_5 - 3\vartheta_3$. (9.55).

We then have

$$A_1 = 2\vartheta_1 \quad A_3 = 5\vartheta_3 - 3\vartheta_1 \quad A_5 = \tfrac{1}{4}(63\vartheta_5 - 70\vartheta_3 + 15\vartheta_1) \qquad (9.56)$$

$$A_7 = \tfrac{1}{8}(429\vartheta_7 - 693\vartheta_5 + 315\vartheta_3 - 35\vartheta_1) \qquad (9.57)$$

$$A_9 = \frac{1}{64}(315\vartheta_1 - 4620\vartheta_3 + 18018\vartheta_5 - 25740\vartheta_7 + 12155\vartheta_9) \tag{9.58}$$

$$A_{11} = \frac{1}{128}(-693\vartheta_1 + 15015\vartheta_3 - 90090\vartheta_5 + 218790\vartheta_7 - 230945\vartheta_9 + 88179\vartheta_{11}) \tag{9.59}$$

Further

$$E_0 = 2(\vartheta_3 - \vartheta_5) \qquad E_2 = 3(6\vartheta_5 - \vartheta_3 - 5\vartheta_7) \tag{9.60}$$

$$E_4 = (5/4)[3\vartheta_3 - 45\vartheta_5 + 105\vartheta_7 - 63\vartheta_9] \tag{9.61}$$

$$E_6 = 7/8\,[924\vartheta_9 - 630\vartheta_7 + 140\vartheta_5 - 5\vartheta_3 - 429\vartheta_{11}] \tag{9.62}$$

and

$$G_1 = 30(\vartheta_1 - \vartheta_3) \qquad G_3 = 5(84\vartheta_3 - 21\vartheta_1 - 63\vartheta_5) \tag{9.63}$$

$$G_5 = \frac{9}{4}(105\vartheta_1 - 875\vartheta_3 + 1771\vartheta_5 - 1001\vartheta_7) \tag{9.64}$$

$$G_7 = \frac{15}{8}(-231\vartheta_1 + 3234\vartheta_3 - 12012\vartheta_5 + 16302\vartheta_7 - 7293\vartheta_9) \tag{9.65}$$

$$G_9 = \frac{15}{64}\left(3003\vartheta_1 - 62063\vartheta_3 + 366366\vartheta_5 - 860574\vartheta_7 + 877591\vartheta_9 - 323323\vartheta_{11}\right) \tag{9.66}$$

For the angular integrals for π_u orbitals, we find

$$A_0' = 2J_0 \;, A_2' = 3J_2 - J_0 \;, A_4' = \frac{1}{4}(35J_4 - 30J_2 + 3J_0) \tag{9.67}$$

$$A_6' = \frac{1}{8}(231J_6 - 315J_4 + 105J_2 - 5J_0) \tag{9.68}$$

$$A_8' = \frac{1}{64}(6435J_8 - 12012J_6 + 6930J_4 - 1260J_2 + 35J_0) \tag{9.69}$$

$$A_{10}' = \frac{1}{128}(46189J_{10} - 109395J_8 + 90090J_6 - 30030J_4 + 3465J_2 - 63J_0) \tag{9.70}$$

Also

$$D_1' = 6(J_2 - J_4) \;, \quad D_3' = 5(10J_4 - 3J_2 - 7J_6) \tag{9.71}$$

$$D_5' = \frac{3}{4}(441J_6 - 231J_8 - 245J_4 + 35J_2) \tag{9.72}$$

$$D_7' = \frac{1}{8}(15444J_8 - 6435J_{10} - 12474J_6 + 3780J_4 - 315J_2) \tag{9.73}$$

$$D_9' = \frac{5}{64}\left(133705J_{10} - 46189J_{12} - 141570J_8 + \right.$$
$$\left. + 66066J_6 - 12705J_4 + 693J_2\right) \tag{9.74}$$

$$D_{11}' = \frac{3}{128}\left(2292654J_{12} - 3002285J_{10} + 1896180J_8 \right.$$
$$- 585585J_6 + 78078J_4 - 3003J_2$$
$$\left. - 676039J_{14}\right) \tag{9.75}.$$

Further we have

$$G_0' = 6(J_0 - J_2)\,, \quad G_2' = 15(8J_2 - J_0 - 7J_4) \tag{9.76}$$

$$G_4' = \frac{35}{4}(153J_4 - 57J_2 - 99J_6 + 3J_0) \tag{9.77}$$

$$G_6' = \frac{5}{8}(18018J_6 - 11088J_4 + 2142J_2 - 63J_0 \tag{9.78}$$
$$- 9009J_8)$$

$$G_8' = \frac{15}{64}\left(231J_0 - 138567J_{10} + 342771J_8 - 294294J_6\right.$$
$$\left. + 102102J_4 - 12243J_2\right) \tag{9.79}.$$

The extra integrals involved for g orbitals are

$$\varphi_0 = 2(J_0 - J_2)\,, \quad \varphi_2 = 3(6J_2 - J_0 - 5J_4) \tag{9.80}$$

$$\varphi_4 = \frac{5}{4}\left(105J_4 - 45J_2 + 3J_0 - 63J_6\right) \tag{9.81}$$

$$\varphi_6 = \frac{7}{8}\left(924J_6 - 630J_4 + 140J_2 - 429J_8 - 5J_0\right) \tag{9.82}$$

$$\varphi_8 = \frac{9}{64}\left(32175J_8 - 30030J_6 + 11550J_4 - 1575J_2 + 35J_0 - 12155J_{10}\right) \tag{9.83}$$

$$\varphi_{10} = \frac{11}{128}\left(277134J_{10} - 328185J_8 + 180180J_6 - 45045J_4 + 4158J_2 - 63J_0 - 88179J_{12}\right) \tag{9.84}$$

and $F_1 = 2J_2$, $F_3 = 5J_4 - 3J_2$, $F_5 = \frac{1}{4}(63J_6 - 70J_4 + 15J_2)$ (9.85)

$$F_9 = \frac{1}{64}\left(12155J_{10} - 25740J_8 + 18018J_6 - 4620J_4 + 315J_2\right) \tag{9.86}$$

$$F_7 = \frac{1}{8}\left(429J_8 - 693J_6 + 315J_4 - 35J_2\right) \tag{9.87}$$

$$F_{11} = \frac{1}{128}\left(88179\,J_{12} - 230945\,J_{10} + 218790\,J_8 \right.$$

$$\left. - 90090\,J_6 + 15015\,J_4 - 693\,J_2 \right)$$

(9.88).

Finally, for the extra angular integrals involved for σ_u orbitals we have

$$L_1 = 6(\vartheta_1 - \vartheta_3) \quad , \quad L_3 = 5(10\vartheta_3 - 3\vartheta_1 - 7\vartheta_5) \tag{9.89}$$

$$L_5 = \frac{3}{4}(441\vartheta_5 - 231\vartheta_7 - 245\vartheta_3 + 35\vartheta_1) \tag{9.90}$$

$$L_7 = \frac{1}{8}(15444\vartheta_7 - 6435\vartheta_9 - 12474\vartheta_5 + 3780\vartheta_3 - 315\vartheta_1) \tag{9.91}$$

$$L_9 = \frac{5}{64}(133705\vartheta_9 - 46189\vartheta_{11} - 141570\vartheta_7 + 66066\vartheta_5 - 12705\vartheta_3 + 693\vartheta_1) \tag{9.92}$$

$$L_{11} = \frac{3}{128}(2292654\vartheta_{11} - 3002285\vartheta_9 + 1896180\vartheta_7 - 585585\vartheta_5 + 78078\vartheta_3) - \frac{3}{128}(3003\vartheta_7 + 676039\vartheta_{13}) \tag{9.93}$$

and finally

$$S_0 = 2\vartheta_1 \,, \; S_2 = 3\vartheta_3 - \vartheta_1 \,, \; S_4 = \frac{1}{4}(35\vartheta_5 - 30\vartheta_3 + 3\vartheta_1) \tag{9.94}$$

$$S_6 = \frac{1}{8}(231\vartheta_7 - 315\vartheta_5 + 105\vartheta_3 - 5\vartheta_1) \qquad (9.95)$$

$$S_8 = \frac{1}{64}(6435\vartheta_9 - 12012\vartheta_7 + 6930\vartheta_5 - 1260\vartheta_3 + 35\vartheta_1) \qquad (9.96)$$

$$S_{10} = \frac{1}{128}(46189\vartheta_{11} - 109395\vartheta_9 + 90090\vartheta_7 - 30030\vartheta_5 + 3465\vartheta_3 - 63\vartheta_1) \qquad (9.97).$$

9.3 BRIEF DESCRIPTION OF PROGRAMMES.

The calculations of the cross sections reported in section 5.2 which were then used in conjunction with Franck-Condon factors to obtain the results of sections 6.3 and 6.5 were performed by means of four main programmes, PHOTO1, PHOTO2, PHOTO3, PHOTO4, one for each orbital type. We have included a listing of the programme PHOTO2 only, all the others being very similar.

The basic input data needed for the programmes are listed in table 9.1.

TABLE 9.1

INPUT FOR PHOTO2.

Programme symbol.	Variable.
ET	Threshold energy I in eV.
R	Internuclear separation of molecule.
S	Slater orbital exponent, ζ_2
DZ(L,N,K)	Coefficients in series (3.20) for σ waves
D1(L,N.K)	" " " " " π "
D2(L,N,K)	" " " " " δ "
TZ(L,K)	Stratton et al's t_{ml} $(R)^{(70)}$ for σ waves
T1(L,K)	" " " " " π "
T2(L,K)	" " " " " δ "

Throughout the programme listing are inserted comment cards which should explain the various stages in the computations. The following steps were taken in obtaining the final results.

EVALUATE SEPARATION CONSTANTS. The $t_{ml}(h)$ tabulated by Stratton et al are here used to find the values of the $A_{ml}(h)$ in accordance with (3.22). Four runs were made for each process considered in order to cover the wavelength range from first ionization potentials to 50A°.

ANGULAR INTEGRATIONS. The various angular integrals defined in sections 4.1 to 4.4 and tabulated in 9.2 are here found from the values of the $J_n(q)$, the latter being called XJ(I). Further, the recurrence relation (4.45) was used to find all the J_n needed so that by means of three DO LOOPS all the angular integrals could be obtained by using the dummy variables BX(I).

EVALUATE SCATTERED WAVES. This involved a tri-nested DO LOOP for values of m = 0,1,2, of l, and of h, the energy variable, (the corresponding symbols being M,L,K).

The COEFFICIENTS OF POWER SERIES section is of course devoted to the determination of the a_n in the expansion for $F(\tau)$ according to (3.30). Recurrence relations

were used for the higher values of n. The values of λ for which the radial functions were evaluated by this method were λ = 1·0, 1·1, 1·2 and this gave the unnormalized functions $G_{ml}(h,\lambda)$ at these values of the radial co-ordinate.

RECURRENCE RELATIONS NOW USED TO GENERATE G FUNCTIONS TO LAM = 10·9.

The $G_{ml}(h,\lambda)$ are programmed as GZ,G1,G2(L,N,K) for σ, π and δ – continuum waves respectively. The subscript N is used for the radial co-ordinate λ. By means of the recurrence relation (3.34), the values of the G_{ml} to λ = 10·9 in ·1 steps of λ are obtained from the first few values by the power series method. The function $\phi(\lambda)$ in (3.36) is programmed as the dummy variable XF(NN) for all m, l and h.

NORMALIZED AMPLITUDES. Here the values of the $Y_{ml}(h)$ given in (3.39) are evaluated, the programme symbols being YZ, Y1 and Y2(L,N,K) where N now represents n in the expansions of the type $\sum_{n=0}^{\infty}{}' d_n(h/0,1)P_n(\mu)$. The first six values of n were employed whereupon the values of the normalized asymptotic amplitudes of the $G_{ml}(h,\lambda)$ could be found. These amplitudes are called

YZZ, Y1Z and Y2Z(L,K).

EVALUATE UNNORMALIZED ASYMPTOTIC AMPLITUDES. We found that calculating the values of $U(\lambda)$ and hence $\alpha(\lambda_1, \lambda_2)$ (see section 3.4) was not satisfactory if λ was less than 10·9 because the condition $w \ll v$ was then not always satisfied. Thus we employed a special subroutine AMP which carried the calculations of the unnormalized $G_{ml}(h,\lambda)$ out to $\lambda = 40{\cdot}7$ by means of (3.34). The values of $G(\lambda)$ in the range $[39{\cdot}7,\ 40{\cdot}7]$ were then used to calculate the $U(\lambda)$ in this range and eventually the values of $D_{ml}(h)$ in (3.40) could be determined.

EVALUATE NORMALIZED RADIAL FUNCTIONS. The normalized $G_{ml}(h,\lambda)$ are used to determine the final radial solutions $\Lambda_{ml}(h,\lambda)$ which are needed to evaluate the electronic matrix elements.

RADIAL INTEGRATIONS. Having found the $\Lambda_{ml}(h,\lambda)$ the programme then computes the λ-dependent parts of the matrix elements in the range $[1{\cdot}0,\ 10{\cdot}9]$. The integrations for each m,l and h are then performed by our subroutine SIMP2 which evaluates integrals by

Simpson's rule. The final radial integrals so obtained are then coupled with the previously determined angular integrals and the resulting squares of the matrix elements obtained. These latter quantities have the programme names TS, TP and TD(L,K) for σ , π and δ - wave contributions. The total of the electronic matrix elements is then found (TOTCO (K)) whereupon the cross section can be immediately found from (1·8). The output consisted of the photon wavelengths and corresponding cross sections together with values of the angular integrals, the normalized radial functions $\Lambda_{nl}(h,\lambda)$, and all the radial integrals.

For the calculations described in section 6.4 the programme PHOTO1 was modified and extended in the following manner. Instead of setting $R = r_e$ the value of R was varied from $R = 1{\cdot}6a_o$ to $3{\cdot}0a_o$ in steps of $\cdot 02a_o$. The matrix elements were then found (for zero energy) for each R. The Morse functions needed for the vibrational wave functions were determined at the corresponding values of R whereupon the complete matrix elements could be obtained by using SIMP2 in the range $[1{\cdot}6, 3{\cdot}0]$. The modified part of the programme for this calculation is also shown in the listings, together

with examples of XNORM which were used to normalize the bound orbitals of Ch. 2.

FORTRAN PROGRAMMES.

1. PROGRAM PHOTO2: Calculation of photoionization cross section for fixed nuclei for an initial $1\pi_u$ molecular orbital.

2. SUBROUTINE XNORM: Evaluation of normalization integrals for $1\pi_u$ molecular orbital.

3. SUBROUTINE AMP: Calculation of asymptotic amplitudes of unnormalized $G_{ml}(k,\lambda)$.

4. PROGRAM VBFC: Calculation of cross sections for different vibrational states using Franck-Condon factors.

5. PROGRAM PHOTO1: Modifications to "photo1" to include the dependence of the electronic transition moment on internuclear separation for the transition to $O_2^+(X^2\Pi_g)$ (for zero kinetic energy of ejected electrons).

```
      PROGRAMPHOTO2(INPUT,OUTPUT)
C     CALCULATION OF PARTIAL PHOTO-IONIZATION CROSS SECTION FROM
C     AN L.C.A.O. 1PI(U) MOLECULAR ORBITAL
C     FOR VARIOUS TRANSITIONS IN N2 AND O2
      DIMENSIONDZ(3,6,7),TZ(3,7),D1(3,6,7),T1(3,7),D2(3,6,7),
     1T2(3,7),AZ(3,7),A1(3,7),A2(3,7),XJ(10),BX(7),AA(7),BB(7),CC(7),
     2DD(6),EE(6),G8(6),Q8(6),TT(5)
      DIMENSIONXX(3,7),PSC(6),XLP(6),GZ(3,7,100),G1(3,7,100),G2(3,7,100)
     1,XF(100),XLAM(100)
      DIMENSIONYZ(3,6,7),YZC(3,6,7),YZZ(3,7),Y1(3,6,7),Y1C(3,6,7),
     1Y1Z(3,7),Y2(3,6,7),Y2C(3,6,7),Y2Z(3,7)
      DIMENSIONYAM(100),YUM(100),XAL(100),XALL(100),PEX(100),BFN(100),
     1T(100),TSA(3,7,6),TSB(3,7,6),TS(3,7),SIGMW(7),TPA(3,7,6),TPB(3,7,
     26),TP(3,7),PYWAV(7),TDA(3,7,5),TDB(3,7,5),TD(3,7),DELWV(7),TOTCO(7
     33),CROSS(7),WAVL(7)
      DIMENSIONTS1(3,7),TS2(3,7),TP1(3,7),TP2(3,7),TD1(3,7),TD2(3,7)
C     READ IN DATA
      READ1,(((DZ(L,N,K),L=1,3),N=1,6),K=2,7)
      READ1,((TZ(L,K),L=1,3),K=2,7)
      READ1,(((D1(L,N,K),L=1,3),N=1,6),K=2,7)
      READ1,((T1(L,K),L=1,3),K=2,7)
      READ1,(((D2(L,N,K),L=1,3),N=1,6),K=2,7)
      READ1,((T2(L,K),L=1,3),K=2,7)
    1 FORMAT(8E10.5)
      DO2L=1,3
      DO3N=1,6
      IF(L.EQ.N)1004,1005
 1004 DZ(L,N,1)=1.
      D1(L,N,1)=1.
      D2(L,N,1)=1.
      GOTO3
 1005 DZ(L,N,1)=0.
      D1(L,N,1)=0.
      D2(L,N,1)=0.
    3 CONTINUE
    2 CONTINUE
      DO86L=1,3
      TZ(L,1)=0.
      T1(L,1)=0.
      T2(L,1)=0.
   86 CONTINUE
C
      PY=3.1415926
      DO1010IX=1,3
      IF(IX.EQ.1)1011,1012
 1011 ET=16.7
      R=2.067369
      S=1.95
      S=SQRT(ET/13.774)*S
      GOTO1013
 1012 R=2.2816611
      S=2.275
      IF(IX.EQ.2)1014,1015
```

```
 1014 ET=16.1
      S=SQRT(ET/11.5)*S
      GOTO1013
 1015 ET=16.8
      S=SQRT(ET/18.95)*S
C     EVALUATE SEPARATION CONSTANTS
 1013 DO6L=1,3
      XL=2*L-2
      DO6K=1,7
      H=(K-1)*.1
      AZ1=(2.*(XL**2)+2.*XL-1.)/(((2.*XL)-1.)*((2.*XL)+3.))
      AZ(L,K)=(XL*(XL+1.))+(H**2)*(AZ1+TZ(L,K))
    6 CONTINUE
      DO7L=1,3
      XL=2*L
      DO7K=1,7
      H=(K-1)*.1
      A11=(2.*(XL**2)+2.*XL-3.)/(((2.*XL)-1.)*((2.*XL)+3.))
      A1(L,K)=(XL*(XL+1.))+(H**2)*(A11+T1(L,K))
      A21=(2.*(XL**2)+2.*XL-9.)/(((2.*XL)-1.)*((2.*XL)+3.))
      A2(L,K)=(XL*(XL+1.))+(H**2)*(A21+T2(L,K))
    7 CONTINUE
      CALLXNORM(R,S,CCO)
      CCC=CCO*SQRT(S**5/(2.*PY))
      ETR=ET/13.595
      AL=R*S/2.
      CA=(EXP(AL)+EXP(-AL))/2.
      SA=(EXP(AL)-EXP(-AL))/2.
      PRINT325,R
  325 FORMAT(1H1,10X,24HINTERNUCLEAR SEPARATION=,F9.7,10HBOHR RADII)
      PRINT326,S
  326 FORMAT(2X,8(/),10X,37HORBITAL EXPONENT FOR ATOMIC ORBITALS=,F5.3)
      PRINT327,ET
  327 FORMAT(2X,8(/),10X,17HTHRESHOLD ENERGY=,F5.2,2HEV)
      PRINT1000,CCO
 1000 FORMAT(2X,8(/),10X,23HNORMALIZATION CONSTANT=,E15.8)
C
C     ANGULAR INTEGRATIONS
      XJ(1)= SA/AL
      DO100 I=2,9
      II  =2*I-2
      I1  = II-1
      I2  = II +1
      XJ(I)= ((AL**II)*SA - II*(AL**I1)*CA + I*II*(AL**I1)*XJ(I-1))/
     1 (AL**I2)
  100 CONTINUE
      DO101 I=1,3
      BX(1)= 2.*XJ(I)
      BX(2)= 3.*XJ(I+1)-XJ(I)
      BX(3)= .25*(35.*XJ(I+2)-30.*XJ(I+1)+ 3.*XJ(I))
      BX(4)= .125*( 231.*XJ(I+3)-315.*XJ(I+2)+105.*XJ(I+1) -5.*XJ(I))
      BX(5)=(6435.*XJ(I+4)-12012.*XJ(I+3)+ 6930.*XJ(I+2)-1260.*XJ(I+1)
     1 +35.*XJ(I))/ 64.
      BX(6)=(46189.*XJ(I+5)-109395.*XJ(I+4)+90090.*XJ(I+3)-30030.*XJ(I+2
     1)+3465.*XJ(I+1)-63.*XJ(I))/128.
```

```
      BX(7)=(676039.*XJ(I+6)-1939938.*XJ(I+5)+ 2078505.*XJ(I+4)-1021020.
     1*XJ(I+3)+225225.*XJ(I+2)-18018.*XJ(I+1)+231.*XJ(I))/512.
      DO 101 I1 =1,7
      IF(I-2)103,104,105
  103 AA(I1)= BX(I1)
      GO TO 101
  104 BB(I1) = BX(I1)
      GO TO 101
  105 CC(I1) = BX(I1)
  101 CONTINUE
      DO106 I=1,2
      BX(1)= 6.*(XJ(I+1)- XJ(I+2))
      BX(2)= 5.*(10.*XJ(I+2)- 3.*XJ(I+1)- 7.*XJ(I+3))
      BX(3)=.75*(441.*XJ(I+3)-231.*XJ(I+4)-245.*XJ(I+2)+35.*XJ(I+1))
      BX(4)=(15444.*XJ(I+4)- 6435.*XJ(I+5)-12474.*XJ(I+3)+3780.*XJ(I+2)
     1 -315.*XJ(I+1))/8.
      BX(5)= 5.*(133705.*XJ(I+5)-46189.*XJ(I+6)-141570.*XJ(I+4)+66066.*
     1XJ(I+3)-12705.*XJ(I+2)+693.*XJ(I+1))/64.
      BX(6)= 3.*(2292654.*XJ(I+6)- 3002285.*XJ(I+5)+ 1896180.*XJ(I+4)
     1- 585585.*XJ(I+3)+ 78078.*XJ(I+2)- 3003.*XJ(I+1)-676039.*XJ(I+7))
     2/128.
      DO106I1 =1,6
      IF(I-1)108,108,109
  108 DD(I1) = BX(I1)
      GO TO 106
  109 EE(I1) =BX(I1)
  106 CONTINUE
      DO110 I=1,3
      BX(1) = 6.*(XJ(I)- XJ(I+1))
      BX(2) = 15.*( 8.*XJ(I+1)-XJ(I)-7.*XJ(I+2))
      BX(3) = 35.*(153.*XJ(I+2)-57.*XJ(I+1)-99.*XJ(I+3) +3.*XJ(I))/4.
      BX(4) = .625*(18018.*XJ(I+3)-11088.*XJ(I+2)+2142.*XJ(I+1)-63.*XJ(I
     1)-9009.*XJ(I+4))
      BX(5)= 15.*(-138567.*XJ(I+5)+231.*XJ(I)+342771.*XJ(I+4)-294294.*
     1XJ(I+3)+102102.*XJ(I+2)-12243.*XJ(I+1))/64.
      DO110I1=1,5
      IF(I-2)111,112,113
  111 G8(I1)=BX(I1)
      GOTO110
  112 08(I1)=BX(I1)
      GOTO110
  113 TT(I1)=BX(I1)
  110 CONTINUE
      PRINT312
  312 FORMAT(1H1,10X,20HANGULAR INTEGRATIONS)
      PRINT313
  313 FORMAT(2X,//,10X,1HN,7X,4HA(N),13X,4HB(N),13X,4HC(N))
      DO314I=1,7
      N=2*I-2
      PRINT315,N,AA(I),BB(I),CC(I)
  314 CONTINUE
  315 FORMAT(10X,I2,3(1X,E15.8))
      PRINT316
  316 FORMAT(2X,//,10X,1HN,7X,4HD(N),13X,4HE(N))
```

```
      DO317I=1,6
      N=2*I-1
      PRINT318,N,DD(I),EE(I)
  318 FORMAT(10X,I2,2(1X,E15.8))
  317 CONTINUE
      PRINT319
  319 FORMAT(2X,//,10X,1HN,7X,4HG(N),13X,4HH(N),13X,4HI(N))
      DO320I=1,5
      N=2*I-2
      PRINT315,N,G8(I),Q8(I),TT(I)
  320 CONTINUE
C
C     EVALUATE SCATTERED WAVES
      DO12M=1,3
      DO12L=1,3
      DO12K=1,7
      PRINT199,M,L,K
  199 FORMAT(2X,2HM=,I2,2HL=,I2,2HK=,I2)
      IF(M-2)18,19,20
   18 XX(L,K)=AZ(L,K)
      GO TO 21
   19 XX(L,K)=A1(L,K)
      GO TO 21
   20 XX(L,K)=A2(L,K)
   21 XM = M-1
      H=(K-1)*.1
C
C     COEFFICIENTS OF POWER SERIES
      XK=XM*(XM+1.)-XX(L,K)+R+H**2
      XH=R+2.*(H**2)
      PSC(1)=-XK/(2.*(XM+1.))
      PSC(2)=-(XH+PSC(1)*(XK+2.*(XM+1.)))/(4.*(XM+2.))
      PSC(3)=-(H**2+XH*PSC(1)+PSC(2)*(6.+4.*XM+XK))/(18.+6.*XM)
      DO328IV=3,5
      V=IV
      PSC(IV+1)=-((H**2)*PSC(IV-2)+PSC(IV-1)*XH+PSC(IV)*(V*(V-1.)+2.*V*
     1(XM+1.)+XK))
      PSC(IV+1)=PSC(IV+1)/(2.*V*(V+1.)+2.*(XM+1.)*(V+1.))
  328 CONTINUE
C
C     OBTAIN STARTING VALUES FOR RADIAL FUNCTIONS AND UNNORMALIZED G FNS
      DO22NN=1,3
      XL=(NN-1)*.1
      DO329JZ=1,6
      XLP(JZ)=XL**JZ
  329 CONTINUE
      IF(M.EQ.1)23,24
   23 GZ(L,K,NN)=1.+PSC(1)*XLP(1)+PSC(2)*XLP(2)+PSC(3)*XLP(3)+PSC(4)*
     1XLP(4)+PSC(5)*XLP(5)+PSC(6)*XLP(6)
      GZ(L,K,NN)=SQRT((XL+1.)**2-1.)*GZ(L,K,NN)
      GOTO22
   24 IF(M.EQ.2)25,26
   25 GI(L,K,NN)=SQRT((XL+1.)**2-1.)*(PSC(1)*XLP(1)+PSC(2)*XLP(2)+ 1. +
```

```
     1PSC(3)*XLP(3)+PSC(4)*XLP(4)+PSC(5)*XLP(5)+PSC(6)*XLP(6))
      G1(L,K,NN)=SQRT((XL+1.)**2-1.)*G1(L,K,NN)
      GO TO 22
   26 G2(L,K,NN)=((XL+1.)**2-1.)*(1.+PSC(1)*XLP(1)+PSC(2)*XLP(2)
     1+PSC(3)*XLP(3)+PSC(4)*XLP(4)+PSC(5)*XLP(5)+PSC(6)*XLP(6))
      G2(L,K,NN)=SQRT((XL+1.)**2-1.)*G2(L,K,NN)
   22 CONTINUE
C
C     RECURRENCE RELATIONS NOW USED TO GENERATE G FUNCTIONS TO LAM=10.9
      IF(M-2)28,29,30
   28 XZ = AZ(L,K)
      GO TO 31
   29 XZ= A1(L,K)
      GO TO 31
   30 XZ =A2(L,K)
   31 DO27NN=2,100
      XL=(NN-1)*.1+1.
      XF(NN)=(-XZ +R*XL +(H**2)*(XL**2))/(XL**2-1.)+(1.-XM**2)/((XL**2-1
     1.)**2)
      XF(NN)=-.01*XF(NN)/12.
   27 CONTINUE
      DO32NN=4,100
      IF(M-2)33,34,35
   33 GZ(L,K,NN)=(2.+10.*XF(NN-1))*GZ(L,K,NN-1)
      GZ(L,K,NN)=GZ(L,K,NN)-(1.-XF(NN-2))*GZ(L,K,NN-2)
      GZ(L,K,NN)=GZ(L,K,NN)/(1.-XF(NN))
      GO TO 32
   34 G1(L,K,NN)=(2.+10.*XF(NN-1))*G1(L,K,NN-1)
      G1(L,K,NN)=G1(L,K,NN)-(1.-XF(NN-2))*G1(L,K,NN-2)
      G1(L,K,NN)=G1(L,K,NN)/(1.-XF(NN))
      GO TO 32
   35 G2(L,K,NN)=(2.+10.*XF(NN-1))*G2(L,K,NN-1)
      G2(L,K,NN)=G2(L,K,NN)-(1.-XF(NN-2))*G2(L,K,NN-2)
      G2(L,K,NN)=G2(L,K,NN)/(1.-XF(NN))
   32 CONTINUE
      DO335NV=1,100
      XLAM(NV)=(NV-1)*.1+1.
  335 CONTINUE
C
C     NORMALIZED AMPLITUDES
      IF(M-2)36,37,38
   36 DO39N=1,6
      YZ(L,N,K)=4.*PY*(DZ(L,N,K)**2)/(4*N-3)
   39 CONTINUE
      YZC(L,1,K)=YZ(L,1,K)
      DO40N=2,6
      YZC(L,N,K)=YZC(L,N-1,K)+YZ(L,N,K)
   40 CONTINUE
      YZZ(L,K)=2./SQRT(PY*R*YZC(L,6,K))
      GOTO41
   37 DO42N=1,6
      Y1(L,N,K)=4.*PY*(D1(L,N,K)**2)*(2*N+1)*N/(4*N+1)
   42 CONTINUE
      Y1C(L,1,K)=Y1(L,1,K)
```

```
      DO43N=2,6
      Y1C(L,N,K)=Y1C(L,N-1,K)+Y1(L,N,K)
   43 CONTINUE
      Y1Z(L,K)=2./SQRT(PY*R*Y1C(L,6,K))
      GOTO41
   38 DO44N=1,6
      Y2(L,N,K)=8.*PY*(D2(L,N,K)**2)*(2*N-1)*N*(2*N+1)*(N+1)/(4*N+1)
   44 CONTINUE
      Y2C(L,1,K)=Y2(L,1,K)
      DO45N=2,6
      Y2C(L,N,K)=Y2C(L,N-1,K)+Y2(L,N,K)
   45 CONTINUE
      Y2Z(L,K)=2./SQRT(R*PY*Y2C(L,6,K))
   41 CONTINUE
C
C     EVALUATE UNNORMALIZED ASYMPTOTIC AMPLITUDES
      IF(M-2)46,47,48
   46 CALLAMP(M,AZ(L,K),H,R,GZ(L,K,99),GZ(L,K,100),C1)
      GOTO49
   47 CALLAMP(M,A1(L,K),H,R,G1(L,K,99),G1(L,K,100),C1)
      GOTO49
   48 CALLAMP(M,A2(L,K),H,R,G2(L,K,99),G2(L,K,100),C1)
   49 CONTINUE
C
C     EVALUATE NORMALIZED RADIAL FUNCTIONS
      DO57NN=2,100
      YAM(NN)=1.+(NN-1)*.1
      YUM(NN) =  1./SQRTF(YAM(NN)**2-1.)
      IF( M-2)58,59,60
   58 GZ(L,K,NN)=YUM(NN)*YZZ(L,K)*GZ(L,K,NN)/C1
      GO TO57
   59 G1(L,K,NN)=YUM(NN)*Y1Z(L,K)*G1(L,K,NN)/C1
      GO TO 57
   60 G2(L,K,NN)=YUM(NN)*Y2Z(L,K)*G2(L,K,NN)/C1
   57 CONTINUE
      IF(M.EQ.1)GZ(L,K,1)=YZZ(L,K)/C1
      IF(M.EQ.2)G1(L,K,1)=0.
      IF(M.EQ.3)G2(L,K,1)=0.
   12 CONTINUE
      DO347M=1,3
      DO347L=1,3
      DO347K=1,7
      KKK=K-1
      PRINT348,M,L,KKK
  348 FORMAT(1H1,10X,2HM=,I1,1X,2HL=,I1,1X,2HK=,I1)
      PRINT349
  349 FORMAT(2X,//,10X,26HNORMALIZED RADIAL FUNCTION)
      PRINT352
  352 FORMAT(10X,48H LAM                          LAM                          LAM)
      DO347NN=1,33
      IF(M.EQ.1)PRINT351,XLAM(NN),GZ(L,K,NN),XLAM(NN+33),GZ(L,K,NN+33)
     1,XLAM(NN+66),GZ(L,K,NN+66)
      IF(M.EQ.2)PRINT351,XLAM(NN),G1(L,K,NN),XLAM(NN+33),G1(L,K,NN+33)
     1,XLAM(NN+66),G1(L,K,NN+66)
```

```
      IF(M.EQ.3)PRINT351,XLAM(NN),G2(L,K,NN),XLAM(NN+33),G2(L,K,NN+33)
     1,XLAM(NN+66),G2(L,K,NN+66)
  351 FORMAT(10X,3(F5.1,1X,E15.8))
  347 CONTINUE
C
C     RADIAL INTEGRATIONS
      DO360N=1,100
      XAL(N)=1.+(N-1)*.1
      XALL(N)=XAL(N)**2-1.
      PEX(N)=EXP(-AL*XAL(N))
      BFN(N)=PEX(N)*SQRT(XALL(N))
  360 CONTINUE
      PRINT363
  363 FORMAT(1H1,10X,32HWAVELENGTH(A) CROSS SECTION(CM2))
      DO81K=1,7
C     SIGMA WAVES CONTRIBUTION TO CROSS SECTION
      DO82L=1,3
      DO361N=1,100
      Y(N)=XALL(N)*PEX(N)*(XAL(N)**2)*GZ(L,K,N)
  361 CONTINUE
      CALL SIMP2(1.,10.,.1,Y,TS1(L,K))
      DO362N=1,100
      Y(N)=XALL(N)*PEX(N)*GZ(L,K,N)
  362 CONTINUE
      CALL SIMP2(1.,10.,.1,Y,TS2(L,K))
      TSA(L,K,1) = DZ(L,1,K)*(AA(1)-BB(1))
      TSB(L,K,1)=DZ(L,1,K)*(CC(1)-BB(1))
      DO68MS=2,6
      TSA(L,K,MS)=  TSA(L,K,MS-1)+ DZ(L,MS,K)*(AA(MS)-BB(MS))
      TSB(L,K,MS)=TSB(L,K,MS-1)+DZ(L,MS,K)*(CC(MS)-BB(MS))
   68 CONTINUE
      TS(L,K)=TSA(L,K,6)*TS1(L,K)+TSB(L,K,6)*TS2(L,K)
      TS(L,K)=CCC*PY*(R**5)*TS(L,K)/16.
      TS(L,K)=TS(L,K)**2
   82 CONTINUE
      SIGMw(K)=  TS(1,K) +  TS(2,K) + TS(3,K)
```

```
C     PI WAVES CONTRIBUTION TO CROSS SECTION
      DO69 L =1,3
      DO70N=1,100
      Y(N)=SQRT(XALL(N))*(XAL(N)**3)*PEX(N)*G1(L,K,N)
   70 CONTINUE
      CALL SIMP2(1.,10.,.1,Y,TP1(L,K))
      DO390N=1,100
      Y(N)=SQRT(XALL(N))*PEX(N)*XAL(N)*G1(L,K,N)
  390 CONTINUE
      CALL SIMP2(1.,10.,.1,Y,TP2(L,K))
      TPA(L,K,1) = D1(L,1,K)*DD(1)
      TPB(L,K,1) = D1(L,1,K)*EE(1)
      DO 72  MT  =2,6
      TPA( L,K,MT)= TPA( L,K, MT-1) + D1(L,MT,K) *DD(MT)
      TPB (L,K,MT) = TPB( L,K,MT-1) + D1( L,MT,K) *EE(MT)
   72 CONTINUE
       TP(L,K)=(TPA(L,K,6)*TP1(L,K)-TPB(L,K,6)*TP2(L,K))* CCC*PY*(R**5)/
     116.
```

```
      TP( L,K) =  TP(L,K)**2
   69 CONTINUE
      PYWAV(K)  = TP(1,K) + TP(2,K)  +  TP(3,K)
C
C     DELTA WAVES
      DO73L=1,3
      DO74N=1,100
      Y(N)=XALL(N)*PEX(N)*(XAL(N)**2)*G2(L,K,N)
   74 CONTINUE
      CALL SIMP2(1.,10.,.1,Y,TD1(L,K))
      DO75N=1,100
      Y(N)=XALL(N)*PEX(N)*G2(L,K,N)
   75 CONTINUE
      CALL SIMP2(1.,10.,.1,Y,TD2(L,K))
      TDA(L,K,1)=D2(L,1,K)*(G8(1)-Q8(1))
      TDB(L,K,1)=D2(L,1,K)*(Q8(1)-TT(1))
      DO76 MU=2,5
      TDA(L,K,MU)=TDA(L,K,MU-1)+D2(L,MU,K)*(G8(MU)-Q8(MU))
      TDB(L,K,MU)=TDB(L,K,MU-1)+D2(L,MU,K)*(Q8(MU)-TT(MU))
   76 CONTINUE
       TD(L,K)=(TDA(L,K,5)*TD1(L,K)-TDB(L,K,5)*TD2(L,K))* CCC*PY*(R**5)/
     132.
       TD(L,K)=TD(L,K)**2
   73 CONTINUE
      DELWV(K) = TD(1,K) + TD(2,K) +TD(3,K)
      TOTCO(K)=SIGMW(K)+PYWAV(K)+2.*DELWV(K)
      CROSS(K)=TOTCO(K)*(ETR+(K-1)**2/(25.*(R**2)))*5.377869*1.E-18
      WAVL(K)=(4.*(((K-1)/10.)**2)*13.595/R**2)+ET
      WAVL(K)=12398./WAVL(K)
      PRINT364,WAVL(K),CROSS(K)
  364 FORMAT(2X,//,10X,F6.1,5X,E15.8)
   81 CONTINUE
C     PRINTOUT OF SEPARATE CONTRIBUTIONS AND BOUND RADIAL FUNCTION
      PRINT454
  454 FORMAT(1H1,5(/),10X,25HSIGMA WAVES CONTRIBUTIONS)
      PRINT455
  455 FORMAT(2X,//,10X,1HK,7X,4HL=0 ,13X,4HL=2 ,13X,4HL=4 )
      PRINT321,(K,TS(1,K),TS(2,K),TS(3,K),K=1,7)
  321 FORMAT(10X,I2,3(1X,E15.8))
      PRINT453
  453 FORMAT(2X,5(/),10X,22HPI WAVES CONTRIBUTIONS)
```

```
      PRINT461
  461 FORMAT(2X,//,10X,1HK,7X,4HL=2 ,13X,4HL=4 ,13X,4HL=6 )
      PRINT321,(K,TP(1,K),TP(2,K),TP(3,K),K=1,7)
      PRINT456
  456 FORMAT(2X,5(/),10X,25HDELTA WAVES CONTRIBUTIONS)
      PRINT461
      PRINT321,(K,TD(1,K),TD(2,K),TD(3,K),K=1,7)
      PRINT458
  458 FORMAT(1H1,10X,29HRADIAL PART OF BOUND FUNCTION)
      PRINT459
  459 FORMAT(2X,5(/),10X,21HLAMBDA BOUND FUNCTION)
      PRINT460,(XAL(N),BFN(N),N=1,40)
  460 FORMAT(11X,F4.1,4X,E15.8)
      PRINT500
  500 FORMAT(1H1,10X,19HRADIAL INTEGRATIONS)
      PRINT501
  501 FORMAT(2X,//,15X,3HTS1,10X,3HTS2)
      DO502K=1,7
      PRINT503,K
  503 FORMAT(15X,2HK=,I2)
      DO502L=1,3
      PRINT504,L
  504 FORMAT(15X,2HL=,I2)
      PRINT505,TS1(L,K),TS2(L,K)
  505 FORMAT(10X,2(1X,E15.8))
  502 CONTINUE
      PRINT506
  506 FORMAT(2X,//,15X,3HTP1,10X,3HTP2)
      DO507K=1,7
      PRINT503,K
      DO507L=1,3
      PRINT504,L
      PRINT505,TP1(L,K),TP2(L,K)
  507 CONTINUE
      PRINT508
  508 FORMAT(2X,//,15X,3HTD1,10X,3HTD2)
      DO509K=1,7
      PRINT503,K
      DO509L=1,3
      PRINT504,L
      PRINT505,TD1(L,K),TD2(L,K)
  509 CONTINUE
 1010 CONTINUE
      STOP
      END
```

```
      SUBROUTINEXNORM(R,S,CCO)
      DIMENSIONP(10)
      PY=3.1415926
      AL=R*S/2.
      DO783J=1,8
      P(J)=AL**J
  783 CONTINUE
      DA=2.*AL
      SD=.5*(EXP(DA)-EXP(-DA))
      CD=.5*(EXP(DA)+EXP(-DA))
      O1=(.5*SD-AL)/AL
      O2=(SD*(.5*P(2)+.25)-.5*AL*CD-P(3)/3.)/ P(3)
      O3=(SD*(.5*P(4)+1.5*P(2)+.75)-.25*CD*(4.*P(3)+6.*AL)-.2*P(5)
     1)/P(5)
      O1=2.+O1
      O2=O2+(2./3.)
      O3=O3+(2./5.)
      ED=EXP(-2.*AL)
      XO1=.5*ED/AL
      XO2=.5*ED*((1./AL)+(1./P(2))+(.5/P(3)))
      XO3=ED*((.5/AL)+(1./P(2))+(1.5/P(3))+(1.5/P(4))+(.75/P(5)))
      CCC=(2./R**2)*SQRT(2./(PY*R))
      CCC=CCC/SQRT(O1*(XO3-XO2)+O2*(XO1-XO3)+O3*(XO2-XO1))
      CCO=SQRT(2.*PY/(S**5))*CCC
      RETURN
      END
```

```
      SUBROUTINE AMP( M,COB,H,R,A,B,C)
      DIMENSIONFF(300),GG(300),YY(11),YL(11),QQ(11),DYL(11),QZ(11)
     1,QY(11),D2LA(11),D2LB(11),D2LD(11),DW(11),UF(11),GUS(2),Y(15)
     2,D2L(11)
      XM=M-1
      DO1I=1,300
      XL=(I-1)*.1+10.8
      FF(I)=(-COB+R*XL+(H**2)*(XL**2))/(XL**2-1.)+(1.-XM**2)/((XL**2-1.)
     1**2)
      FF(I)=-.01*FF(I)/12.
    1 CONTINUE
      GG(1)=A
      GG(2)=B
      DO2I=3,300
      GG(I)=(2.+10.*FF(I-1))*GG(I-1)
      GG(I)=GG(I)-(1.-FF(I-2))*GG(I-2)
      GG(I)=GG(I)/(1.-FF(I))
    2 CONTINUE
      XM=  1. -(M-1.)**2
      DO52J=1,11
      YY(J)=(J-1)*.1+39.7
      YL(J)=( -COB      + R*YY(J)  +(H**2)*(YY(J)**2))/(YY(J)**2-1.)
     1 +   ( 1.-(M-1.)**2)/((YY(J)**2-1.)**2)
      QQ(J) =   YY(J)**2 - 1.
      H2 = H**2
      DYL(J)=((QQ(J)*(R + 2.*(H2)*YY(J))) +( R*YY(J)- COB      + H2*
     1(YY(J)**2))*(2.*YY(J)))/(QQ(J)**2) - (4.*YY(J)*XM)/(QQ(J)**3)
      QZ(J) = YY(J)**3
      QY(J) = YY(J)**2
      D2LA(J)=2.*(6.*H2*QY(J)+3.*R*YY(J)-H2-COB      )
      D2LB(J)=4.*H2*QZ(J)+3.*R*QY(J)-YY(J)*(2.*H2+2.*COB      )-R
      D2LD(J)=-4.*XM*(5.*QY(J)+1.)/(QQ(J)**4)
      D2L(J)=(QQ(J)*D2LA(J)-4.*YY(J)*D2LB(J))/(QQ(J)**3)
      D2L(J)=D2L(J)-D2LD(J)
      DW(J) = S.*(DYL(J)**2)/(16.*(YL(J)**2))  -  D2L(J)/(4.*YL(J))
      UF(J)=YL(J)+DW(J)
      IF(UF(J).LE.0.)400,401
  400 UF(J)=1.
      GOTO52
  401 UF(J)=SQRT(UF(J))
   52 CONTINUE
      PRINT53
   53 FORMAT(10X,6HLAMBDA,8X,1HW,16X,1HV     ,16X,1HU)
      DO54J=1,11
      PRINT55,YY(J),DW(J),YL(J),UF(J)
   55 FORMAT(10X,F5.2,3(1X,E15.8))
   54 CONTINUE
      DO56J=1,2
      JH=(J-1)*10+290
      KH=(J-1)*10+1
      GUS(J)=SQRT(UF(KH))*GG(JH)
   56  CONTINUE
      DO345I=1,11
```

```
      Y(I)=UF(I)
  345 CONTINUE
      CALLSIMP2(39.7,40.7,.1,Y,XA)
      XA=.5*XA
      GAS  = GUS(1) + GUS(2)
      GOS  =  GUS(1) - GUS(2)
      GES  =  1./ (COSF(XA)**2)
      GIS  =  1./ ( SINF(XA)**2)
      C =.5*SQRTF((GAS**2)*GES+(GOS**2)*GIS)
      RETURN
      END
```

```
      PROGRAMVBFC(INPUT,OUTPUT)
      DIMENSIONEVIB(21),FC(21),A(5),B(5),EN(5,21),WL(5,21),CR(5,21)
      CALCULATION OF PHOTOIONIZATION CROSS SECTIONS FOR VARIOUS FINAL
      VIBRATIONAL STATES OF O2+A2PIU
      READ1,(EVIB(J),J=1,21)
    1 FORMAT(16F5.3)
      READ2,(FC(J),J=1,21)
    2 FORMAT(16F5.4)
      DO3J=1,21
      FC(J)=FC(J)/10.
      EVIB(J)=EVIB(J)+16.8
      EVIB(J)=EVIB(J)/13.595
    3 CONTINUE
      A(1)=.5628$A(2)=.5628$A(3)=.5894$A(4)=.6285$A(5)=.6895
      B(1)=0.$B(2)=.00768$B(3)=.03073$B(4)=.06915$B(5)=.12294
      DO4K=1,5
      DO4J=1,21
      EN(K,J)=EVIB(J)+B(K)
      WL(K,J)=911.953/EN(K,J)
      CR(K,J)=2.6889*EN(K,J)*A(K)*FC(J)
    4 CONTINUE
      PRINT5
    5 FORMAT(1H1,5X,18HPHOTON WAVELENGTHS)
      DO6J=1,21
      K=J-1
      PRINT7,K ,WL(1,J),WL(2,J),WL(3,J),WL(4,J),WL(5,J)
    7 FORMAT(2X,I3,5(2X,F9.4))
    6 CONTINUE
      PRINT9
    9 FORMAT(2X,5(/),5X,14HCROSS SECTIONS)
      DO8J=1,21
      K=J-1
      PRINT7,K,CR(1,J),CR(2,J),CR(3,J),CR(4,J),CR(5,J)
    8 CONTINUE
      STOP
      END
```

MODIFICATIONS TO 'PHOTO1' TO INCLUDE THE DEPENDENCE OF THE ELECTRONIC TRANSITION MOMENT ON INTER-NUCLEAR SEPARATION.

```
      WE=1580.361
      WX=12.073
      RE=2.2816611
      UA=8.
      ALP=.1288721*SQRT(UA*WX)
      XKK=WE/WX
      XKM=XKK-1.
      CALLGAMMA(XKM,GKM)
      CON=.5*(ALOG(ALP)-GKM)
C     DATA FOR O2+(X)
      WEF=1876.4
      WXF=16.53  $REF=2.121604  $UAF=7.99986
      XKKF=WEF/WXF
      ALPF=.1288721*SQRT(UAF*WXF)
      DO3000JR=1,71
      R=1.6+(JR-1)*.02
      WAV(JR)=.5*XKM*(ALOG(XKK)-ALP*(R-RE))
      WAVI(JR)=-.5*XKK*EXP(-ALP*(R-RE))
      WAVI(JR)=CON+WAV(JR)+WAVI(JR)
      WAVI(JR)=EXP(WAVI(JR))
      PRINT3001,R,WAVI(JR)
 3001 FORMAT(2X,F5.2,2X,E15.8)
C     VIBRATIONAL WAVE FUNCTIONS FOR ION STATES
      ZEX(JR)=XKKF*EXP(-ALPF*(R-REF))
      DO3000JV=1,10
      V=JV-1
      BV=XKKF-1.-2.*V
C     NORMALIZATION CONSTANT
      VV=V+1
      BVV=BV+V+1.
      BBB=BV+1.
      CALLGAMMA(BBB,GBB)
      CALLGAMMA(BVV,GBV)
      CALLGAMMA(VV,GVV)
      CONF=.5*(ALOG(ALPF)+ALOG(BV)+GBV-GVV)-GBB
C
      POWF=BV/2.
      CALLSUPER(JV,BV,ZEX(JR),GIN)  ---Confluent hypergeometric subroutine.
      ZEXX(JR)=POWF*(ALOG(XKKF)-ALPF*(R-REF))
      WAVF(JR,JV)=CONF-.5*ZEX(JR)+ZEXX(JR)
      WAVF(JR,JV)=EXP(WAVF(JR,JV))
      WAVF(JR,JV)=GIN*WAVF(JR,JV)    ---Ion vibrational wave functions.
 3000 CONTINUE
      PRINT3002,(RR(JR),WAVF(JR,1),WAVF(JR,2),WAVF(JR,3),WAVF(JR,4),WAVF
     1(JR,5),JR=1,141)
      PRINT3002,(RR(JR),WAVF(JR,6),WAVF(JR,7),WAVF(JR,8),WAVF(JR,9),WAVF
     1(JR,10),JR=1,141)
 3002 FORMAT(2X,I2,5(2X,E15.8))
      DO3009JV=1,10
      DO3010L=1,3
      DO3008JR=1,71
      Y(JR)=TSR(L,JR)*WAVI(JR)*WAVF(JR,JV)
```

```
 3008 CONTINUE
      CALLSIMP2(1.6,3.0,.02,Y,TSV(L,K,JV))
      TSV(L,K,JV)=TSV(L,K,JV)**2
 3010 CONTINUE
      TVS(JV,K)=TSV(1,K,JV)+TSV(2,K,JV)+TSV(3,K,JV)
      DO30111L=1,3
      DO3012JR=1,71
      Y(JR)=TPR(L,JR)*WAVI(JR)*WAVF(JR,JV)
 3012 CONTINUE
      CALLSIMP2(1.6,3.0,.02,Y,TPV(L,K,JV))
      TPV(L,K,JV)=TPV(L,K,JV)**2
 3011 CONTINUE
      TVP(JV,K)=TPV(1,K,JV)+TPV(2,K,JV)+TPV(3,K,JV)
      DO3013L=1,2
      DO3020JR=1,71
      Y(JR)=TDR(L,JR)*WAVI(JR)*WAVF(JR,JV)
 3020 CONTINUE
      CALLSIMP2(1.6,3.0,.02,Y,TDV(L,K,JV))
      TDV(L,K,JV)=TDV(L,K,JV)**2
 3013 CONTINUE
      TVD(JV,K)=TDV(1,K,JV)+TDV(2,K,JV)
      TOTV(JV,K)=TVS(JV,K)+TVP(JV,K)+2.*TVD(JV,K)
C     FOLLOWING ONLY APPLIES AT THRESHOLD FOR LEVEL
      CROSSV(JV,K)=TOTV(JV,K)*EVIB(JV)*2.688934E-18
 3009 CONTINUE
      PRINT3016,K
 3016 FORMAT(1H1,5X,2HK=,I2)
      PRINT3017
 3017 FORMAT(5X,13HION VIB LEVEL,13HCROSS SECTION)
      DO3018JV=1,10
      JJ=JV-1
      PRINT3019,JJ,CROSSV(JV,K)
 3019 FORMAT(10X,I3,8X,E15.8)
 3018 CONTINUE
      DO3050JV=1,10
      KV=JV-1
      PRINT3051,KV,EVIB(JV)
 3051 FORMAT(2X,2HV=,I3,9HEN LEVEL=,F8.6)
 3050 CONTINUE
      STOP
      END
```

REFERENCES.

1. DIRAC, P.A.M., 1957, "Principles of Quantum Mechanics". (Clarendon Press, Oxford).

2. HEITLER, W., 1954, "The Quantum Theory of Radiation". (Clarendon Press, Oxford).

3. SCHIFF, L.I., 1955, "Quantum Mechanics". (McGraw-Hill).

4. POWELL, J.L. and CRASEMANN, B., 1961, "Quantum Mechanics". (Addison-Wesley).

5. BATES, D.R., 1939, M.N.R.A.S., 100, 25.

6. CHANDRASEKHAR, S., 1945, Astrophys. J., 102, 223.

7. ROOTHAAN, C.C.J., 1951, Rev. Mod. Phys., 23, 69.

8. BATES, D.R., 1946, M.N.R.A.S., 106, 432.

9. DITCHBURN, R.W. and OPIK, U., 1962, In "Atomic and Molecular Processes", BATES, D.R. (Ed.). (Academic Press, New York).

10. MARR, G.V., 1967, "Photoionization processes in gases". (Academic Press).

11. MESSIAH, A., 1961, "Quantum Mechanics", Vol I. (North Holland, Amsterdam).

12. BEYNON, J.D.E. and CAIRNS, R.B., 1965, Proc. Phys. Soc. (London), 86, 1343.

13. MENZEL, D.H. and PEKERIS, C.L., 1935, M.N.R.A.S., 96, 77.

14. ERBER, T., 1959, Ann. Phys., 8, 435.

15. SLATER, J.C., 1930, Phys. Rev., 36, 57.

16. SLATER, J.C., 1939, Phys. Rev., 42, 32.

17. BATES, D.R., 1946, M.N.R.A.S., 106, 423.

18. HARTREE, D.R. and HARTREE, W., 1935, Proc. Roy. Soc. A, 150, 9.

19. BURHOP, E.H.S., 1935, Proc. Roy. Soc. A., 148, 272.

20. HARTREE, D.R., 1928, Proc. Camb. Phil. Soc. 24, 89, and 24, 426.

21. CONDON, E.U., and SHORTLEY, G.H., 1963,"The Theory of Atomic Spectra".(Cambridge).

22. HARTREE, D.R., 1955,"The Calculation of Atomic Structures". (N.Y. Wiley).

23. BATES, D.R. and MASSEY, H.S.W., 1941, Proc. Roy. Soc. A., 177, 329.

24. BATES, D.R. and SEATON, M.J., 1949, M.N.R.A.S., 109, 68.

25. DALGARNO, A., HENRY, R.J.W., and STEWART, A.L., 1964, Planet. Space. Sci., 12, 235.

26. BATES, D.R., 1947, Proc. Roy. Soc., 188, 350.

27. DALGARNO, A., 1962, Advan. Phys., 11, 281.

28. BUCKINGHAM, R.A., 1937, Proc. Roy. Soc. A., 160, 94.

29. DITCHBURN, R.W., TUNSTEAD, J., and YATES, J.G., 1943, Proc. Roy. Soc. (London), A181, 386.

30. TAIT, J.H., 1964, In "Atomic Collision Processes", McDowell, M.R.C. (Ed). (North Holland).

31. JAMES, H.M. and COOLIDGE, A.S., 1936, Phys. Rev., 49, 688.

32. GELTMAN, S., 1963, Astrophys. J., 136, 935.

33. MARR, G.V., 1963, Proc. Phys. Soc. (London), 81, 9.

34. COOPER, J.W., 1962, Phys. Rev., 128, 681.

35. BURGESS, A., and SEATON, M.J., 1960, M.N.R.A.S., 120, 121.

36. BATES, D.R. and DAMGAARD, A., 1949, Phil. Trans. Roy. Soc. (London), A242, 101.

37. SEATON, M.J., 1958, M.N.R.A.S., 118, 504.

38. SEATON, M.J., 1955, C.R. Acad. Sci. (Paris), 240, 1317.

39. HERMAN, F. and SKILLMAN, S., 1963, "Atomic Structure Calculations", (Prentice-Hall).

40. BATES, D.R., OPIK, U., and POOTS, G., 1953, Proc. Phys. Soc. (London), A66, 1113.

41. BATES, D.R., LEDSHAM, K., and STEWART, A.L., 1953, Phil Trans. Roy. Soc. A, 246, 215.

42. JAFFE, G., 1934, Z. Phys., 87, 535.

43. WINANS, J.G. and STUECKELBERG, E.C.G., 1928, Proc. Nat. Acad. Sci., Wash., 14, 867.

44. HERZBERG, G., 1967, "Spectra of Diatomic Molecules". (Van Nostrand).

45. DALGARNO, A., 1952, Proc. Phys. Soc. (London), A65, 663.

46. BUCKINGHAM, R.A., MASSEY, H.J.W. and TIBBS, S.R., 1941, Proc. Roy. Soc. A, 178, 119.

47. METZGER, P.H. and COOK, G.R., 1964, J. Chem. Phys. 41, 642.

48. DITCHBURN, R.W., 1955, Proc. Roy. Soc. A., 229, 44.

49. SHIMIZU, M., 1960, J. Phys. Soc. Jap., 15, 1440.

50. FLANNERY, M.R. and OPIK, U., 1965, Proc. Phys. Soc., 86, 491.

51. WEINBAUM, S., 1933, J. Chem. Phys., 1, 593.

52. BATES, D.R. and POOTS, G., 1953, Proc. Phys. Soc., 66, 784.

53. WAINFAIN, N., 1955, Phys. Rev., 99, 542.

54. COOK, G.R. and METZGER, P.H., 1964a, J. Opt. Soc. Am., 54, 968.

55. GELTMAN, S., 1958, Phys. Rev., 112, 176.

56. BORN, M. and OPPENHEIMER, J.R., 1927, Ann. d. Physik, 84, 457.

57. SAMSON, J.A.R., and CAIRNS, R.B., 1965, J. Opt. Soc. Am., 55, 1035.

58. COHEN, H.D. and FANO. U., 1966, Phys. Rev., 150, 30.

59. BATES, D.R. and OPIK, U., 1968, J. Phys. B. Ser. 2., 1, 543.

60. POPLE, J.A. and NESBET, R.K., 1954, J. Chem. Phys., 22, 571.

61. SCHERR, C., 1955, J. Chem. Phys., 23, 569.

62. SAHNI, R.C. and LORENZO, E.J.De., 1965, J. Chem. Phys., 42, 3612.

63. COOK, G.R. and METZGER, P.H., 1964b, J. Chem. Phys., 41, 321.

64. GILMORE, F.R., 1965, J.Q.S.R.T., 5, 369.

65. MORSE, P.M. and FESHBACH, H., 1953, "Methods of Theoretical Physics". (McGraw-Hill).

66. SMITH, W.V. and HOWARD, R., 1950, Phys. Rev., 79, 1.

67. MOTT, N.F. and MASSEY, H.S.W., 1965, "The theory of Atomic Collisions". (Oxford).

68. FISK, J.B., 1936, Phys. Rev., 49, 167.

69. FLAMMER, C., 1957, "Spheroidal Wave Functions". (Stanford Univ. Press).

70. STRATTON, J.A., MORSE, P.M., CHU, L.J., LITTLE, J.D.C., and CORBATO, F.J., 1956, "Spheroidal Wave Functions". (Wiley).

71. BUCKINGHAM, R.A., 1962, "Numerical Methods". (Pitman).

72. HARGREAVES, J., 1929, Proc. Camb. Phil. Soc., 25, 75.

73. ABRAMOVITZ, M. and STEGUN, I.A., (Ed.), 1965, "Handbook of Mathematical Functions". (Dover).

74. MORSE, P.M., 1929, Phys. Rev., 34, 57.

75. PEKERIS, C.L., 1934, Phys. Rev., 45, 98.

76. LEARNER, R.C.M., 1962, Proc. Roy. Soc. A., (G.B.), 269, 311.

77. NICHOLLS, R.W., 1961, J. Res. Nat. Bur. Stds., A, 65, 451.

78. BATES, D.R., 1952, M.N.R.A.S., 112, 614.

79. WACKS, M.E., 1964, J. Chem. Phys., 41, 930.

80. BAHR, J.L., 1969, Private Communication.

81. BLAKE, A.J. and CARVER, J.H., 1967, J. Chem. Phys., 47, 1038.

82. KAPLAN, I.G. and MARKIN, A.P., 1968, Optics and Spectroscopy, 24, 475.

83. MATZANUGA, F.M. and WATANABE, K., 1967, Sci. of Light, 16, 31.

84. HALMANN, M. and LAULICHT, I., 1965, J. Chem. Phys., 43, 438.

85. NICHOLLS, R.W. and JARMAIN, W.R., 1956, Proc. Phys. Soc., 69, 253.

86. WEISSLER, G.L. and PO LEE, 1952, J. Opt. Soc. Am., 42, 200.

87. SAMSON, J.A.R. and CAIRNS, R.B., 1964, J. Geophys. Res., 69, 4583.

88. ABOUD, A.A., CURTIS, J.P., MERCURE, R. and RENSE, W.A., 1955, J. Opt. Soc. Am., 45, 767.

89. PO LEE, 1955, J. Opt. Soc. Am., 45, 703.

90. WEISSLER, G.L., 1962, J.Q.S.R.T., 2, 383.

91. BRION, H., MOSER, C. and YAMAZAKI, M., 1959, J. Chem. Phys., 30, 673.

92. BRION, H., MOSER, C. and YAMAZAKI, M., 1961, J. Chem. Phys., 33, 1871.

93. MARMO, F.F., 1953, J. Opt. Soc. Am., 43, 1186.

94. WATANABE, K., MATZANUGA, F.M. and SAKAI, H., 1967, Applied Optics, 6, 391.

95. WATANABE, K., 1954, J. Chem. Phys., 22, 1564.

96. WATANABE, K., 1958, Advan. Geophys., 5, 153.

97. KUMAR, VIJAY, 1969, Private Communication.